GEOLOGICAL SURVEY OF WESTERN AUSTRALIA

REPORT 31

A STRUCTURAL STUDY OF THE SOUTHERN PERTH BASIN WESTERN AUSTRALIA

by
R. P. Iasky

DEPARTMENT OF MINERALS AND ENERGY

GEOLOGICAL SURVEY OF WESTERN AUSTRALIA

REPORT 31

A STRUCTURAL STUDY OF THE SOUTHERN PERTH BASIN WESTERN AUSTRALIA

by
R. P. Iasky

Perth 1993

13843—1

MINISTER FOR MINES
The Hon. George Cash, J.P., M.L.C.

ACTING DIRECTOR GENERAL
L. C. Ranford

DIRECTOR, GEOLOGICAL SURVEY OF WESTERN AUSTRALIA
Pietro Guj

National Library of Australia
Cataloguing-in-publication entry

Iasky, R. P. (Robert Paul), 1956-
A structural study of the Southern Perth Basin, Western Australia

ISBN 0 7309 4480 8.

1. Geology — Western Australia — Perth Basin.
2. Basins (Geology) — Western Australia.
3. Perth Basin (W.A).
I. Geology Survey of Western Australia.
II. Title. (Series: Report (Geological Survey of Western Australia); no. 31).

559.41

ISSN 0508–4741

Copies available from:
Mining Information Centre
Department of Minerals and Energy
100 Plain Street
EAST PERTH Western Australia 6004
Telephone (09) 222 3459

Contents

Appendices

Plates

Plates are provided on microfiche in an envelope inside the back cover; full scale plates can be provided on request.

Figures

A structural study of the southern Perth Basin Western Australia

Abstract

The southern Perth Basin lies south of the Harvey Ridge; it consists of the Bunbury Trough and Vasse Shelf. It differs from the central and northern Perth Basin in having Precambrian basement outcropping on both its eastern and western margins. The structural framework of the southern Perth Basin has been re-interpreted using three geophysical methods: seismic, potential field, and geothermal.

Nearly 4000 km of seismic reflection data were used to map five horizons in the basin. Analysis of these data shows that the major fault trend is northerly and that strike-slip faulting, previously thought to be of minor importance in the formation of the basin, had a major impact in its evolution.

Gravity modelling indicates that crustal thickness beneath the basin is consistent with average continental thickness. The crust thins rapidly westwards towards the continental margin, and thickens eastwards. The Darling and Busselton Faults are normal faults, which extend into the lower crust and control the structure of the southern Perth Basin. An isostatically balanced basin would have a thinner crust under it. However, the gravity modelling in the southern Perth Basin shows that the crust is thicker than expected, implying isostatic imbalance.

Burial history and vitrinite-reflectance modelling on nine petroleum wells and five traverses across the basin have shown that there was a Late Permian–Triassic and a Cretaceous period of tectonism in the basin. Vitrinite-reflectance modelling of Lake Preston 1 provides strong evidence for a Late Permian event. Similar modelling on Sue 1 provides supporting evidence for a widespread event in the basin. Vitrinite-reflectance contours on burial histories over the nine wells show that the oil window is found within the Triassic and Permian strata onshore, and within the Late Jurassic strata offshore. The southern Perth Basin has the source rocks, the structures, and the seal needed for hydrocarbon accumulation; Permian, Triassic, and Jurassic exploration drilling objectives should be considered.

Deposition in the basin may have begun in the Silurian — although Permian sediments are the oldest found — and deposition continued through to the Quaternary. The evolution of the southern Perth Basin has had three major periods of tectonism which re-activated major faults. These were:

(a) right-lateral strike-slip motion along the Darling Fault in the Late Permian–Triassic, and the eventual rise of the Harvey Ridge;

(b) a phase of tectonism with associated left-lateral strike-slip motion along the Dunsborough Fault in the Jurassic, which marks an active period of deposition and faulting; and

(c) separation of Australia from India in the Early Cretaceous. This produced uplift with a predominantly tensional, but also some oblique–transcurrent right-lateral, faulting.

KEYWORDS: Seismic reflection, seismic interpretation, structural interpretation, geological structures, tectonism, gravity modelling, geohistory, geological history, vitrinite-reflectance modelling, geothermal gradients, hydrocarbon maturation, Perth Basin, Western Australia.

Introduction

The Perth Basin is in the southwest of the Australian continent; it is a deep, elongated, north-trending, sediment-filled trough, approximately 1000 km long. The eastern boundary is the Darling Fault, which marks a discontinuity between the sediments of the basin and the Precambrian rocks of the Yilgarn Craton. The western and southern boundaries are the edge of the continental shelf. To the north, the Perth Basin passes gradually into the Carnarvon Basin.

The area of investigation is the southern portion of the Perth Basin (Fig. 1). It includes the Bunbury Trough and Vasse Shelf, onshore and offshore, and lies south of 32°S latitude or, geologically, south of the Harvey Ridge. The area is bounded by the Yilgarn Craton and Leeuwin Complex at its eastern and western boundaries respectively; it spans an approximate length of 225 km, an approximate width of 75 km, and has a total area of 16 875 km^2.

Previous investigations

The first geological investigation of the southwestern part of Western Australia was conducted by Saint-Smith (1912) and this was followed by geological investigations

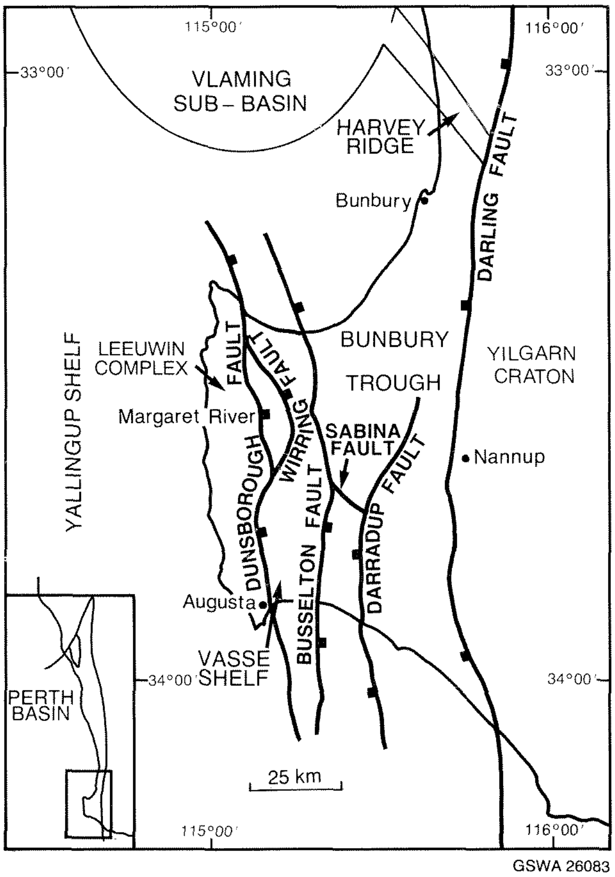

Figure 1. Location and tectonic elements of southern Perth Basin

of the Perth Basin by Maitland (1919), Clarke et al. (1944), Teichert (1947), and Fairbridge (1948 and 1953). The first comprehensive regional geological survey of the Perth Basin was conducted between 1954 and 1958 by Playford, Willmott, and Johnstone, while they were working for West Australian Petroleum Pty Ltd (WAPET) (Johnstone and Playford, 1955; Playford and Willmott, 1958). WAPET conducted several other investigations, the results of which were used in the compiling of *Geology of the Perth Basin, Western Australia* (Playford et al., 1976).

It was not until 1948 that Vening Meinesz (1948) described the findings of gravity expeditions which had been carried out off the southern coast of Western Australia between 1923 and 1938; and it was then that the thickness of the sedimentary sequence in the basin was first appreciated. This was followed by a gravity traverse through Bullsbrook by Thyer (1951), regional gravity and magnetic surveys of the basin (Thyer and Everingham, 1956; Quilty, 1963), and the Busselton seismic-reflection survey in 1956 (Lodwick, 1962): all were carried out by the Bureau of Mineral Resources (BMR).

An important contribution was also made by Cockbain and Lehmann (1971), who produced detailed geophysical maps and cross-sections of the Perth Basin.

As well as having been explored for oil and coal by a number of exploration companies, the study area has been extensively drilled for water by the Geological Survey. The primary target for oil and coal exploration has been the Permian Sue Coal Measures in both the Bunbury Trough and the Vasse Shelf; whereas the objective of the water drilling has been to evaluate the deep groundwater resources in the basin.

Petroleum exploration in the Bunbury Trough started in 1902, when Westralian Mining and Oil drilled three shallow wells. Renewed interest in the basin occurred in the second half of the 1960s and the early 1970s, when WAPET and Union Oil conducted a new round of exploration. In the late 1970s, Wainoco International conducted a seismic survey in the southern offshore area; further exploration was carried out between 1980 and 1982 by BP Australia, Mesa Australia Ltd., and Weaver Oil and Gas Corporation Australia.

Fifteen wells have been drilled and 42 geophysical surveys carried out for petroleum exploration in the southern Perth Basin. These include one gravity, one seismic-reflection, and two aeromagnetic surveys undertaken by the BMR.

The Geological Survey has drilled numerous bores in several traverse lines across the basin for groundwater assessment. From north to south, the hydrogeological drilling includes the Harvey line in 1983–84 (Deeney, 1989a), the Binningup line in 1984 (Deeney, 1989b), the Picton line in 1978 (Wharton, 1980), the Boyanup line in 1981 (Smith, 1982), the Quindalup line in 1966–80 (Wharton, 1981), the Cowaramup line in 1988 (Appleyard, 1989), and the Karridale line in 1989–90 (Baddock, 1991). This drilling totalled 36 bores spread throughout the basin from latitude 32°50' to 34°10'. In addition, the Bunbury shallow drilling program was conducted in 1981 (Commander, 1981, 1982).

Considerable drilling for coal has been conducted on the Vasse Shelf by BHP, Mallina–Bond, CRA, and Griffin. The data utilized in the present study are tabulated in Appendices 1–5.

Physiography

The area being investigated may be divided into three physiographic provinces, the Darling Plateau, an intermediate plain, and the Leeuwin–Naturaliste Ridge. The intermediate plain can be split into three areas, the Swan Coastal Plain, the Blackwood Plateau, and the Scott Coastal Plain (Lowry, 1967; Wilde and Walker, 1982; Wilde and Walker, 1984).

The Darling Plateau is an ancient erosion surface that has an average elevation of 300 m above sea level. The Darling Scarp, whose relief is 40 m in the south and up to 200 m in the north, is the eroded western edge of the Darling Plateau, and is the surface expression of the Darling Fault.

The Swan Coastal Plain extends west from the Darling and Whicher Scarps to the Indian Ocean (Woolnough, 1920), and is underlain by Quaternary alluvium and littoral dunes. Along the coastline, there is a narrow belt of active dunes and lagoons; the plain rises to 60 m above sea level at the foot of the Whicher Scarp. The Whicher Scarp is a complex erosional marine feature which marks the northern edge of the Blackwood Plateau and separates it from the Swan Coastal Plain. The scarp parallels the coastline; its relief ranges from 100 m in the east to 30 m in the west.

The undulose surface of the Blackwood Plateau, which consists of laterite, lateritic gravel, and sand, ranges from 120 to 180 m above sea level (Cope, 1972; Low, 1972). Remnants of an early drainage system are preserved, and it supports a jarrah forest.

The Scott Coastal Plain has an average elevation of 40 m. It is a swampy region, but remnants of dunes form scattered hills and ridges; and there is a belt of active dunes and lagoons along the coast.

The climate is temperate Mediterranean type; and the average annual rainfall ranges from 800 mm in the north to 1500 mm in the south. The Margaret, Blackwood, and Scott Rivers, are the only permanently flowing rivers in the southern Perth Basin.

Geology of the southern Perth Basin

Tectonic setting

The Bunbury Trough, which is bounded by the Darling Fault to the east and Busselton Fault to the west, is a deep graben that contains up to 11 km of Permian–Holocene sedimentary rocks. To the north, the Harvey Ridge separates the Bunbury Trough from the Dandaragan Trough. Figure 1 shows the main tectonic elements of the area.

The Harvey Ridge starts at the Darling Fault and extends for a short distance offshore before plunging under the Vlaming Sub-basin in a northwesterly direction.

The Vasse Shelf is a shallow fault block, bounded by the Busselton Fault to the east and the Dunsborough Fault to the west. It consists of Permian to Holocene sedimentary rocks ranging in thickness from 0.5 to 3 km.

In the northern offshore part of the area, the sequence thickens; and sediments of the Vlaming Sub-basin onlap sediments of the Bunbury Trough. To the west, the Busselton Fault continues to be a major discontinuity; and the sequence thins as it approaches the oceanic crust.

In the southern offshore part of the area, the Bunbury Trough and the Vasse Shelf sediments thin as they approach the continental margin. The Darradup Fault is a major west-dipping fault in the southern portion of the Bunbury Trough. It divides the Bunbury Trough into a higher block to the west and a lower block to the east. A cross-cutting fault (herein named the Sabina Fault) to the north of the high block, separates it from the rest of the trough.

Offshore, where there is a strong magnetic positive anomaly, the northern part of the Leeuwin Complex appears to be oriented in a northwesterly direction; whereas seismic data suggests that the southern part swings in a southeasterly direction. It is not a southern extension of the Beagle Ridge (to the north) because dating of rocks of the Leeuwin Complex has shown them to be much younger than those of the Beagle Ridge (Fletcher et al., 1985).

Regional geology

Outcrop in the southern Perth Basin is sparse: the area is covered by Cainozoic rocks and a few scattered outcrops of the Cretaceous Bunbury Basalt. The coastal areas are covered by Quaternary sands of the Bassendean Sand, the Guildford Formation, strips of Tamala Limestone, and occasional Safety Bay Sand. All of the inland area is covered by laterite and associated sand. The Phanerozoic sediments in the Bunbury Trough are about 11 km thick (Plate 11), but on the Vasse Shelf, they thin to 3 km.

Remnants of Middle to Late Proterozoic deposition are found in the Moora, Cardup, and Yandanooka Groups, immediately to the east and west of the Darling Fault. These sediments do not outcrop anywhere south of latitude 33°, and it is unlikely that they are present in the southern Perth Basin.

In the onshore part of the southern Perth Basin, the sedimentary sequence includes up to 4 km of Permian, 3 km of Triassic, 4 km Jurassic, and some 300 m of Cretaceous. These sedimentary rocks increase rapidly in thickness to the northwest offshore area. The Triassic and Jurassic sediments are not present in the northern part of the Vasse Shelf, but Triassic sediments have been intersected in both Sue 1 and Alexandra Bridge 1 in the southern part of the Vasse Shelf. Tertiary sediments are present in the Vlaming Sub-basin, offshore, but do not extend into the Bunbury Trough. Permian sediments that correlate with the Sue Coal Measures are exposed in the Collie and the northern Perth Basins. Triassic and Jurassic rocks also outcrop in the north of the basin.

Stratigraphy

This section describes the stratigraphy of the Bunbury Trough and Vasse Shelf (Fig. 2). Formation tops for most of the wells drilled in the southern Perth Basin are summarized in Appendix 6.

Permian

The Sue Coal Measures of Early to Late Permian age (Williams and Nicholls, 1966), and the Sabina Sandstone of Late Permian to Early Triassic age (Young and Johanson, 1973), are up to 4 km thick and overlie basement rocks. The sequence is intruded by dolerite sills which are probably comagmatic with the Cretaceous Bunbury Basalt (Williams and Nicholls, 1966). These sills are also seen in the Triassic Lesueur Sandstone in Whicher Range 2 (Poynton and Hollams, 1980).

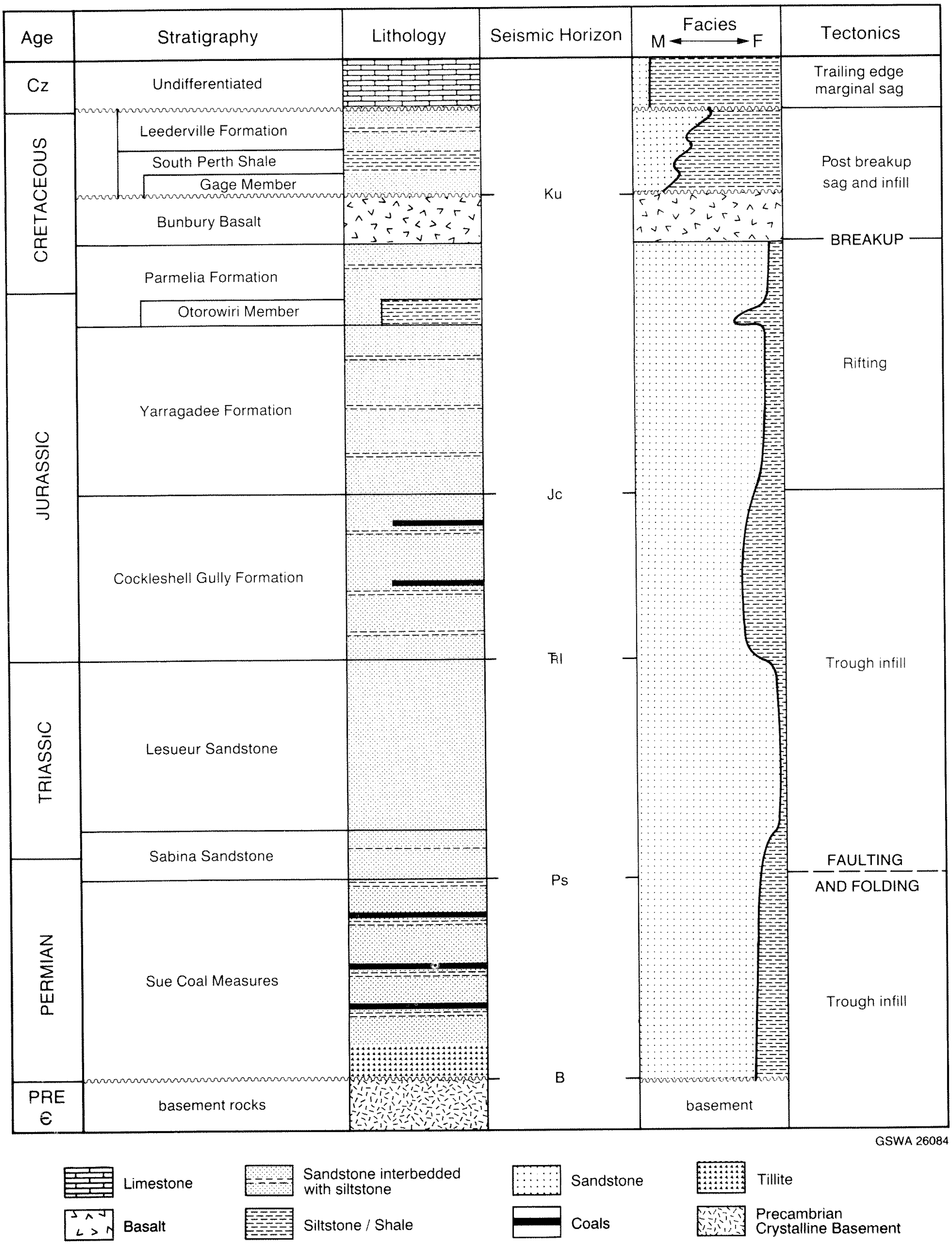

Figure 2. Stratigraphic column; lithological screens after Berkman (1976); M = marine; F = fluvial

The Sue Coal Measures are a sequence of interbedded sandstone, siltstone, and coal above a thin basal conglomerate (Williams and Nicholls, 1966). The unit is a continental deposit consisting of alternating fluvial and paludal sediments over a thin glacial sequence at the base. The sediments are equivalent to Permian deposits in the Collie Basin and the northern Perth Basin.

The Permian sequence has proved to contain hydrocarbon source rocks (Nosiara and Hogg, 1982) and has been the principal target for petroleum exploration. The coal seams generally are bituminous throughout the Permian sequence, but may become sub-bituminous in the Upper Permian: they are the target for coal exploration on the Vasse Shelf.

The Sabina Sandstone is a thin unit, which conformably overlies the Sue Coal Measures; its maximum recorded thickness is 561 m in Lake Preston 1. It is a sequence of medium- to coarse-grained quartz sandstone that contains thin beds of interbedded shale. This unit is believed to be predominantly a fluvial deposit, although it may become paralic to the north (Playford et al., 1976).

Triassic

The Lesueur Sandstone, mainly fine- to coarse-grained quartz sandstone but containing small amounts of siltstone, probably disconformably overlies the Sabina Sandstone. The age of this sequence in the Bunbury Trough has been interpreted to be Early to Late Triassic (Union Oil Development Corp., 1968, 1972).

This unit, which is widespread in the Bunbury Trough and the southern part of the Vasse Shelf, is as much as 3 km thick on the northeastern side of the trough (Plates 7 and 9). It is believed to be a fluvial unit, whose deposition began in the southern Perth Basin during the Early Triassic and whose depocentre shifted north in the Middle to Late Triassic (Burdett, 1963; Elie et al., 1965).

Jurassic

The Jurassic sequence in the southern Perth Basin includes: the Early Jurassic Cockleshell Gully Formation (Lehmann, 1966; Bird and Moyes, 1971); the Middle to Late Jurassic Yarragadee Formation (Bird and Moyes, 1971); and the Late Jurassic Parmelia Formation. The sequence has not been intersected by drilling on the Vasse Shelf: it is only present in the Bunbury Trough. The whole Jurassic sequence has a maximum thickness of 4 km (Plates 3 and 5).

The Cockleshell Gully Formation is a fluvial deposit of fine- to coarse-grained sandstone with interbedded claystone and siltstone. Some coals are present in the Cowaramup 6 and 7 water bores (Appleyard, 1989), suggesting that this part of the sequence is equivalent to the Jurassic sequence in the northern Perth Basin. In the south, the maximum thickness of the Cockleshell Gully Formation is about 1 km, and it conformably overlies the Lesueur Sandstone.

The hydrocarbon potential of the Cockleshell Gully Formation has been underestimated in the southern Perth Basin. It has been shown to possess reasonable source-rock potential (Nosiara and Hogg, 1982).

The Yarragadee Formation, a fluvial deposit, consists of interbedded sandstone and siltstone, and subordinate shale, claystone, and conglomerate. It varies in thickness in the Bunbury Trough because much of it was removed during rifting. The maximum thickness of approximately 550 m was intersected in Sabina River 1. It conformably overlies the Cockleshell Gully Formation, which is lithologically similar; this makes it difficult to distinguish the two formations.

The Parmelia Formation was defined by Backhouse (1984): it consists of continental, paralic, and shallow marine sediments, and includes the marine Carnac and the Otorowiri Members in the southern Perth Basin. These members are well-defined shaly and silty units, and display strong seismic reflections. The Otorowiri Member is found in the Vlaming Sub-basin and the offshore Bunbury Trough, whereas the Carnac Member is only found in the Vlaming Sub-basin north of the study area. The sequence conformably overlies the Yarragadee Formation.

In the Offshore Vlaming Sub-basin, the Parmelia Formation is very thick (Cockbain, 1990), but it thins to the south and is mostly absent onshore. In the onshore Bunbury Trough, the sequence was intersected in the Cowaramup 6 and 7 water bores (Appleyard, 1989, 1991), Karridale 7 (Baddock, 1991), and has been identified in the Quindalup 7 and 9 bores (Wharton, 1981). The formation consists of poorly consolidated clayey sandstone, siltstone, and shale. It is believed to be scattered in small pockets throughout the onshore Bunbury Trough.

In the offshore Vlaming Sub-basin, where it is thick, the Parmelia Formation is one the main targets for petroleum exploration. Unfortunately, the hydrocarbon potential of the onshore sequence is poor because it is very thin and shallow.

Cretaceous

The Early Cretaceous Bunbury Basalt and the Leederville Formation of the Warnbro Group are present in the southern Perth Basin.

The Bunbury Basalt, which is widespread in the onshore part of the southern Perth Basin, consists of lava flows within valleys in the eroded Yarragadee Formation. The basalt flows are porphyritic or microporphyritic basalt (Edwards, 1938; Trendall, 1963; Burgess, 1978). Potassium–argon dating by McDougall and Wellman (1976) suggests an age of at least 90 Ma. It was probably extruded during the breakup of India and Australia; Backhouse (1988) and Playford et al. (1976) suggested a Valanginian (136 Ma) age. Felcman and Lane (1963) used aeromagnetic and gravity data to map the distribution of the basalts. Davies et al. (1989) produced evidence to suggest that the Bunbury Basalt flows are similar to the basalts on the Kerguelen Plateau, which formed above the

13843—2

Dupal mantle plume during the opening of the Indian Ocean. As the continents separated, the plume, which is now situated beneath Heard Island, left a winding trail along the moving plate.

In the southern Perth Basin, the Warnbro Group has been described as undifferentiated sediments equivalent to the Leederville Formation (Appleyard, 1989, 1991). These sediments have previously been identified as belonging to the Leederville Formation in the Busselton area (Hirschberg, 1989).

The Warnbro Group unconformably overlies the Yarragadee and Parmelia Formations or older units. It consists primarily of interbedded continental sandstone and siltstone, minor amounts of conglomerate, and thin seams of coal or lignite. It is a thin blanket of sediments, up to 300 m thick onshore, which covers both the Bunbury Trough and Vasse Shelf. It has no hydrocarbon potential in the southern Perth Basin.

Quaternary

A thin layer of sediments covers the Cretaceous rocks of the southern Perth Basin. These sediments, which range from 20 to 100 m thick, include laterite and associated sand, Bassendean Sand, Tamala Limestone, Safety Bay Sand, and Guildford Formation.

This sequence, which consists of eolian dunes near the shoreline, lake and swamp deposits in the interdune areas, and alluvial and estuarine deposits along rivers, unconformably overlies the older Mesozoic sequences.

The laterite, which is composed of iron and aluminium oxides, is a vesicular or concretionary rock that overlies weathered bedrock. It is, in turn, generally overlain by as much as 10 m of podsolized quartz sand.

The Tamala Limestone is coarse- to medium-grained calcarenite containing some quartz sand. The rest of the Quaternary sediments comprise mainly varying thicknesses of quartz sand.

Basin evolution

The Perth Basin formed along the divergent western margin of the Australian continent during the Palaeozoic and Mesozoic. Cockbain (1990) suggested that the geological evolution of the basin occurred in three main phases:

(a) Silurian to Carboniferous;
(b) Permian to early Neocomian; and
(c) Late Neocomian to Holocene.

During the first phase, the Early Silurian Tumblagooda Sandstone was deposited in the north. Drilling and seismic data indicate that the oldest sediments in the southern Perth Basin are Early Permian.

The second phase was the interior-fracture rifting stage, and the third phase was the extensional–transtensional stage in the development of the Perth Basin (Fig. 2).

The development of the Perth Basin has been influenced by the history of the Darling Fault. The main period of normal movement of the Darling Fault was between the Early Triassic and Middle Jurassic; but there is evidence to suggest that the fault follows a line of crustal weakness initiated in the Archaean (Wilson, 1958; Blight et al., 1981).

Baxter and Harris (1979) recognized three phases in the Darling Fault's history:

(a) early Archaean ductile and brittle–ductile transcurrent movement, which resulted in a Proterozoic intracratonic basin;
(b) Proterozoic brittle and brittle–ductile reverse movement; and
(c) Phanerozoic brittle fractures, which include Silurian and Late Permian strike-slip, and Jurassic and Cretaceous normal and transtensional movements.

The Yilgarn Craton (>2.3 Ga), the Leeuwin Complex (0.65 Ga), and basement rocks of the southern Perth Basin (1.8–2.0 Ga) contain crustal material of different ages. Fletcher et al. (1985) suggested that crustal Proterozoic mobile belts were accreted on to the western margin of the Archaean Yilgarn Craton.

Palaeozoic

Between 450 and 500 Ma, significant heating and uplift occurred in the southwestern part of Yilgarn Craton (de Laeter and Libby, in press) and possibly in the adjacent Perth Basin. Deposition of the fluvial to shallow-marine Tumblagooda Sandstone is possibly associated with this uplift; and right-lateral strike-slip movement along the Darling Fault could have moved these rocks northwards to the southern Carnarvon Basin.

In the northern offshore part of the basin, a phase of tectonism associated with rifting occurred in the Early Permian; and glacial sediments were deposited throughout the Perth Basin and on the Yilgarn Craton. This was followed by deposition of coal measures in the southern Perth Basin. This period experienced little faulting; but sedimentation extended across the Yilgarn Craton, and pockets of Permian sediments, such as the Collie and Wilga Basins, are remnants of this widespread deposition.

A Late Permian tectonic event caused some faulting, which is thought to have produced a deep graben in the basin (Johnstone et al., 1973). During this period, mantle upwelling (Middleton and Hunt, 1989) throughout the western margin caused the reactivation of major crustal weaknesses such as the Darling and Busselton Faults. The formation of the Harvey Ridge probably occurred at this time, as significant uplift is suggested in various parts of the basin. It is possible that this regional event caused some right-lateral strike-slip movement along the Darling Fault.

The uplift caused erosion of the Permian sediments on the Yilgarn Craton; but, in the Bunbury Trough and Vasse Shelf, deposition of fluvial and alluvial plain sediments (Sabina Sandstone) continued in the very Late Permian to Early Triassic. Further to the north, deposition of the Late Permian Wagina Sandstone occurred as alluvial fan deltas spread westwards from the Darling Fault.

Mesozoic (pre-breakup)

In the north Perth Basin, a marine transgression resulted in the deposition of the Kockatea Shale. At the beginning of the Middle Triassic, basin-margin faults (Darling, Dunsborough, and Busselton Faults) were reactivated, and basement blocks (Yilgarn and Leeuwin) were uplifted. This important period of block faulting in the basin coincided with a marine regression and the deposition of the Woodada Formation in the north. It was followed by the deposition, which continued to the Late Triassic, of thick fluvial and alluvial-fan deposits (Lesueur Sandstone) throughout the Perth Basin.

In the Early Jurassic, fluvial, swamp, and marsh environments developed, and the Cockleshell Gully Formation was deposited. In the north, this was followed by brief transgressions and deposition of paralic sediments during the Middle Jurassic. To the south, and associated with the breakup of the southern margin of Western Australia, there was a left-lateral activation of the Dunsborough Fault.

The breakup of the northwestern margin of Western Australia resulted in the reactivation of major faults during the Late Jurassic (Crostella and Barter, 1980); thick fluvial and alluvial-plain sediments of the Yarragadee Formation were deposited; and extensive movement took place along the Darling Fault.

In the latest Jurassic to Early Cretaceous, the depocentre shifted from the Dandaragan and Bunbury Troughs to the Vlaming Sub-basin; lacustrine shales and silts (Parmelia Formation) were deposited over most of the Vlaming Sub-basin and extended as far as the south Bunbury Trough (Appleyard, 1989).

During the breakup stage in the Early Cretaceous, considerable transcurrent movement occurred along the Perth–Wallaby transform fault system; this set up a transtensional regime in the basin.

Mesozoic (post-breakup) to Holocene

When the breakup of Australia and India along the western margin of the continent occurred in the Early Cretaceous (Falvey and Mutter, 1981), basaltic lava flows were extruded over the erosion surface in the Bunbury Trough. Uplift and erosion over the basin produced an unconformity in offshore areas. A subsequent marine transgression from the west brought marine sediments to the offshore areas, while continental deposits were deposited in onshore areas (Warnbro Group).

In the onshore Bunbury Trough, the Cretaceous terrigenous clastic sediments of the Leederville Formation, which onlap the Yilgarn Craton and Leeuwin Complex, are very thin.

The Neocomian breakup event initiated the last major faulting in the basin, but subsidence has continued to the present; while in the south of the Bunbury Trough, rifting of the Australian–Antarctic southern margin occurred in the mid-Cretaceous (Cande and Mutter, 1982).

As oceanic circulation and favourable warm, shallow environments were established along the continental margins in the Late Cretaceous and the Tertiary, carbonates were deposited.

The Tertiary was a period of clastic and carbonate sedimentation offshore and a period of erosion and lateritization of the onshore Perth Basin.

A small amount of uplift of the Yilgarn Craton has occurred since the Eocene and may still be continuing. Middle to Late Tertiary uplift has also occurred along the Jarrahwood axis on the Blackwood Plateau (Cope, 1972). However, in general, the Quaternary has been a period of subsidence with little active faulting other than movement resulting from differential compaction.

Mantle convection stress patterns under Australia show that the western margin is continuing to experience upwelling convection currents which has caused uplift of the western shield areas since the Pliocene (Liu, 1979).

Hydrocarbon potential

A summary of the hydrocarbon discoveries in the Perth Basin was given by Elliott et al. (1985). Most discoveries have been in the northern Perth Basin. However, the Whicher Range wells had good gas flows; and Wonnerup 1 had shows of hydrocarbons in the Permian.

The petroleum discovered in the north of the basin occurs in Permian, Triassic, Jurassic, and Early Cretaceous rocks. The stratigraphic sequence in the southern Perth Basin is similar to that in the north, and both Jurassic and Permian coal measures could be potential source beds.

Both the source rocks and reservoir sands for the discoveries in the southern Perth Basin are in the Sue Coal Measures. This Permian sequence is too deep to have retained good porosities, although maturation studies show that it lies within the oil-maturation window. In the Jurassic and Triassic sequences, which are shallower, there are potential reservoirs; and, given favourable migration paths, hydrocarbon could be found in these. Although the Jurassic has not been considered a target in the past, it has been shown to possess source material (Nosiara and Hogg, 1982) and could be a target in the future.

Reservoir rocks are present in the Permian to Jurassic sequence, and structural and stratigraphic traps are possible. The basin is strongly fractured and faults play an important role in hydrocarbon migration. Although there have only been a few hydrocarbon discoveries in the southern Perth Basin, it offers the right ingredients of source, seal, and structure, to encourage further exploration.

Seismic interpretation and structural maps

Using both onshore and offshore seismic reflection data, seismic time and depth structure contours have been mapped on five horizons (Plates 3–12). Figure 3 shows the location of petroleum wells in the basin, and the position of the seismic sections displayed in this section. The mapped horizons are:

(a) Early Cretaceous, break-up unconformity (base of Warnbro Group, horizon *Ku*)
(b) Top Early Jurassic (top of Cockleshell Gully Formation, horizon *Jc*)
(c) Top Triassic (top of Lesueur Sandstone, horizon *Ŧl*)
(d) Top Permian (top of Sue Coal Measures, horizon *Ps*)
(e) Top Precambrian (basement, horizon *B*).

The aim of the seismic mapping was to determine the structural framework of the Bunbury Trough and the Vasse Shelf. The five horizons were chosen because they are major stratigraphic horizons in the depositional history of the southern Perth Basin. These horizons may not necessarily display strong seismic reflections.

The data were collected from 1964 to 1982, and the quality varies from poor to good. The type of data used in the seismic interpretation, together with the limits, assumptions, methodology, and procedures used to compile the maps, are discussed in this section.

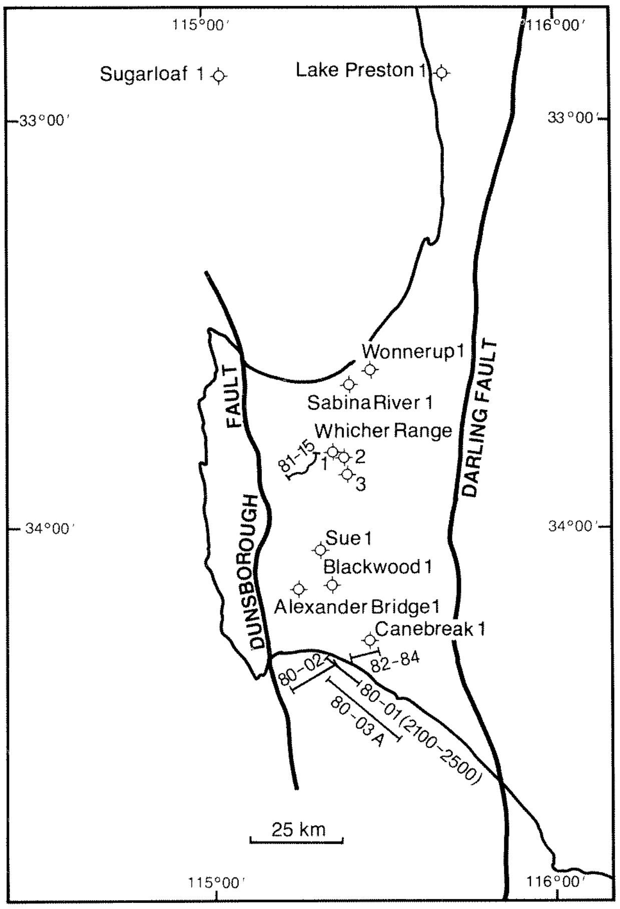

Figure 3. Locations of petroleum wells and seismic sections discussed in text

Quality of data

The quality of the onshore seismic data is generally very poor to bad; this is a result of both acquisition and processing parameters. The poor penetration of energy was caused by geophone decoupling which, in turn, was due to surface laterite and other energy-dissipation factors, such as near-surface Bunbury Basalt and Tamala Limestone (Taylor, 1969).

Furthermore, the recording parameters of some of the earlier surveys were selected to enhance reflections at a two-way travel time of two seconds so that the reflections from the primary target, the top of the Sue Coal Measures, could be recognized easily. To achieve this, long source and receiver arrays, which attenuated the shallower events, were used in the recording.

Good energy transfer was achieved by Ampol Exploration in the northern Perth Basin permit EP 321 by placing dynamite at depths of 150–200 m in shot holes that had been drilled well below the weathered layer. This method of acquisition may be applicable to the southern Perth Basin. Improvements could also be expected with an increased energy-source pattern and increased fold cover.

The quality of the southern offshore data is very good and the mapping horizons can easily be picked. However, the tops of the Cockleshell Gully Formation and the Lesueur Sandstone could not be correlated from the onshore interpretation, and were not mapped in the southern offshore area. Figure 4 shows the correlation between the closest onshore and offshore seismic sections.

The quality of the northern offshore data is poor because the area is highly faulted. The breakup unconformity (base of the Warnbro Group) is a good reflector, but reflections below it are hard to identify. The sections are highly overmigrated which causes reflectors to become concave upwards below 4.0 seconds. The acquisition and processing parameters were selected to enhance the 1–2 seconds time window.

Characteristics of reflections

There are two sources of strong reflections in the section: these are the dolerite intrusives, and the coal measures in the Permian sequence. They can easily be recognized in the synthetic seismograms for Whicher Range 2 (Fig. 5) and Canebreak 1 (Fig. 6).

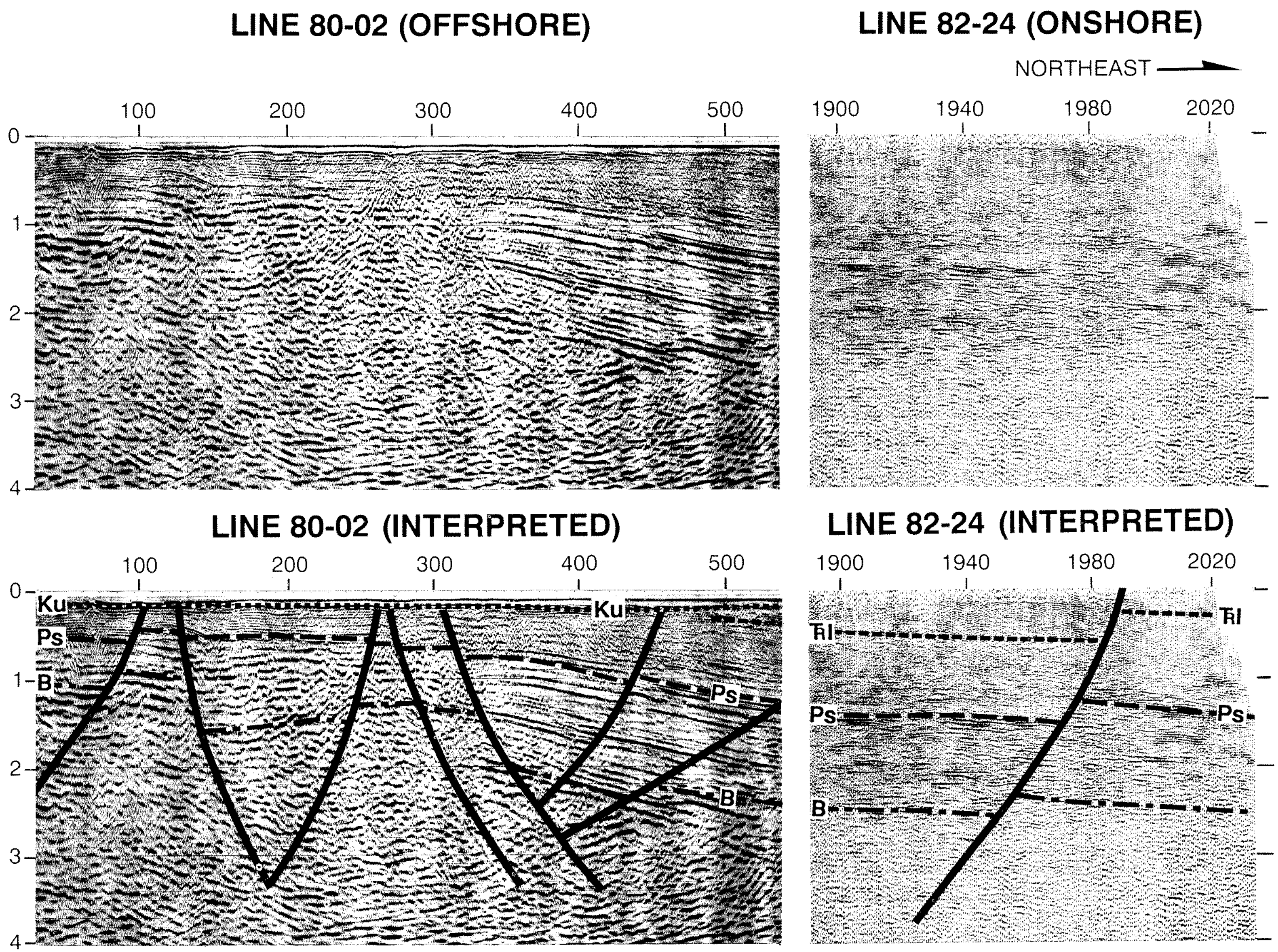

Figure 4. Onshore and offshore seismic correlation

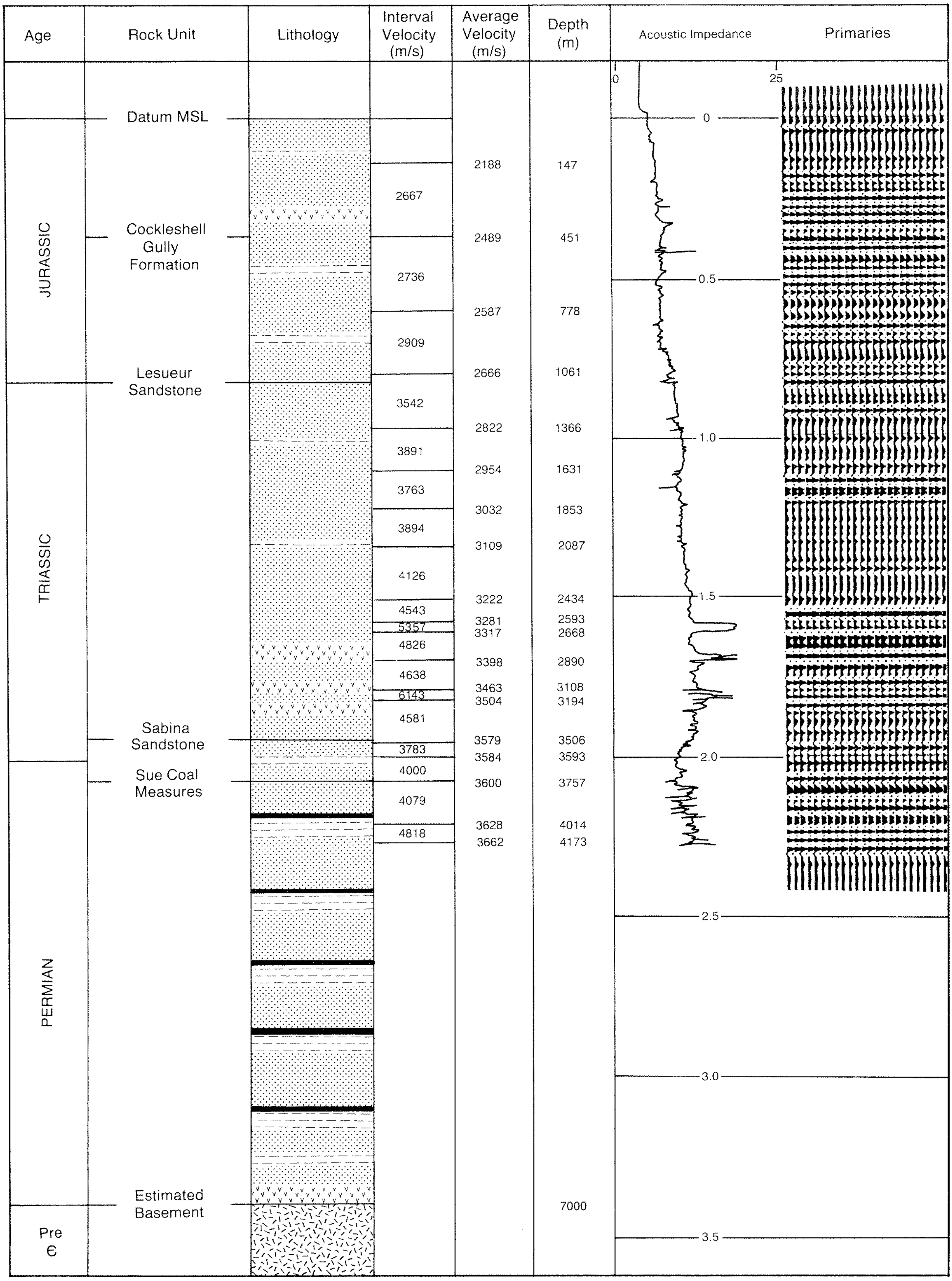

GSWA 26087

Figure 5. Synthetic seismogram of Whicher Range 2

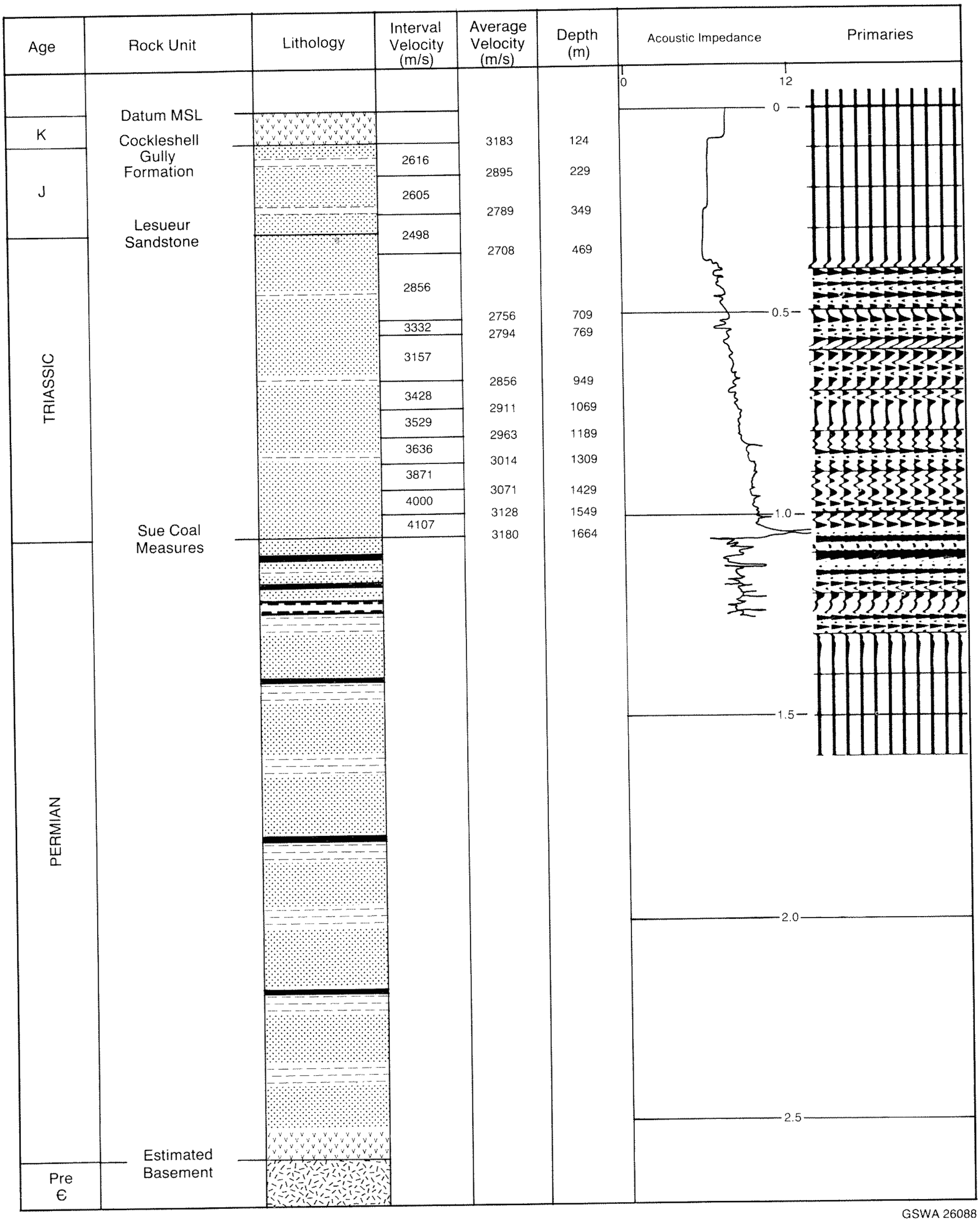

Figure 6. Synthetic seismogram of Canebreak 1

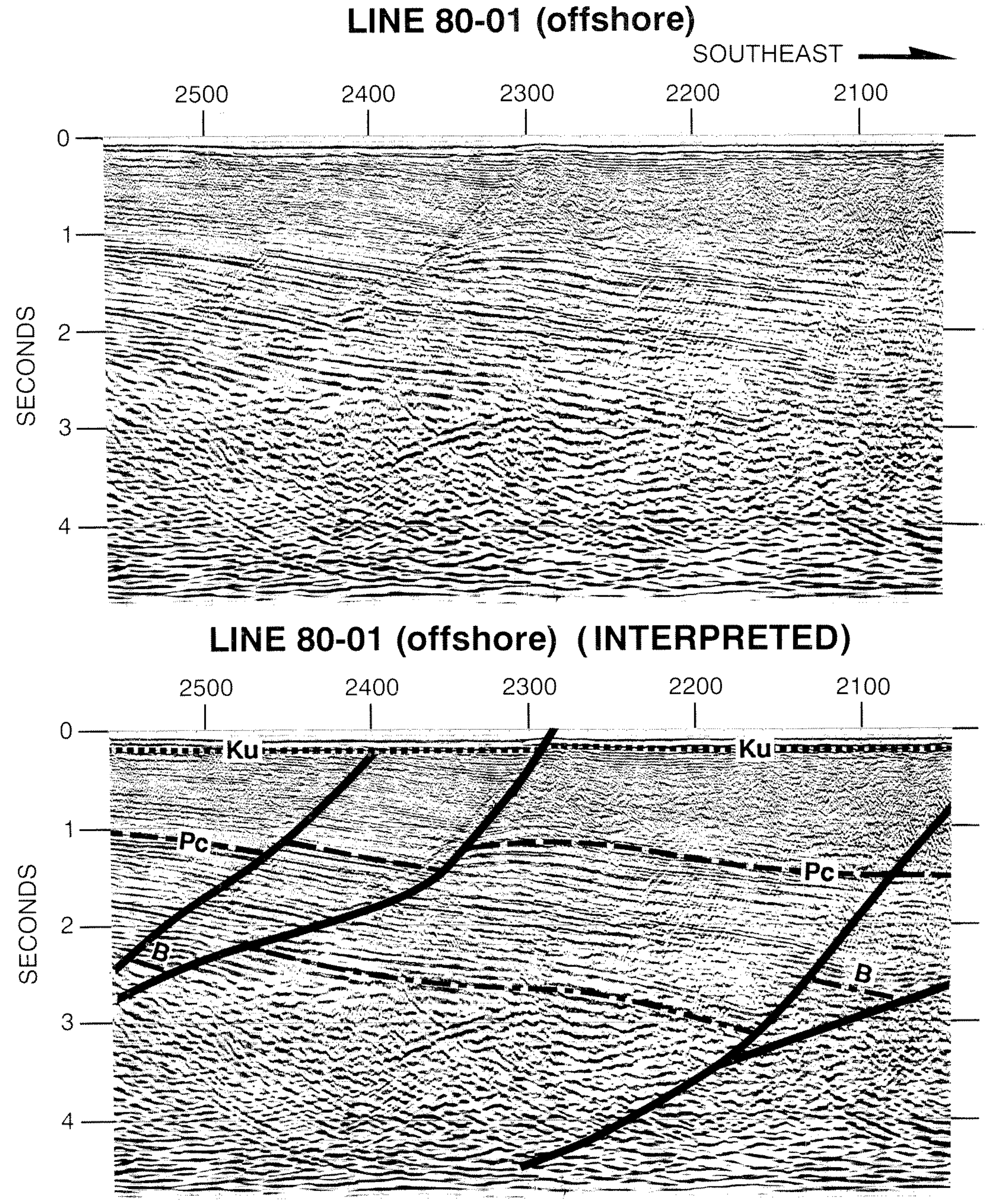

Figure 7. Seismic section showing offshore basement reflection features

The Bunbury Basalt is usually too shallow to display a seismic event on the section onshore, but the dolerite intrusives may appear at any depth along the section (Fig. 5).

The base of the Warnbro Group is too shallow to be seen onshore; but in the offshore areas it can be easily recognized as a characteristic angular unconformity. There is no distinct lithological difference between the Warnbro Group and the underlying sediments and consequently this interface does not have a characteristic reflector.

The Jurassic sequence is made up of sandstone with interbedded shale, siltstone, and clay. There is very little difference between the lithologies of the Yarragadee Formation and the Cockleshell Gully Formation; consequently, the acoustic-impedance contrast does not display a signature of consistent character through the sub-basin. This is seen in the synthetic seismogram (Fig. 5), where the Yarragadee Formation overlies the Cockleshell Gully Formation.

Occasional strong reflectors are seen in the Jurassic section in the southern part of the Bunbury Trough. These are possibly due to coal measures, seen in the Cockleshell Gully Formation in Blackwood 1, or to siltstone layers in the sequence. In contrast, the Jurassic Cattamarra Coal Measures of the Cockleshell Gully Formation are persistently strong reflectors in the northern Perth Basin.

The top of the Lesueur Sandstone is also a discontinuous seismic marker. The lithology seems to grade from sandstone and interbedded siltstone in the Cockleshell Gully Formation, to sandstone in the Lesueur Sandstone with no distinct break between the two formations. The acoustic-impedance contrast in Whicher Range 2 (Fig. 5) displays a small drop at this boundary. However, this signature is not continuous throughout the Bunbury Trough and the horizon is difficult to pick.

The event at the top of the Permian occurs at about 2 seconds onshore, and it is the easiest one to identify in the Bunbury Trough. There are a number of coal seams in the section; these create high acoustic-impedance contrasts and good seismic events. The first coal seam is near the top of the Permian, and provides a good reflection at the boundary with the Permo-Triassic Sabina Sandstone (Fig. 6).

The top of the Permian remains a strong event in the southern offshore area, but it becomes harder to identify in the northern offshore area as, to the northwest, the horizon deepens very quickly below 4 seconds.

The crystalline basement is usually a good seismic marker in the Bunbury Trough as, in most areas, it provides strong acoustic impedance contrast against the overlying sedimentary sequence.

In the southern offshore area, basement displays multiple reflections of low frequency (8–10 Hz), while onshore it displays a higher frequency reflector (20–40 Hz, depending on depth) (Fig. 7). The low-frequency reflections in the southern offshore area are probably a result of the low-frequency cut-off point of the time-variant filter applied at the 2.6 to 5.0 seconds time window.

Structural mapping

Velocity analysis

All the available well-velocity survey data were used to convert surface seismic time to depths. Many of the wells did not intersect the mapped horizons, and extrapolation of the velocity curves was needed to convert the time values at the deeper horizons.

To carry out seismic interpretation, the two-way travel time (TWT) values to the formation tops is needed. Appendix 7 is a summary of these values, which were determined by using the well-velocity survey data. A least-squares curve-fitting program to fit a straight line, exponential, power, and polynomial curves to the data was developed by Iasky (1990a).

An appropriate function for use in the depth conversion of time contours is one that can provide a reasonable fit to the time-depth points obtained from well-velocity surveys, and also produce an acceptable estimate of depth to basement.

The linear and exponential curves produced very large deviations from the measured points, and their velocity functions were disregarded. The second-order polynomial gives a very good fit to the points, but the curve becomes inaccurate below the deepest point in the wells. Therefore, the curve cannot be used to extrapolate depths to basement level as it seems to overestimate depths by more than 1 km relative to both the results from the power curve, and previous estimates of basement depths by Cockbain and Lehmann (1971).

The power function provided the best and most reliable fit, and a velocity function was calculated for each well using the power equation employed by Acheson (1981).

$$d = at^b$$

where: a, b = coefficients
d = depth to horizon in metres
t = two-way time to horizon in seconds

The function with the appropriate coefficients is shown in Appendix 8.

Figure 8 shows the well-velocity data points for each of the wells used plotted on the curves calculated from the functions in Appendix 8.

The velocity data were too sparse to draw a meaningful velocity contour map over the study area and the depth conversion consisted of applying well-velocity functions to areas near the well. Where there were wells very close to each other, such as the three Whicher Range wells, an average function was used.

Different velocity functions were applied to different areas. These areas were chosen to correspond to major southerly trending faulted blocks within the basin, and by applying an arbitrary circle of influence in the north–south direction, where there are not any distinguishing breaks in the sedimentary sequence. Figure 9 shows the areal influence of the velocity functions used.

At the junction between areas of influence, where different functions were applied, depth-derived contours have been averaged and smoothed.

Seismic maps

The time and depth structure contour maps are shown in Plates 3–12.

Six major structural features can be identified from the mapping. From west to east, they are the Dunsborough Fault, the Wirring Fault, the Busselton Fault, the Sabina Fault, the Darradup Fault, and the Darling Fault. Figure 10 shows the major faults in a perspective view of the basin at basement level.

The position of the Dunsborough Fault has been interpreted from the BMR regional gravity data, which shows a steep gradient that becomes steeper towards the Leeuwin Complex. There is, however, little change in the gradient along the fault; this indicates little change in the throw.

The Busselton Fault is clearly identifiable on the seismic profile; it has a northerly trend throughout

13843—3

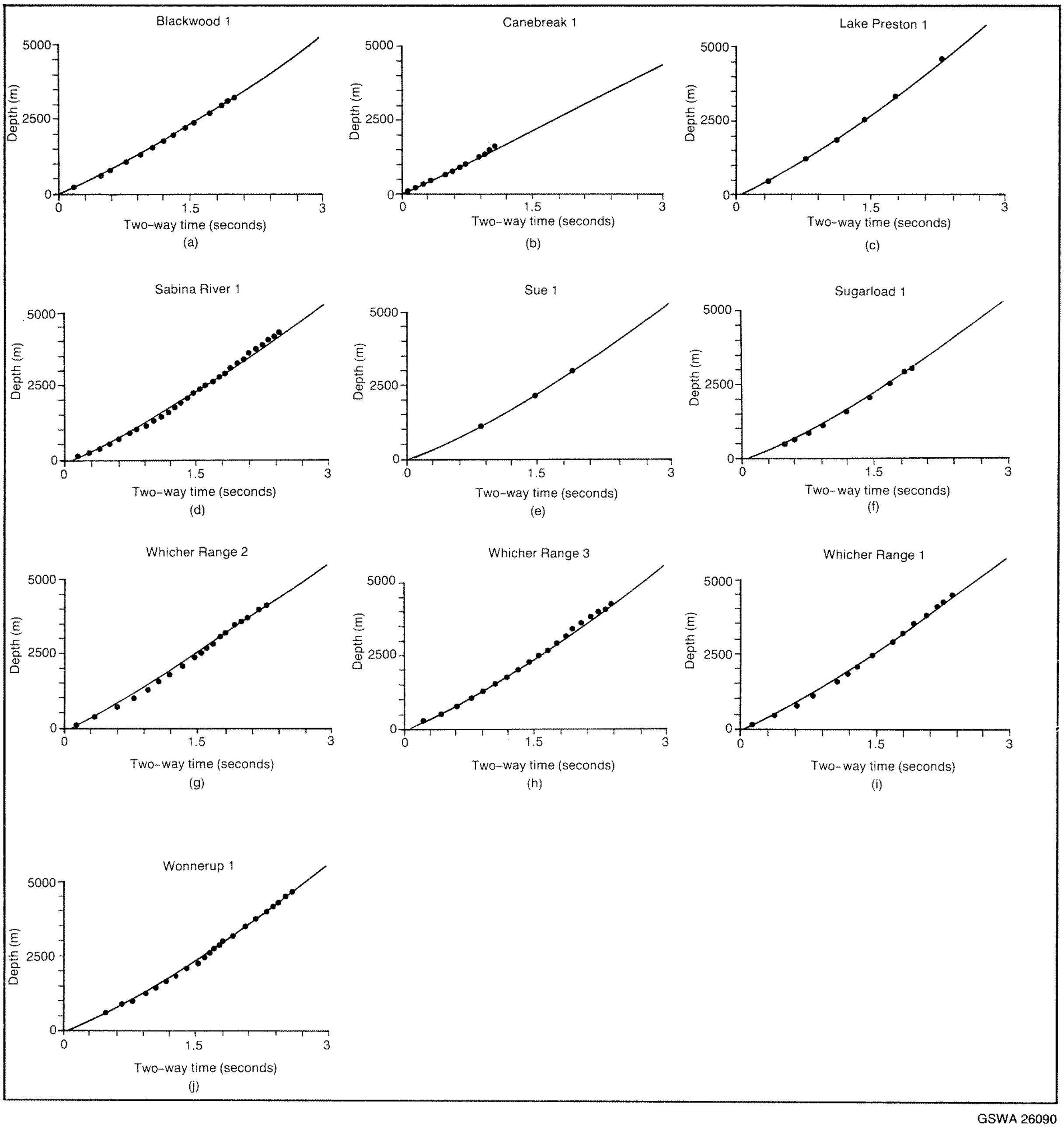

Figure 8. Well-velocity curves for all wells

the mapped area (Plate 12), and cuts the whole sedimentary sequence except for the post-breakup Warnbro Group. The Busselton Fault is the dominant feature in the northern part of the area, but it becomes smaller in the southern offshore area. The size and straightness of this fault indicate that it is an important fracture in the earth's crust, that it might have formed early in the development of the Perth Basin, and that it might have been reactivated during the Phanerozoic tectonic events.

Two samples of crystalline basement (from coal bores CRCH1 and DDH2 on the northern Vasse Shelf) were dated at approximately 2.0 Ga (W. G. Libby, pers. comm., 1989) using Sm–Nd model-age analysis from Fletcher et al. (1985). This dating is in accord with the dating of basement rock from Sue 1, but is quite different from the dating of 0.65 Ga (Fletcher et al., 1985) in the Leeuwin Complex. W. G. Libby (pers. comm., 1989) suggested that this confirms speculation that the Dunsborough Fault, rather than the Busselton Fault, is the boundary between the Perth Basin and the Leeuwin Complex. However, the much larger throw on the Busselton Fault implies that it may, in fact, be the major bounding fault between the Bunbury Trough and the Leeuwin Complex.

The Sabina Fault is intersected on seismic line AA of the Sabina River Seismic Survey, and does not conform to the major northerly trend. Together with the Wirring Fault (Fig. 10), which can be seen in the basement and Permian horizons, it introduces a northwesterly trend in the basin.

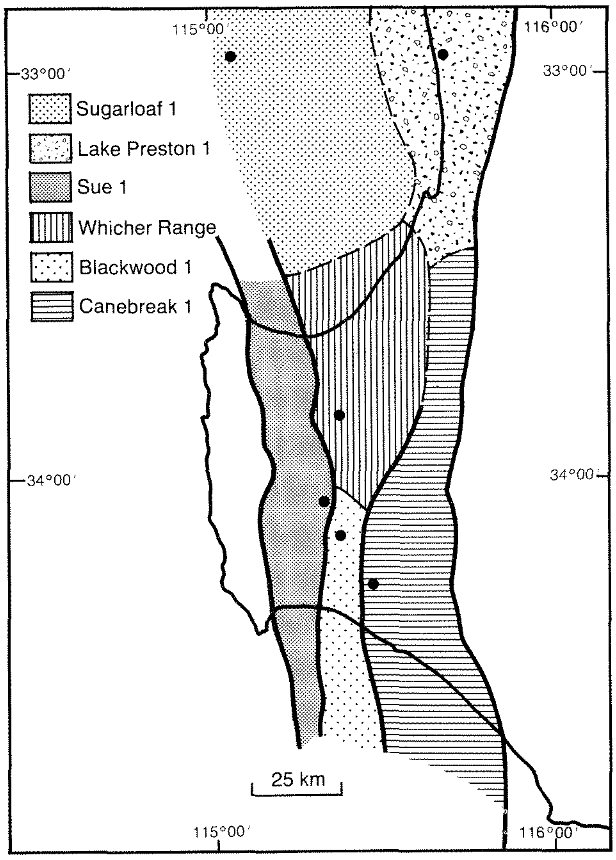

Figure 9. Areal influence of velocity functions

The Wirring Fault is intersected on the edges of lines 81-14, 81-15 and 81-18 (Fig. 11). It is not clearly identifiable on the seismic profile, but well data provide a good fix for the central part of the fault. The northern part of the fault follows a northwesterly trend along the Whicher Scarp and joins to the Dunsborough Fault to the north. This contrasts with a previous interpretation by Cockbain and Lehmann (1971) which had the fault oriented north–south and intersecting the coast between Quindalup 2 and 3 water bores. Quindalup 2 intersects the Top Permian at 109 m; but Quindalup 3, to the west of Quindalup 2, intersects the Top Permian at 209 m. Furthermore, the Permian sequence in Quindalup 2 is older than that in Quindalup 3 (Probert, 1968); this implies that the Permian sequence of Quindalup 2 is relatively higher than Quindalup 3, and that the younger Permian sediments in Quindalup 2 have been eroded. If there were a fault between the two bores, the west block, not the east, as is the case with the Wirring Fault, would be downthrown (Plate11). This suggests that the fault does not strike between the two bores as suggested by Cockbain and Lehmann (1971).

The Darradup Fault is easily identifiable in the southern offshore seismic data (Fig. 12) as a low-dipping fault with a large throw (approximately 1 second). To the north, the throw diminishes, the fault loses character, and it becomes debatable whether it continues any further north than 33°50'S latitude. This fault cuts through the whole sedimentary sequence up to the breakup unconformity (Plates 5–12).

The Darling Fault can only be seen at the edge of the most eastern seismic lines. It has a throw of more than 11 km in the northern Bunbury Trough (Plate 11), but this diminishes to 3.5 km in the southern offshore area.

An important feature of the Darling Fault is its bowing to the west between 33°S and 34°30'S in the Bunbury Trough. Geological mapping of the Perth Basin (Playford et. al, 1976) shows that the fault has slight kinks throughout its length; but one of its most notable features is the distinct curvature at the southern extremity near the coast (Plate 11).

Another important feature in the mapping is the structurally high block between the Busselton Fault and the Darradup Fault in the southern portion of the Bunbury Trough (Fig. 10). Blackwood 1 was drilled in this high basement area, which shows a reduced thickness of sediments.

The predominant structural trend in the Bunbury Trough and Vasse Shelf is northerly, but there is a slight scattering of fault trends on either side of the main northerly trend (Fig. 13). This trend continues unchanged up to latitude 31°S, where the main northerly trend appears to change to north-northwesterly. In a fault-azimuth analysis, Middleton (1990) has shown that the spread of directions of faulting in the Perth Basin is restricted to a narrow envelope of azimuths, commonly less than 50°. This azimuth spread is consistent with the effect of wrench tectonics as seen in other parts of the world, such as the Gulf of Suez, the Los Angeles Basin, and the San Andreas Fault system; therefore, the Perth Basin does not appear to have been affected by a simple orthogonal extensional faulting regime.

The contours of the horizon maps in Plates 5–12 show undulating topography. Some of the difference between horizons may be due to differential compaction caused by overlying sediments. The basement map shows a notably undulate topography, but this may be the result of lateral velocity variations. The increasing magnitude of undulation with depth is probably a function of the increased uncertainty in velocity.

Faulting in the area appears to be predominantly normal, although a strike-slip component is likely. In the Bunbury Trough, the pre-breakup sediments are undulating and tilt towards the east. However, the Vasse Shelf is not predominantly tilted in any direction (Fig. 10). The thickness of sediments in the Bunbury Trough increases towards the north, where the travel time is approximately two seconds more. This amounts to an approximate regional dip of 3° over a distance of 200 km.

Discussion

The mapping shows that the major structural trends in the basin are oriented in a northerly direction with very little deviation. According to Middleton (1990), the small deviation from the predominant northerly trend implies a

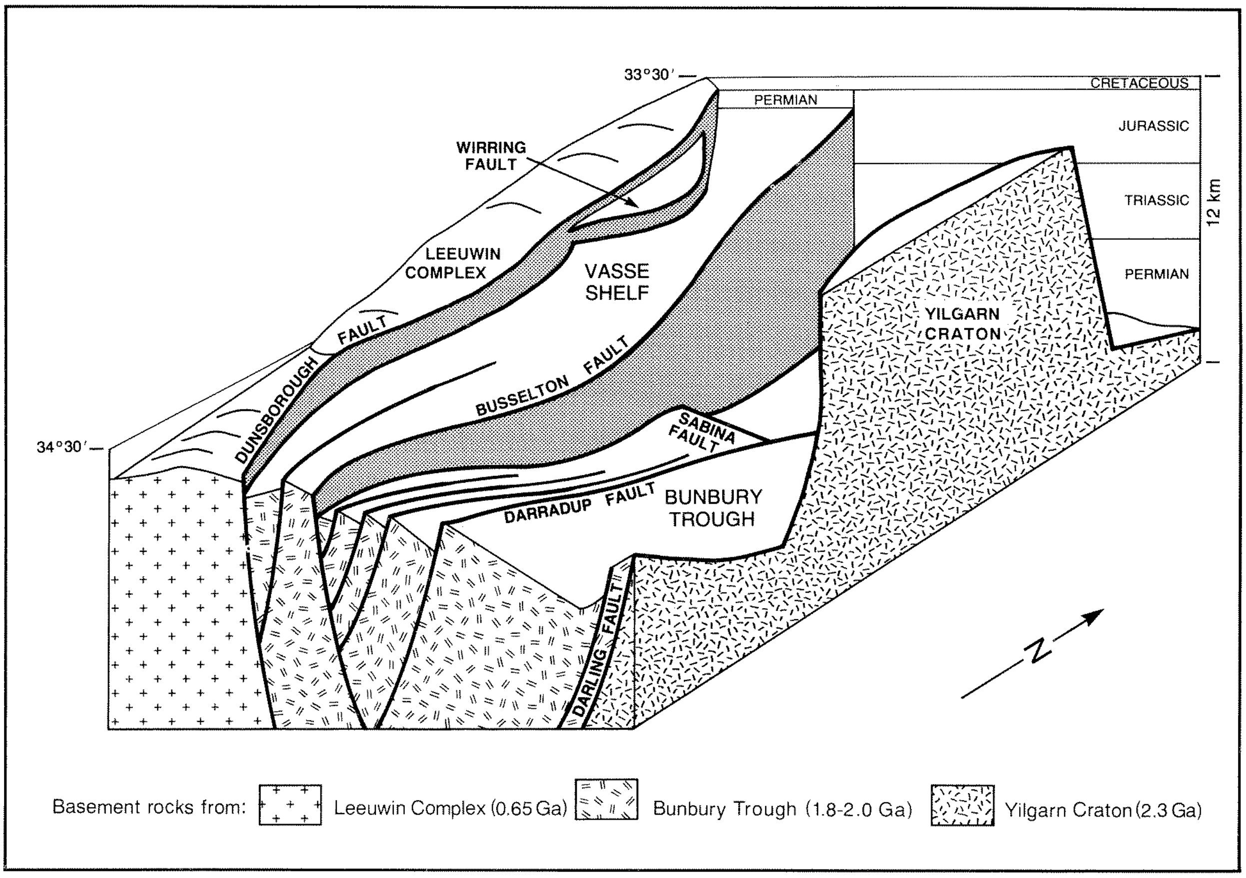

Figure 10. Diagrammatic perspective view of basin at basement level

low-drag, strike-slip movement in the basin. Further physiographic evidence of strike-slip motion is the strong linearity of the Darling and the Busselton Faults (Sylvester, 1988) — in particular the Darling Fault, a feature that extends more than 1000 km in a northerly direction.

The Darling Fault is a deep, crustal fracture that was established in the Precambrian, when it underwent strike-slip movement (Blight et al., 1981). It continued to play an important role during the Phanerozoic: it was re-activated during the Silurian, Permian, Jurassic, and Cretaceous; and most of the motion was restricted to existing zones of crustal weakness. Therefore, the strike-slip imprint of earlier times influenced the tectonism of later events.

The Darling, Dunsborough, and Busselton Faults, have undergone several periods of activation, although the faulting now appears to be predominantly extensional. The strike-slip component in the basin can be diagnosed from the strong, northerly, linear trend of the major faults, and the associated subordinate northwesterly trends.

Biotite dating, using Rb–Sr ratio analysis, conducted by Libby and de Laeter (1979) over the southwestern Yilgarn Craton, suggests that at 400–500 Ma (de Laeter and Libby, in press), a triangular zone east of the Darling Fault from Perth to Albany was uplifted by 5 to 10 km. This uplift would have produced a sizable influx of Ordovician to Silurian clastic sediments. The nearest package of sediments of that age is the Tumblagooda Sandstone in the southern Carnarvon Basin (Hocking, 1991). Libby and Hocking (pers. comm., 1990) suggest that the offset of the Silurian sediments could be explained by invoking a right-lateral strike-slip movement along the Darling Fault at that time. However there is the possibility that the 400–500 Ma rocks on the southwestern Yilgarn Craton are a result of superposition by thrusting, rather than an indication of basement uplift (Pidgeon, 1989).

There is no direct evidence of Silurian tectonism because Silurian sediments are absent in the southern Perth Basin. However, the presence of more than 10 km of Permian and younger sediments suggests considerable tectonism after the Permian deposition. The Darling Fault is a normal fault, and its seismic profile shows a dip of approximately 70°. The oldest sediments in the basin are Permian; this indicates that the fault must have been active after the Permian, and that it probably underwent more than one period of activation.

The first post-Permian activity is believed to have occurred at the end of the Permian deposition; it may have been responsible for the rise of the Harvey Ridge and the deposition of the Sabina Sandstone. Evidence for this stage of tectonism is based on vitrinite-reflectance modelling, which will be discussed below. The Harvey

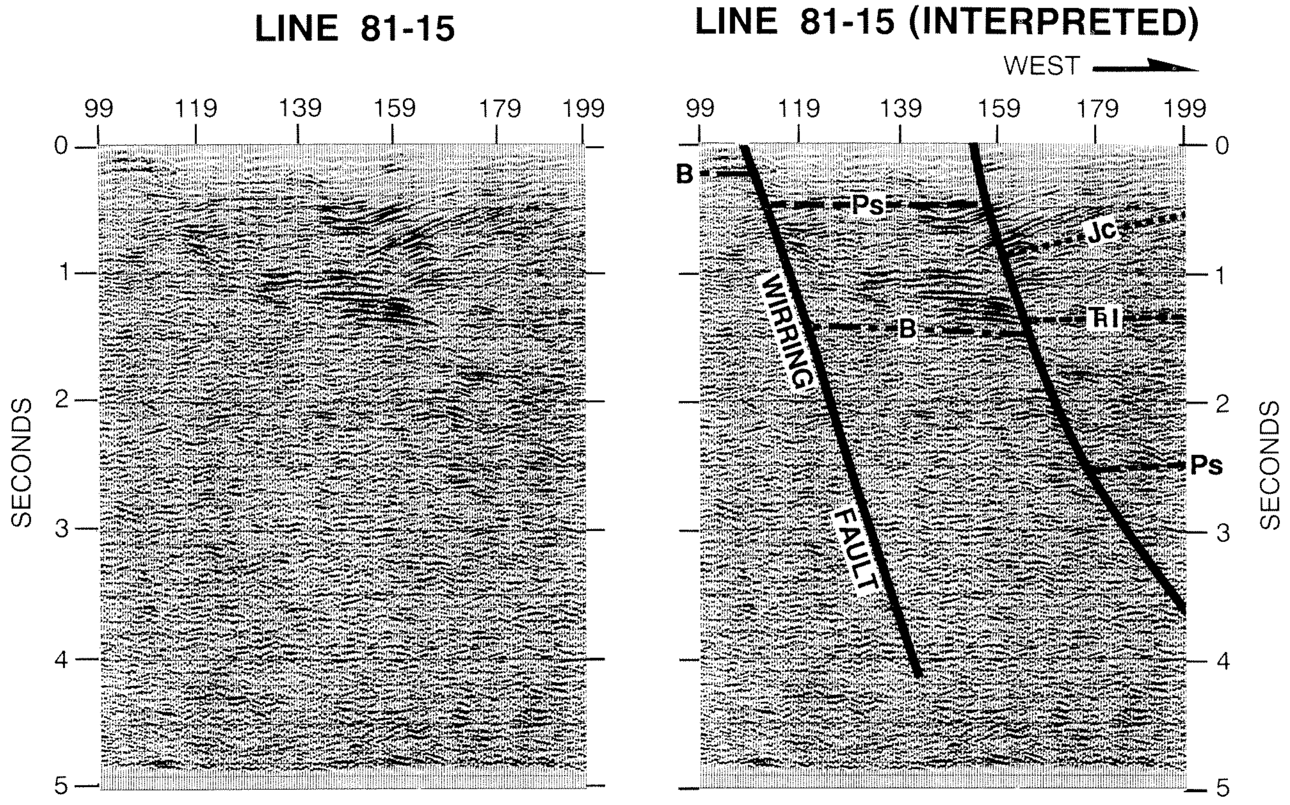

Figure 11. Seismic section 81-15 showing Wirring Fault

Ridge is oriented in a northwesterly direction; and a strain ellipsoid (Fig. 14) shows that folding in this direction may have been caused by right-lateral strike-slip motion on the Darling Fault. Lowry (1976), while trying to correlate coal seams across the Stockton Ridge in the Collie Basin, recognized Late Permian tectonism. He suggested that the absence of correlation between the two sides of the ridge might be the result of faulting at that time.

The strain ellipsoid (Fig. 14) indicates that the Sabina Fault in the Bunbury Trough is a typical fracture associated with left-lateral strike-slip faulting (Le Blanc-Smith, 1989; Middleton, 1990). If the principal fracture in the stress ellipsoid is aligned with the major north-trending faults in the basin, then the orientation of the Sabina Fault is consistent with the northwesterly trending normal faults expected from the stress ellipsoid.

Further evidence of strike-slip tectonics may be found on the Vasse Shelf, where synthetic faults are seen to diverge from the Dunsborough Fault. The Wirring Fault is an example of synthetic normal faulting, as is the fault immediately west of the Alexandra Bridge Fault (Plate 11). These faults may be interpreted as shears, or as extensional and contractional duplexes from the principal motion in a left-lateral-moving strike-slip Dunsborough Fault (Sylvester, 1988).

A good example of the effect of such motion was described by Roberts et al. (1990) when discussing the transtensional regime in the inner Moray Firth, northeastern Scotland. Figure 15 shows an example of oblique transcurrent movement in a left-lateral sense. It is important to note the contractional duplex — which is associated with a higher basement seen in the seismic mapping — in the centre. Also, the northwesterly turn to the north, and the southeasterly turn to the south seem to fit the fault pattern mapped in association to the Dunsborough fault. It is difficult to put a date to this tectonism; however, the strain ellipsoid shows that the direction of faulting is inconsistent with the forces in place during the Late Permian event or at breakup. Middleton (1984a) and Etheridge et al. (1989) suggest a left-lateral strike-slip motion along the southern margin during the Jurassic rifting between Australia and Antarctica. It is probable that the tectonism along the southern margin influenced, and was contemporaneous with, the strike-slip motion along the Dunsborough Fault.

The only distinct unconformity seen on the seismic sections is at the base of the Warnbro Group; this unconformity coincides with the breakup between Australia and India. This phase of tectonism is typically extensional, although it has a strike-slip component along the transform faults which offset rifting centres at the continental margins. The largest of these transform faults is the Wallaby Fault; but magnetic stripes show that there are at least four others (Middleton, 1985; Marshall et al., 1989) which, if extended southeast, would cut through the

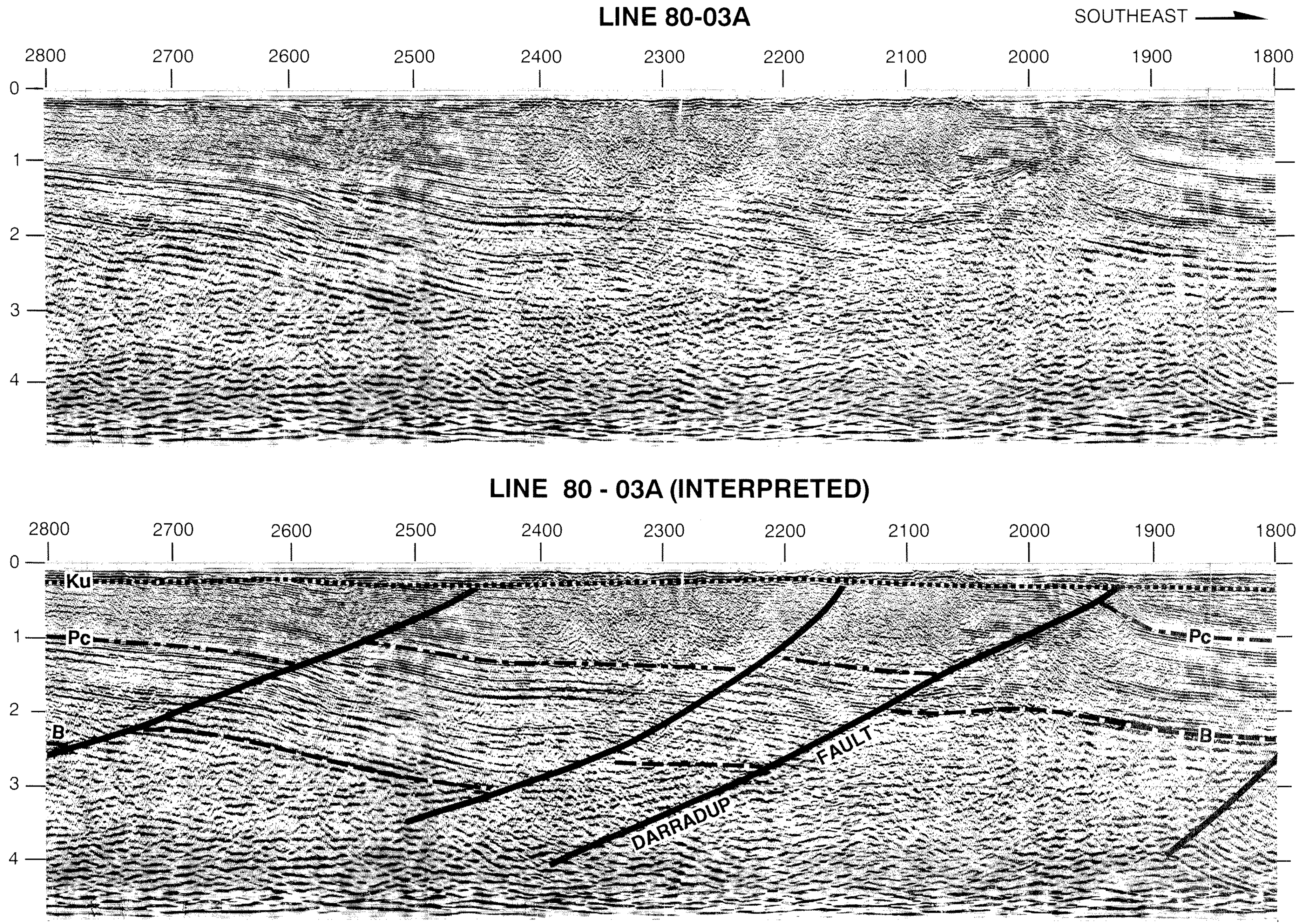

Figure 12. Seismic section 80-03A showing Darradup Fault

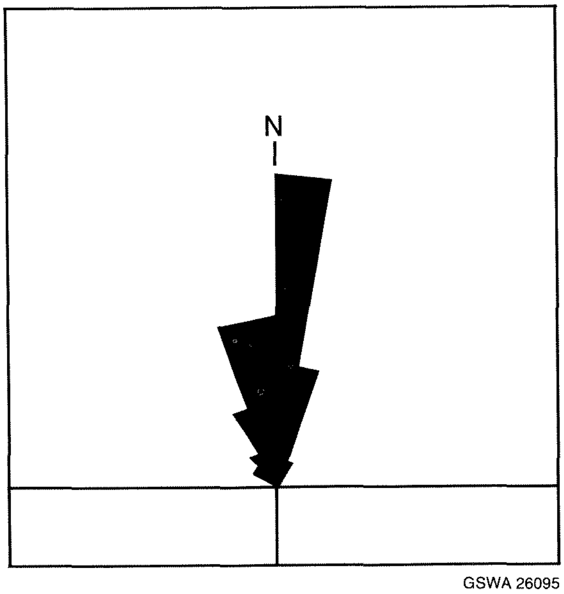

Figure 13. Rose diagram of fault trends

southern Perth Basin and across the southwestern part of the Yilgarn Craton. The Darling Fault has various kinks along its length, and these seem to line up with the transform faults (Middleton, 1985). Northwesterly trending lineaments on the Yilgarn Craton also line up with the Cretaceous transform faults; the northwesterly trending Boyup Brook, Tenterden, and other faults in the southwest, offset rocks in the Albany–Fraser Orogen, and indicate a right-lateral strike-slip motion along this trend (Myers and Hocking, 1988).

The Permian coal strata of the Perth Basin correlate with the Collie Coal Measures. There is evidence to show that the Permian sequence accumulated as an areally extensive platform deposit and that the faulting in Collie Basin grabens is post-depositional. The Permian strata in the basin are faulted, and those faults are truncated by a Cretaceous unconformity (Backhouse and Wilson, 1989). Mapping by Cockbain and Lehmann (1971) indicates that the bounding faults of the Collie Basin are oriented parallel to the northwest transform trend; other faults in the basin also match the transform trend. Thus, it appears that Early Cretaceous tectonism extended into the southwest Yilgarn Craton and produced the uplift, tilting, and erosion, of the sediments in the Collie Basin.

Interestingly, two larger features of the Darling Fault in the southern Perth Basin are a broad westerly bowing of the fault, and the large curvature near Point D'Entrecasteaux on the southern coast. These features may have resulted from pre-Permian tectonism, because the apparent motion of the fault at these points does not conform to Late Permian, Mid Jurassic, or Early Cretaceous events. If this curvature existed at the time, the right-lateral movement of the Darling Fault in the Late Permian would have produced an uplift. Gravity modelling supports this hypothesis, because modelling on the gravity traverse at latitude 34°36'S (Fig. 23) shows uplift in the second crustal layer, immediately east of the Darling Fault.

The faults in the basin, both onshore and offshore, dip at low angles (between 45° and 60°), and are indicative of a typical extensional rifting environment (Lowell, 1985). The structural evidence is supported by the geological evidence: post-breakup paralic and marine sediments are draped over fault blocks of continental sediments that were rotated before the breakup. This kind of sedimentation is consistent with marine transgression during a rifting and breakup phase in the formation of the basin. Clearly, the Mesozoic sequence in the southern Perth Basin has been dominated by an extensional regime of faulting in the later stages of evolution in the basin.

Interpretation of potential field data

Five gravity traverses across the basin were modelled to obtain information on crustal thickness, and to gain a better understanding of the major tectonic features in the deeper part of the geological section. Furthermore, the modelling is intended to provide information on density variations within the crust, and to investigate whether movement on the Darling Fault is normal, reverse, or strike-slip (Lambeck, 1987).

The seismic mapping provides three-dimensional information on both the sedimentary sequence and depth to crystalline basement in the southern Perth Basin. In contrast, the gravity modelling carried out in this study is only a two-dimensional approach, and it cannot provide the detailed information of the seismic maps. However, the seismic data are shallow and do not enable the interpretation of deeper structure, so gravity must be used to determine the density variations to the Moho.

A previous investigation of this kind was undertaken by Felcman and Lane (1963), who modelled three traverses to define broad areas of interest for petroleum exploration. This work — using a density contrast of 0.4 g/cm^3 between the sediments (2.35 g/cm^3) and the basement rocks (2.75 g/cm^3) — identified the main fault blocks and the regional dip of the sediments by modelling the residual gravity.

Gravity data

Data were extracted from the BMR 1:250 000-scale gravity and magnetic maps. Offshore data were obtained from free-air gravity profiles drawn from the BMR Marine surveys 1970–1973.

The BMR applied the free-air correction to the offshore data to reduce the shipboard gravity readings to sea level datum. Onshore, the height above datum is as much as 100 m, and the free-air correction does not allow for the layer of crust above datum. A correction, in the form of the Bouguer correction, for this layer of crust has been applied.

The correction applied by the BMR on their contour maps was calculated by using a rock density of 2.2 g/cm^3

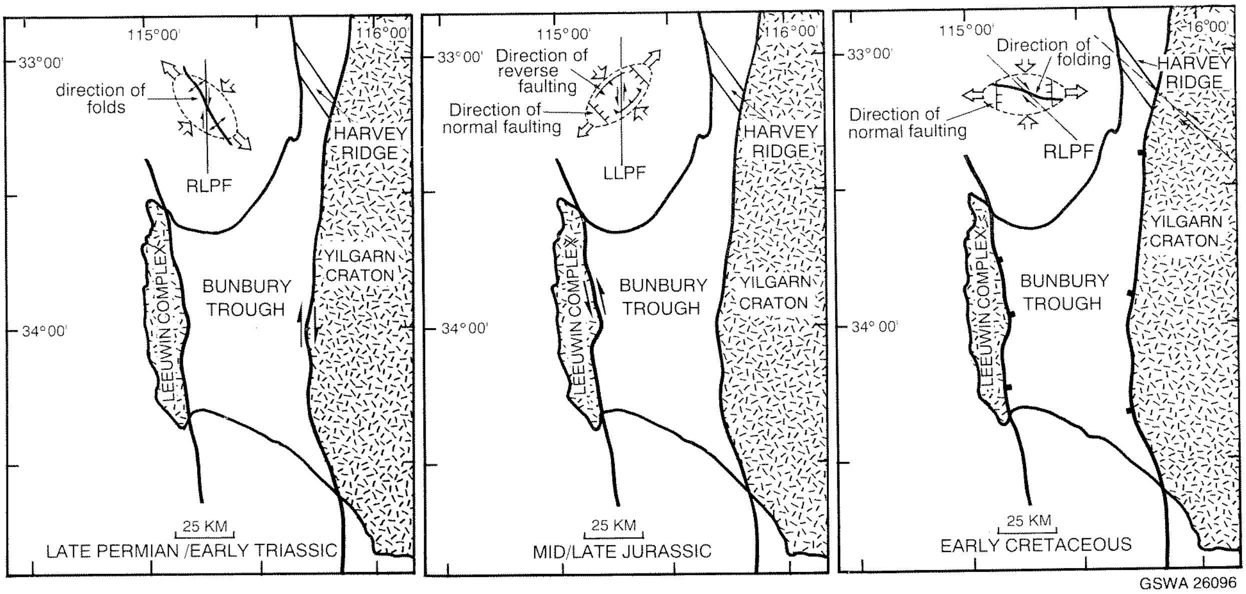

Figure 14. Diagram showing the three major tectonic events in the southern Perth Basin

between the station and the datum plane. It is reasonable to assume a density of 2.2 g/cm^3 for the top 100 m of unconsolidated sand and clay in the southern Perth Basin. This correction is derived by assuming a slab of infinite horizontal extent between the datum and the station; it is, however, an incomplete Bouguer correction because topography has not been corrected.

The absolute gravity values used to compile this series of maps are based on the BMR pendulum stations at Perth, Albany, Watheroo, and Geraldton; the nominal station spacing for the grid is 10 km. Because of the relatively large station spacing, the contours do not show short wavelength anomalies.

Gravity data analysis

Gravity contours (Fig. 16) show three areas of rapidly changing gradient; these coincide with the Darling, Busselton, and Dunsborough Faults. The basin has a strong negative anomaly of 1000 µm/sec^2 (100 mgal). The Harvey Ridge, to the north of the Bunbury Trough (Fig. 1), displays a positive 250 µm/sec^2 (25 mgal) residual anomaly relative to the deepest part of the basin (Fig. 16).

The contours on the Vasse Shelf (Fig. 1) suggest that the largest throw on the northern portion of the Dunsborough Fault is transferred to the northern portion of the Busselton Fault. Plate 11 shows that, in the southern portion of the Vasse Shelf, the sediment is up to 2 km thick; whereas, in the northern Vasse Shelf, a high block of basement that is covered by up to 500 m of sediment is bounded by the Dunsborough Fault and the Wirring Fault. To the east of the Wirring Fault, the sediment is up to 2 km thick, as in the southern Vasse Shelf. The Wirring and Busselton Faults are about 5 km apart, but the gravity contours do not resolve the gradient — which appears to be continuous — of either fault. From the gravity contours, the Wirring Fault cannot be readily seen, and the Busselton Fault appears to include the throw of both faults. However, seismic data show that the throw is transferred to the Wirring Fault.

The throw of the Busselton Fault diminishes from 7 km in the northern Bunbury Trough, to 2 km in the south (Plate 11); this has the effect of reducing the steepness in the gravity contour map.

The steep gradient along the southern portion of the Dunsborough Fault near Augusta signifies that the denser gneiss of the Leeuwin Complex continues to be adjacent to the less dense sedimentary rocks. Further south, seismic mapping (Plate 11) shows that the throw of the fault diminishes to less than 100 m, and it is probable that, offshore, the Leeuwin Complex plunges beneath a sedimentary cover as much as 1 km thick.

To the north, the Dunsborough Fault is probably associated with a series of faults — one of which is the Wirring Fault (Plate 11) — which are synthetic to it, and step down onto the Vasse Shelf. These faults have the effect of decreasing the steepness of the gradient on the gravity contour map.

The Bouguer contours represent accurately the major tectonic features mapped on the seismic data. In the Bunbury Trough, the gravity map shows a difference of 400 µm/sec^2 (40 mgal) between the most southwestern portion and the deepest northwestern portion. This corresponds to an increase in sedimentary thickness of 6.5 km (Plate 11). Both sets of data confirm the thickening sedimentary sequence to the east towards the Darling Fault. The deepest part of the basin contains 11 km of sediments and corresponds with the largest negative anomaly of 800 µm/sec^2 (80 mgal).

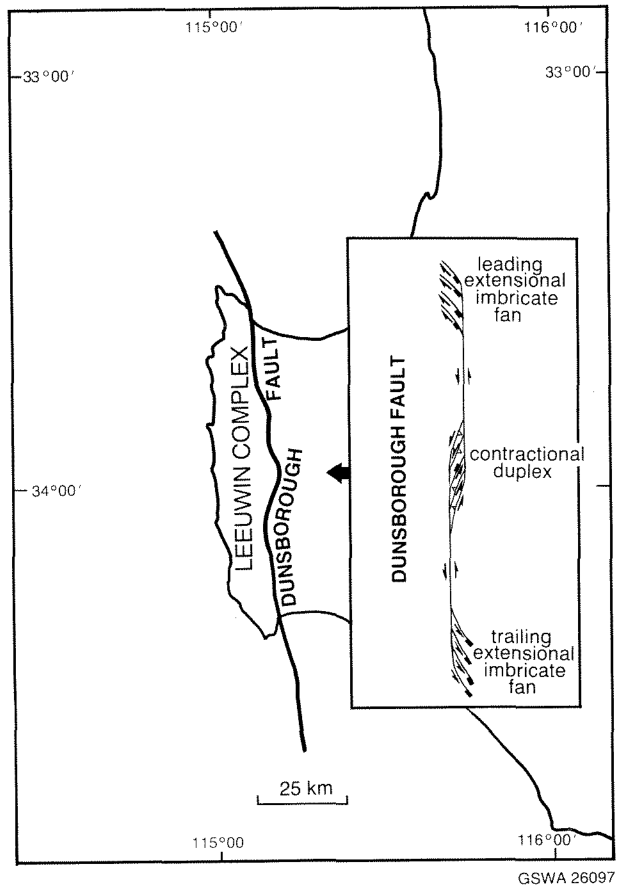

Figure 15. Example of left-lateral strike-slip movement as applied to the Dunsborough Fault

Magnetic data

A total magnetic intensity contour map was used in this study (Fig. 17).

This map is a compilation of the airborne magnetometer survey of the Perth Basin carried out in 1957 by the BMR (Quilty, 1963) and offshore data from the Leeuwin Aeromagnetic Survey carried out by WAPET in 1969. The survey was flown at an altitude of 457 m above sea level along lines spaced 1609 m apart and total field was measured with a proton magnetometer. Flight lines were flown east–west. A continuous-strip film was used for flight-path and station recovery.

The ages of the Yilgarn Craton, the basement of the basin, and of the Leeuwin Complex, all differ from one another (Fletcher et al, 1985); consequently, the directions of their remanent magnetization may be different. The unknown magnitude and angle of remanent magnetization, together with interference from near-surface basalt flows, makes magnetic modelling in the basin difficult.

Magnetic maps show a strong correlation to gravity maps in sedimentary basins because the deep basement has the greatest influence on both sets of data. Magnetic data are bound to show higher frequency variations because susceptibility is more variable than density values between different crystalline rocks in the basement. Both magnetic and gravity data can provide an estimate of depth to basement. However, because of the complexity of the crust, it is difficult to interpret deeper features, such as depth to Moho, from magnetic data.

Magnetic data analysis

The Darling, Busselton, and Dunsborough Faults, are the three major recognizable features of the magnetic intensity map. They have different characters, but all have steep gradients. The positions of these magnetic features agree with the positions of the same features on the Bouguer gravity map. The magnetic signature of the Busselton Fault is slightly to the east of its signature as found on the gravity map, and is more consistent with the position of the fault as mapped from seismic data (Figs 16 and 17).

Both the Dunsborough and the Darling Faults are distinguishable features in the total magnetic intensity contour map. The basement blocks (Yilgarn and Leeuwin) display a more rapid magnetic variation and a higher overall total magnetic intensity. The basin displays a 500–600 nT negative anomaly with respect to the blocks. Because the contours in the basin do not show the high-frequency variation that is seen on the blocks, the contours are considerably smoother.

The Busselton Fault is identified as having a constant broad gradient from the Leeuwin Complex to the Bunbury Trough with a total magnetic intensity difference of about 300 nT throughout its length. The position of the fault on the magnetic map correlates strongly with the seismically mapped position of the fault (Fig. 17). The gradient steepens slightly from north to south; the greatest magnetic response, 1800 nT (Fig. 16), is in the Bunbury Trough near the Sabina Fault and immediately east of the Darradup Fault. The steeper gradient in the south may be due to the shallower basement south of the Sabina Fault.

The southern portion of the Vasse Shelf displays an area of steep gradient caused by the Alexandra Bridge Fault. The magnetic signature in this area of the Vasse Shelf differs from that in the northern portion, and it probably marks the presence of a cross-cutting discontinuity in the basement rocks just north of Sue 1.

The near-surface basalt was mapped by Felcman and Lane in 1963 from magnetic data. Their interpretation is broadly supported by the BMR's more recent image-processed data, which seem to outline the basalt flows clearly. The main differences between the BMR image and Felcman and Lane's interpretation are that, in the former, the flow channels are thinner and are not restricted to the middle of the Bunbury Trough. Flows appear to extend east of the Darling Fault between latitudes 33°45' and 34°15'; and the BMR image shows that the basalt flows extend north of latitude 33°00'.

Gravity modelling

The gravity anomaly was calculated by a forward modelling process, whereby the gravity effect of an assumed body or number of bodies is calculated, and the observed data are compared to the calculated values over a number of station points in a traverse. The shape of the model body and the densities are adjusted and the

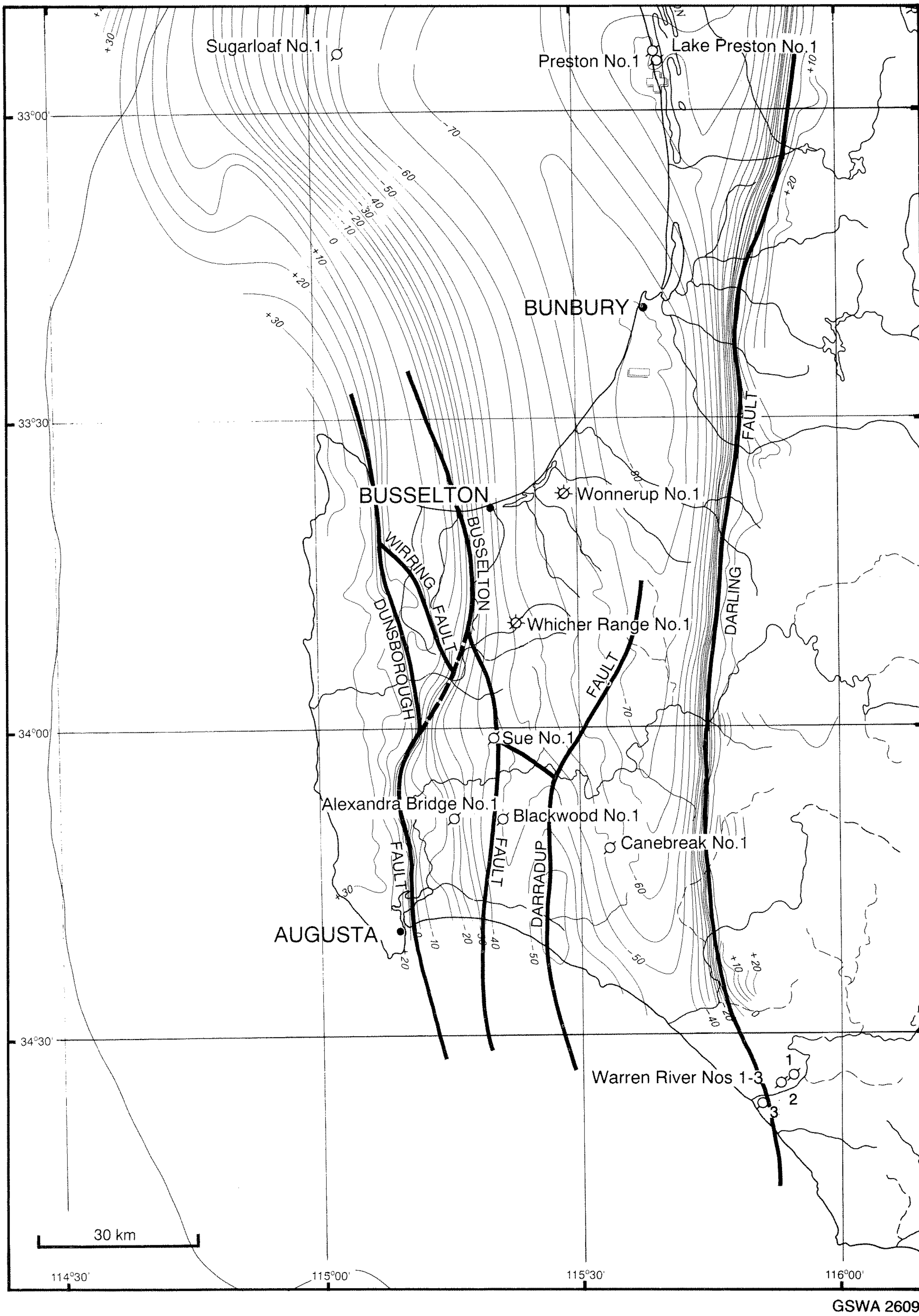

Figure 16. Major faults overlaid on the gravity contours

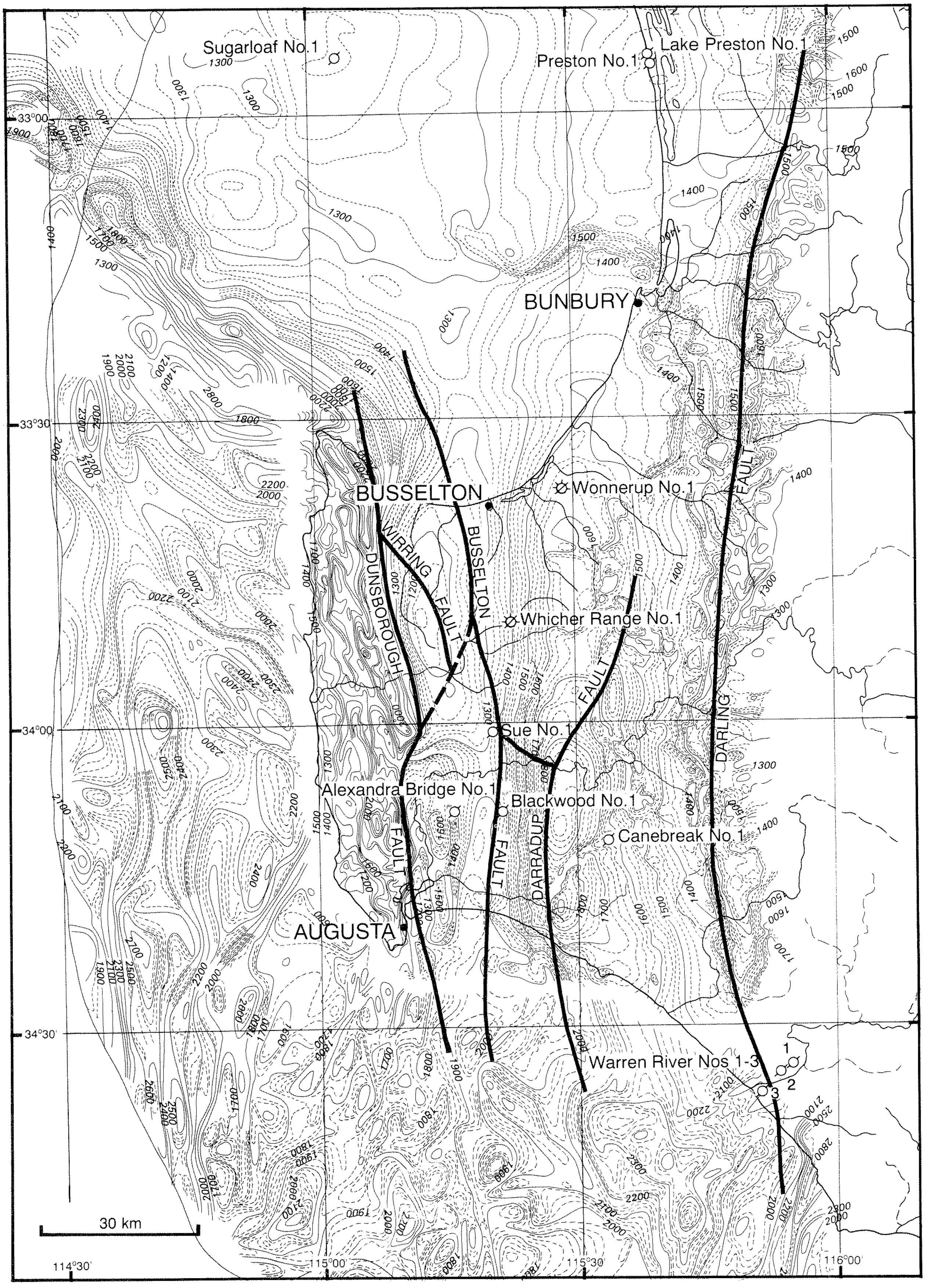

Figure 17. Major faults overlaid on the magnetic contours

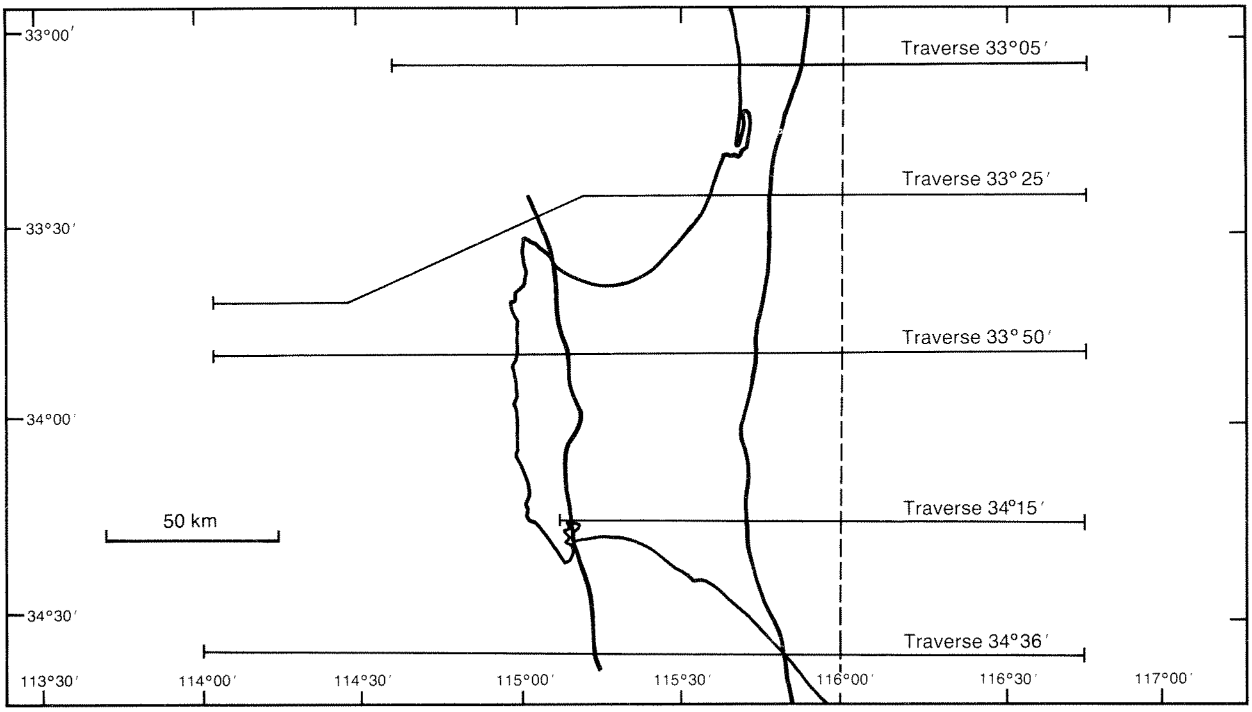

Figure 18. Location diagram of gravity traverses

calculation is repeated until the calculated values match the observed ones.

This type of modelling can only be done efficiently on a computer. A computer listing of the program is given in Iasky (1990b), and the data used for the modelling is in Iasky (1990a).

The densities used in the gravity modelling are listed below.

0 – 2 km = 2.30 g/cm^3
2 – 4 km = 2.50 g/cm^3
4 – 6 km = 2.55 g/cm^3
6 – 8 km = 2.60 g/cm^3
8 – 10 km = 2.65 g/cm^3

Near-surface sedimentary bodies thinner than 2 km have been assigned a density of 2.1–2.2 g/cm^3.

Generally, the log data fits the modelled densities, which have been averaged over the sedimentary section in two-kilometre intervals. There is a density inversion in Wonnerup 1 in the interval 4000–4500 m, in Whicher Range 1 in the interval 4000–4250 m, and in Whicher Range 2 between 4000 and 4100 m. This inversion is restricted to a relatively narrow interval, and is probably only a local feature.

The traverses were oriented east–west, starting at least 50 km east of the Darling Fault and traversing the basin through to the offshore, so that the total length of the traverses is between 200 and 250 km depending on the availability of the data offshore (Fig. 18).

The starting model for each traverse was derived by adopting the sediment thickness mapped from the seismic data (Plate 11). The sedimentary basin was then divided into a number of stratified sequences and the initial densities were estimated by using petroleum exploration well density logs.

There are no data on deep-crustal refraction in the southern Perth Basin. However, Mathur et al. (1977) conducted deep-crustal investigations on the Yilgarn Craton which indicated that the depth to the Moho at the Darling Fault is approximately 40 km and that it rises to approximately 32 km some 600 km to the east.

Seismic refraction from the 1956 atomic explosions at Maralinga indicated a single-layered crust 32 km thick (Bolt, Doyle, and Sutton, 1958). Doyle and Everingham (1964) recomputed the crustal thickness in the eastern part of Western Australia to be 35 km.

The crust thins to an oceanic type to the west and south. Hawkins et al. (1965) indicated shallowing of the base of the oceanic crustal layer towards the continent to a depth of approximately 10.5 km some 120 km south of Point D'Entrecasteaux. Information on oceanic crust is available from refraction studies in the Indian Ocean by Francis and Raitt (1967).

Dooley (1972) has shown that the P velocities increase from east to west in the Yilgarn Craton and that the depth to the mantle is 35 to 40 km.

Empirical velocity–density relationships for crystalline rocks, based on world-wide data, were established by Nafe and Drake (1961), Woollard (1959, 1968), and Nettleton (1976). The crystalline rock densities used in the modelling lie between the model 1 and 2 values determined by Mathur (1974, 1977) in the southwestern Yilgarn Craton.

The crystalline part of the crust was subdivided into three layers, as in the Mathur et al. (1977) model, and the densities used are 2.7, 2.9, and 3.0 g/cm^3. The upper mantle density used is 3.30 g/cm^3. There may be considerable lateral variation of the density in the crystalline rocks; however, this is on a small scale compared with the depth to the rocks, and an average density for each layer was used to represent the gravity anomaly. These densities are similar to Mathur's three layers of 2.78, 2.94 and 3.10 g/cm^3, with an Upper Mantle density of 3.45 g/cm^3. The greatest difference between the two sets of values is the density of the upper mantle.

Application of two-dimensional modelling

The objective of the gravity modelling over the basin was to determine the lateral and vertical variation in thickness and density of the crust. The depth to basement shown in the models was determined from the seismic mapping and provided a good datum for modelling the deeper structures.

To obtain a three-dimensional picture of crustal structure, five traverses were modelled across the basin; their positions are shown in Figure 18. The intersection of longitude 116° 00' with the traverses is assumed to be an arbitrary distance of 500 km along the traverses.

The layers used in the models were defined by different densities and were represented by 'n' sided polygons. The coordinates of each polygon are listed in Iasky (1990a). It is important to note that the resulting models represent a simplified interpretation of the geological structure.

For all models, the sedimentary basin was stratified into layers, each with a constant density that increased with the depth of the layer. This was in accord with the density logs from petroleum exploration wells, which generally display an increase in density with depth. Each density layer was assigned a thickness of 2 km which provided a reasonable representation of the well density logs. The deepest petroleum well is Wonnerup 1 which reached a depth of 4727 m and thereby provided density data for less than half of the sedimentary column in the basin. Density values for the lower part of the sedimentary section were estimated using velocity versus density curves drawn by Gardner et al. (1974). Velocity functions, to be used with the curves, were developed from well velocity survey data and were applied to each density layer.

The crystalline rock underlying the sediments is represented by three layers to the level of the Mohorovicic discontinuity (Moho). This is an approximation of the true density variation which consists of several more layers of increasing density with depth. The models are not very sensitive to the position of boundaries between these layers, but are more sensitive to the overall thickness to the Moho. The assumed density of the mantle at the Moho was kept constant at 3.3 g/cm^3 for all the traverses.

Changes in the thickness of the crust to the extreme west of the models influence strongly the anomaly at the east of the models. The dip of the faults bounding the basin is an important parameter in matching the calculated with the observed Bouguer gravity along the traverse. The impact on the calculated gravity of changing model boundaries, depends on the depth and magnitude of the change. However, even small changes affect, to some extent, the calculated gravity at all stations along the traverse. The difference in calculated gravity values becomes smaller with increasing distance from changes to the model.

The modelling is quite sensitive to the dip of the Darling and Busselton Faults and the depth to the Moho. Deeper changes to the model affect the calculated Bouguer gravity over a broader area of the traverse. Generally, the greater the sedimentary thickness the larger the negative anomaly. Similarly, greater crustal thickness decreases the gravity value for the region.

Traverse 1, at latitude 33° 05' (Fig. 19), shows the presence of the Harvey Ridge and the regional easterly dip of the basement layers. The crust is thickening towards the east in contrast to Mathur's model. The modelling shows that the Darling Fault, with a very steep dip of approximately 75° to the west, is a dominant feature down to the Moho. The depth to the Moho varies from 34 km in the east to 17 km in the west. At the Darling Fault the Moho is 30 km deep, which is substantially less than the Australian continental average of 37 km (Dooley, 1976) and does not agree with the thickness of approximately 40 km reported by Mathur et al. (1977).

Traverse 2, at latitude 33° 25' (Fig. 20), crosses the Darling and Busselton Faults. Both faults cut through the basement and extend into the Moho. The easterly increase in crustal thickness and the effect of the Leeuwin Complex can be observed in this traverse. The depth to the Moho varies from 32 km in the east to 17 km in the west.

Traverse 3, at latitude 33° 50' (Fig. 21), shows the Darling Fault to the east and the Busselton–Dunsborough Fault to the west of the basin. Both sets of faults extend to the Moho. It is difficult to separate the Dunsborough and Busselton Faults, as the gravity gradient is continuous from one to the other. The effect of the Leeuwin Complex is seen in the observed gravity profile as the crystalline basement outcrops. The density layering beneath the Leeuwin Complex remains unaffected by any faulting as the crust thins to the west. The model shows that the depth to the Moho varies from 33 km in the east to 10 km in the west. The density layering east of the Darling Fault is not dipping to the east as in traverses 1 and 2, so that crustal thickness remains constant at approximately 33 km beneath the Yilgarn Craton.

Traverse 4, at latitude 34° 15' (Fig. 22), shows the presence of a denser body (2.65 g/cm^3) near the surface at traverse distance 450 km. This body was introduced into the model to match the observed curve. An alternative model is one with a much shallower basement, although this is not consistent with the seismic mapping. The positive anomaly in the basin is a sizeable feature which extends south and may be due to a large area of

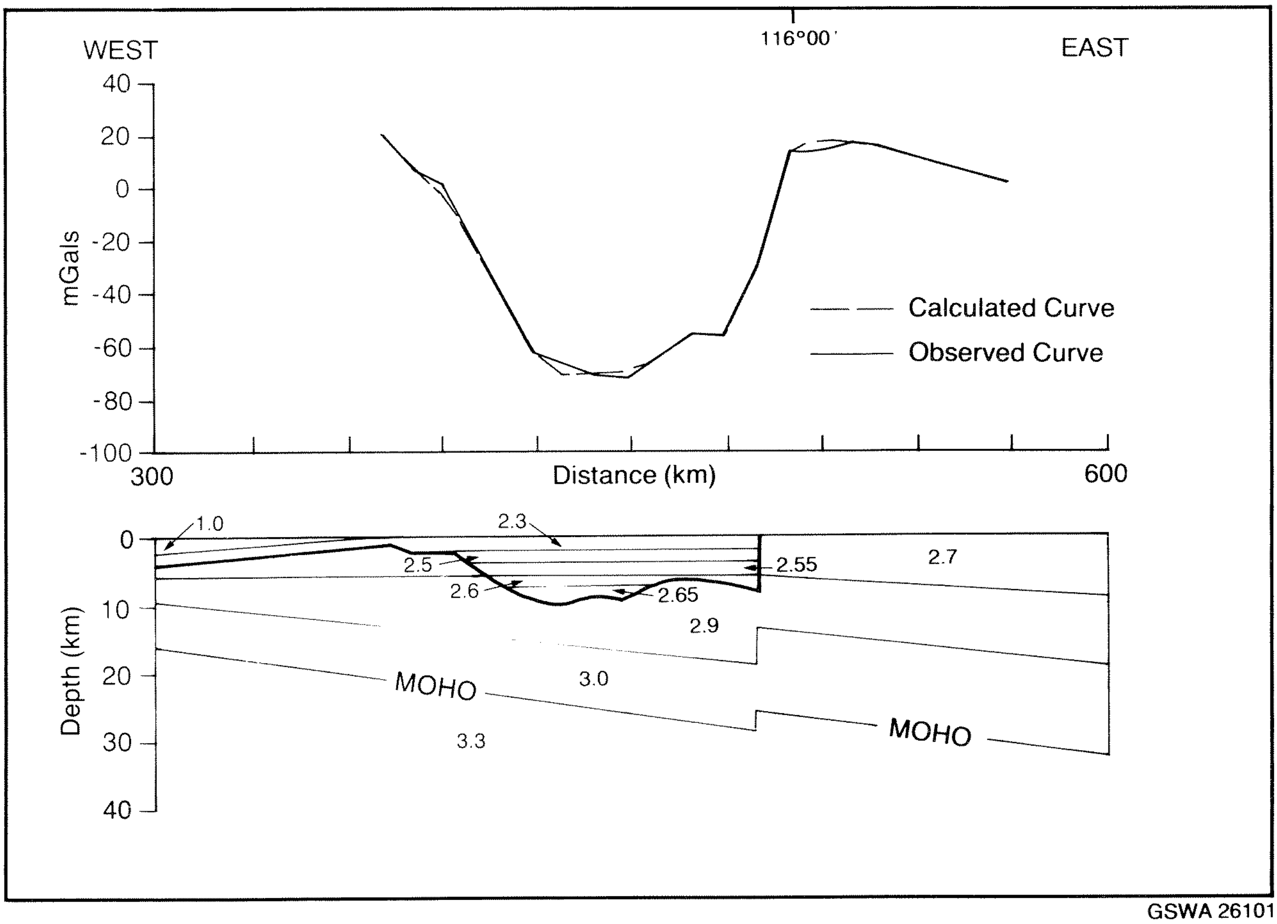

Figure 19. Gravity model for traverse at 33°05'

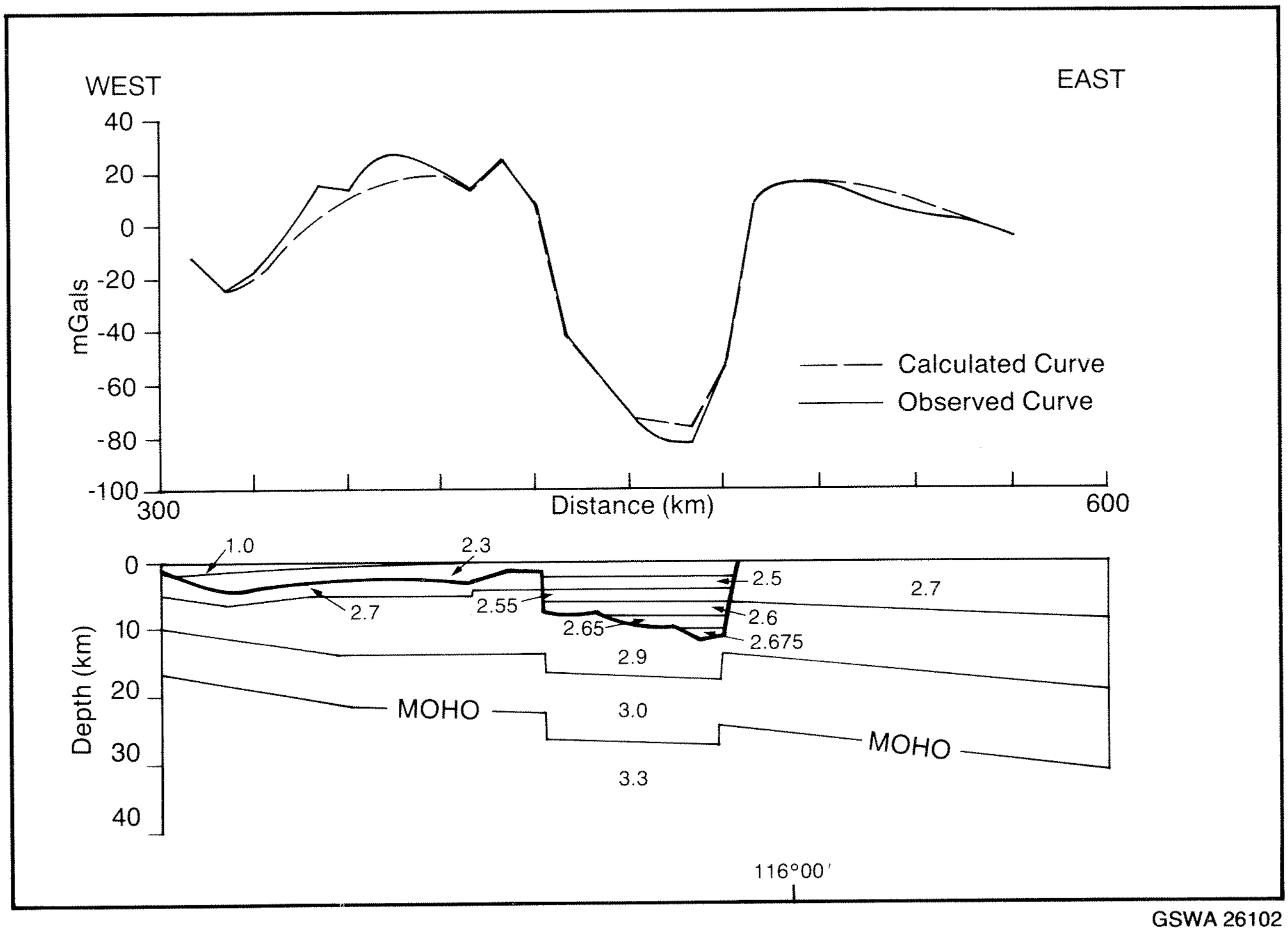

Figure 20. Gravity model for traverse at 33°25'

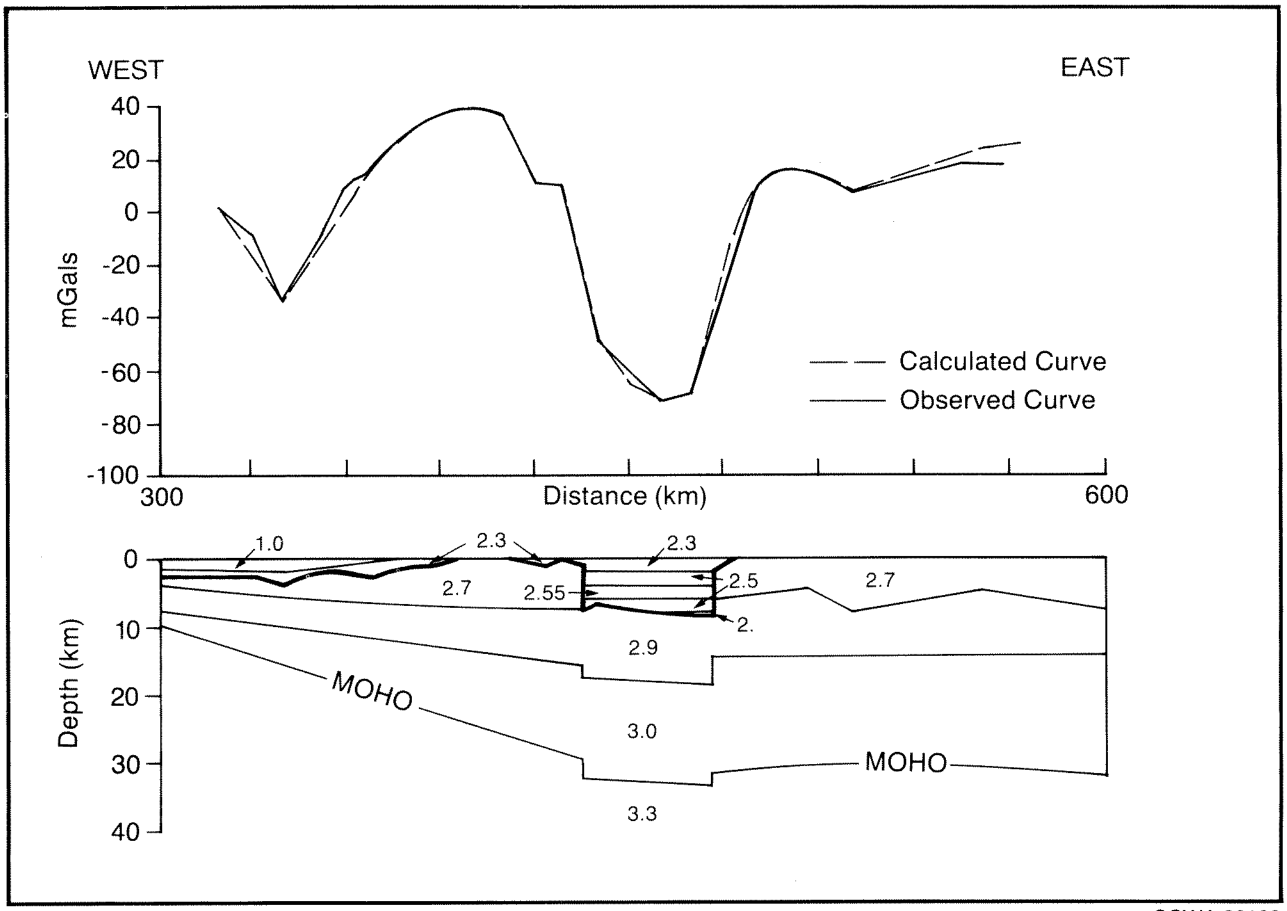

GSWA 26103

Figure 21. Gravity model for traverse at 33°50'

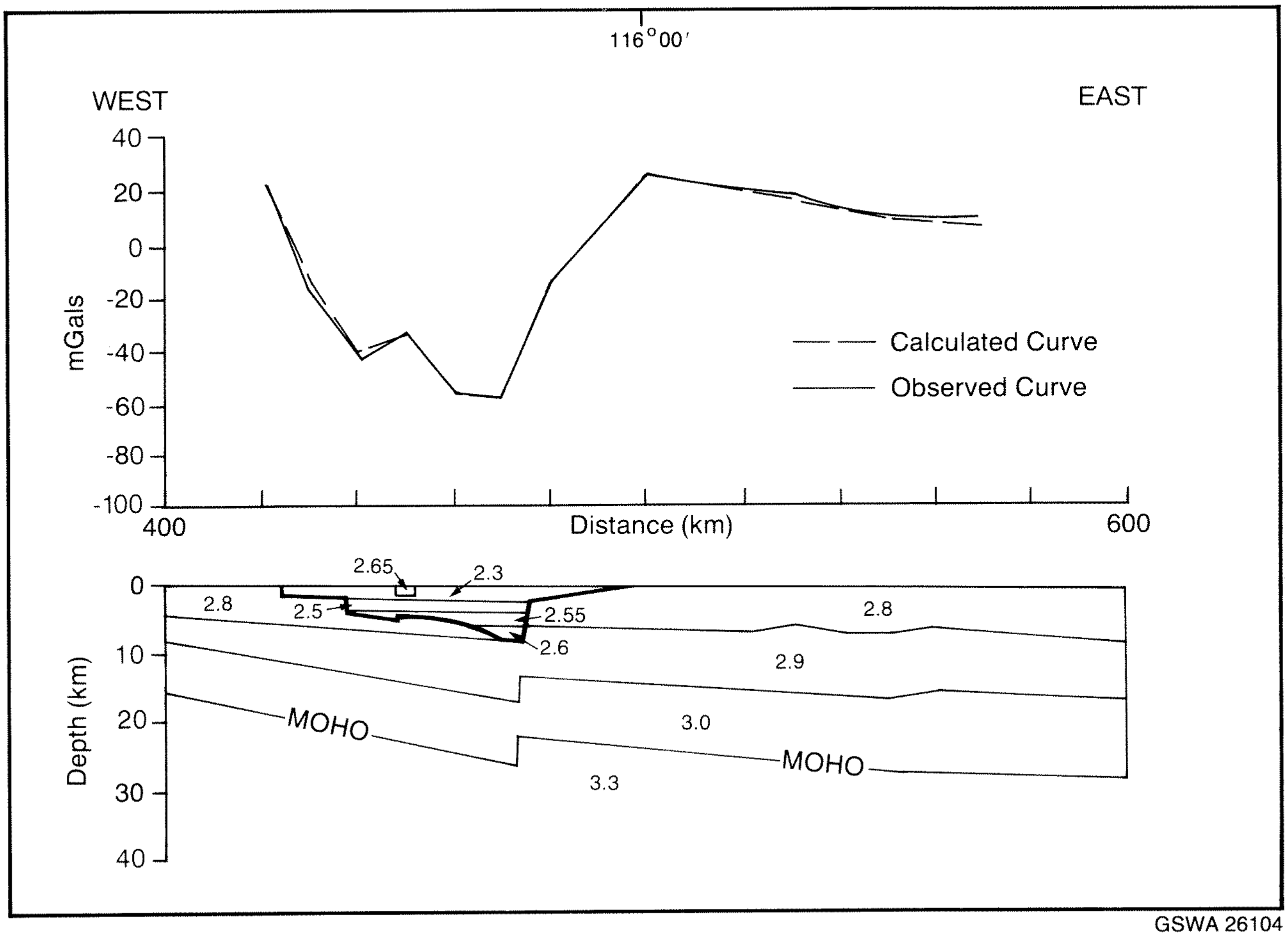

Figure 22. Gravity model for traverse at 34°15'

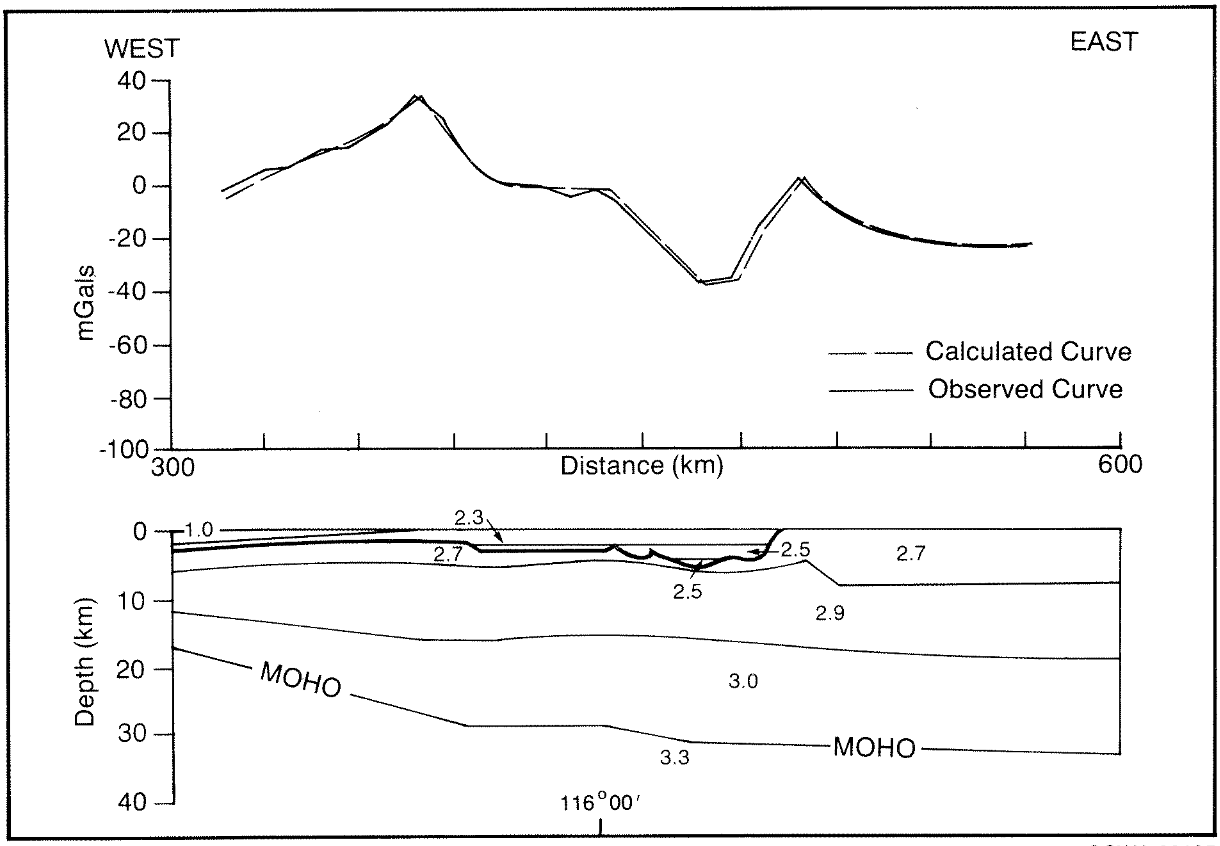

GSWA 26105

Figure 23. Gravity model for traverse at 34°36'

Bunbury Basalt or a large intrusion. A thin near-surface wedge of low-density material was introduced to the east of the Darling Fault to match the decreased slope of the observed curve.

In traverse 4, the Darling Fault is a dominant feature as in the other traverses, and the Busselton Fault becomes insignificant at depth. The Leeuwin Complex continues to be an important feature as it marks the western edge of the gravity anomaly and the basin. The model of traverse 4 shows that the depth to the Moho varies from 30 km in the east to 17 km in the west.

In traverse 5, at latitude 34° 36' (Fig. 23), the effect of the Darling Fault is seen clearly, but the model shows it as a shallow feature that does not extend into the lower crustal layers as in the northern traverses. An interesting feature of this model is the uplift of the first basement layer immediately east of the Darling Fault. This feature may be explained as part of a compressional uplift caused by the right-lateral movement of the Darling Fault along its southern curvature. To the east of the Darling Fault, the model shows basement layering with only a small regional easterly dip. The depth to the Moho varies from 33 km in the east to 17 km in the west.

Discussion

The Darling Fault is a normal fault with a large displacement that is characterized by a steep gravity gradient on the eastern side of the southern Perth Basin. According to modelling, the fault extends to the Moho except on the southernmost traverse. The Busselton Fault is also a major feature that extends through the lower crustal layers in the northern part of the Bunbury Trough.

Models for traverses 1 and 2 indicate a regional easterly dip of the crystalline layers and the Moho east of the Darling Fault. The modelling on all traverses also shows considerable westward thinning of the crust, a feature to be expected in a transition from continental to oceanic crust. The average thickness of the crust according to the models is: 16 km (approximately 170 km west of the Darling Fault); 30 km (below the Darling Fault); and 32 km (approximately 100 km east of the Darling Fault).

The principle of isostasy requires an upwelling in the upper mantle to compensate for the presence of overlying lower density sediments. The models demonstrate a local isostatic imbalance since the crust thickens beneath the basin. This is consistent with Lambeck's (1987) hypothesis of an isostatically imbalanced Perth Basin held in place by compressive stresses acting on the whole continent.

Geohistory analysis

In this text, geohistory analysis is a term used to describe the reconstruction of burial history by progressively backstripping shallower stratigraphic units, allowing for palaeobathymetry, compaction, and erosional episodes. The term also includes the analysis of geothermal history.

Five traverses were modelled for geohistory analysis to understand the structural and depositional history of the Bunbury Trough and Vasse Shelf in the southern Perth Basin (Fig. 43). Three of the traverses cross the basin in an easterly direction; the other two are in a northerly and a northwesterly direction.

Geohistory analysis and thermal-maturation modelling were carried out on all the petroleum exploration wells in the Bunbury Trough and Vasse Shelf. The thermal maturation modelling was done by calculating vitrinite reflectance and comparing it with measured values. Vitrinite reflectance contours were drawn in the geohistory diagram for each well (Figs 25, 27, 29, 31, 33, 35, 37, 39, 41) and indicate the hydrocarbon maturation window. Burial geohistory diagrams were plotted using a computer program written by Iasky (1990b).

The thermal-maturity modelling provides information on the timing and depth of hydrocarbon maturation in the stratigraphic section, as well as providing a basis on which the hydrocarbon maturity of a basin can be determined.

Depths to stratigraphic units used to model burial history were obtained by digitizing seismic maps at 5 km intervals for the east–west onshore traverses, and 10 km intervals for the offshore traverses. The seismic horizons mapped represent the major stratigraphic subdivisions used in the modelling (Plates 3–12). The temperature data were obtained from Bestow (1982), who tabulated bottom-hole temperature and geothermal gradient for petroleum exploration wells in Western Australia.

Thermal-maturation modelling was carried out by assuming a constant palaeotemperature gradient through time. However, a heat pulse at tectonically active times was applied to wells where uplift or increased heat flow was estimated by modelling.

Episodes of erosion and/or uplift are important in the determinination of the maturation history. The amounts of uplift were initially estimated from regional geological cross sections, and later refined by modelling vitrinite reflectance data.

Thermal modelling of Sue 1 and Lake Preston 1 indicate that there were two periods of uplift. The first occurred in the Late Permian, and the second in the Late Jurassic preceding Australia's breakup with India (Falvey, 1974). An uplift of 1 km was assumed when modelling the Permian and Early Cretaceous events. This amount of uplift is consistent with the Early Cretaceous erosion observed in the geological cross sections drawn by Cockbain and Lehmann (1971).

The mid-Neocomian breakup produced uplift and tilting of faulted blocks (Falvey and Mutter, 1981). The faulting at this time was mostly tensional, but was accompanied by an oblique-angle strike-slip (transtensional) component that resulted from transcurrent motion along the offsets of spreading ridges (Wallaby transform fault). This component created the low-frequency north-trending folds over the whole Perth Basin that have been illustrated in cross-sections drawn by Cockbain and Lehmann (1971). Much of the younger sequence is preserved in the synclines, but there has been erosion of approximately 1 km of Late Jurassic sediments from the anticlines.

Geothermal modelling

Well analysis

Geohistory analysis and maturation modelling were carried out for nine wells. Vitrinite reflectance measurements are only available for 4 wells (Appendices 2, 9); but, on the basis of the modelling from these wells, similar parameters were used for the maturation modelling of the remaining wells. Appendix 6 shows the interpreted stratigraphic sequence for each well; data files used in the burial history and vitrinite reflectance modelling are in Iasky (1990a). Figures 24, 26, 28, and 30 plot vitrinite reflectance versus depth for a number of wells. Lake Preston 1 and Sue 1 provide the most interesting vitrinite reflectance measurements because significant tectonism occurred during their geological histories.

Lake Preston 1 (Fig. 24) has high vitrinite reflectance values that increase rapidly below 4000 m and produce a strongly curved reflectance profile. A two-kilometre uplift with an increase in thermal gradient from 20° to 120°C/km at 250 Ma provides a fit to the observed values (Fig. 25). The pronounced discontinuity in the observed vitrinite reflectance curve just below 4000 m occurs near the top of the Permian. This sudden change in gradient can only be modelled by introducing an intense heat pulse of 120°C/km at 250 Ma (Late Permian). A two-kilometre uplift was also introduced to add to the thermal effect, although this figure could vary considerably because the modelling is insensitive to the degree of uplift.

An increase in geothermal gradient from 20°C/km to 120°C/km is too large to attribute to tectonism alone. There is a magnetic anomaly near Lake Preston 1 and it is possible that a Late Permian intrusion created the heat flow necessary for the observed maturation. The nearest known evidence for a Permian intrusion is in Edel 1 in the south Carnarvon Basin (Smith and Cowley, 1987), and this event is dated Late Permian to Early Triassic. Such an event may have been responsible for the formation of the Harvey Ridge.

Cook and Kantsler (1980) suggested that Permian coal measures underwent rapid coalification in the Triassic because they do not show signs of carbonization. Low vitrinite reflectance values in the Lower Jurassic imply that little uplift has occurred on the Harvey Ridge since the Triassic. The rapid coalification recognized by Cook and Kantsler (1980) may be a result of the Permian–Triassic tectonism proposed by Middleton and Hunt (1989). The latter authors suggested that upwelling mantle convection currents on the western margin of the continent caused heating and tectonism during the Late Permian–Triassic. This hypothesis is consistent with the Lake Preston 1 maturation model.

The vitrinite reflectance values in Sue 1 (Fig. 26) increase below 2700 m and follow a similar pattern to the values in Lake Preston 1. The Sue 1 well was drilled to basement and it could provide a good example for modelling vitrinite reflectance. However, the observations below 2700 m show scatter, and they are insufficient to provide an appropriate sample for modelling.

Sue 1 is on the Vasse Shelf where the Busselton Fault has a throw of 2 km, and a considerable volume of sediment was removed with the uplift of the shelf. The modelling does not allow for more than 1 km displacement of the Busselton Fault during breakup in the Early Cretaceous, so that the remaining 1 km displacement has to be accounted for in the Late Permian event. Unlike the Lake Preston 1 model, the thermal gradient of Sue 1 was kept at a constant 20°C/km throughout to obtain a fit in the modelling (Fig. 27). It is suggested that significant movement of the major faults occurred in the Late Permian or Early Triassic to account for some of the uplift and erosion on the Vasse Shelf.

Maturation in Whicher Range 1 (Fig. 28) can be modelled by assuming 1 km uplift in the Early Cretaceous. The vitrinite-reflectance values are low and increase only slightly with depth. The model shows that depth of burial is the main cause of thermal maturation in Whicher Range 1 as there were few tectonic movements or heating episodes. The thermal gradient used in modelling this well is a constant 19°C/km throughout its depositional history. Thermal history for Whicher Range 1 is shown in Figure 29.

Modelling of Whicher Range 1 indicates that the Bunbury Trough has undergone extensive subsidence, with a reasonably constant low temperature gradient and minimal uplift, throughout its history.

The observed vitrinite reflectance values in Sugarloaf 1 (Fig. 30) extend down to 2700 m within the Yarragadee Formation, but there are insufficient samples to allow comprehensive modelling. A model resembling that of Whicher Range 1 seems to fit Sugarloaf 1; however, the sediments offshore have undergone a slightly different thermal history. The temperature gradient must have increased during rifting (Middleton, 1984b) and this resulted in the exponential increase in vitrinite reflectance with depth. The thermal modelling adopted a constant thermal gradient of 20°C/km before breakup at 120 Ma and thereafter a constant 29°C/km through to the present. Thermal history for Sugarloaf 1 is shown in Figure 31.

The current geothermal gradient in the onshore southern Perth Basin is quite low, ranging from 18 to 20° C/km (Fig. 42). The high geothermal gradient that occurred during breakup appears to have had little effect on the onshore Bunbury Trough and Vasse Shelf because there is no indication of a heat pulse during that time. This is consistent with rapidly declining heat flow from an active spreading centre. Middleton (1984b) suggested that the geothermal gradient over a spreading ridge could be more than 70°C/km and that it decreases by more than half its original value in the first 100 million years. The maximum heat flow during breakup would occur at the ridge because of upwelling of mantle material, and it should decrease rapidly with distance from it.

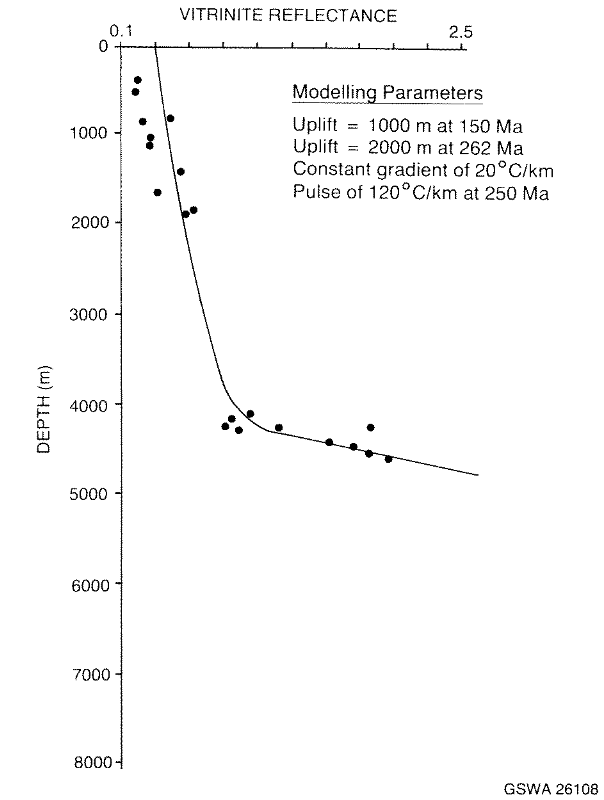

Figure 24. Lake Preston 1, vitrinite reflectance plotted against depth

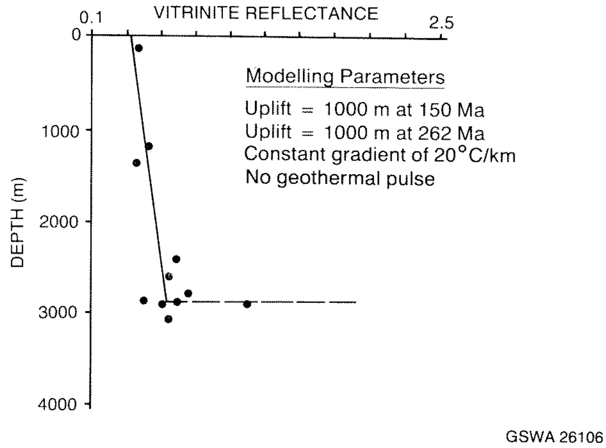

Figure 26. Sue 1, vitrinite reflectance plotted against depth

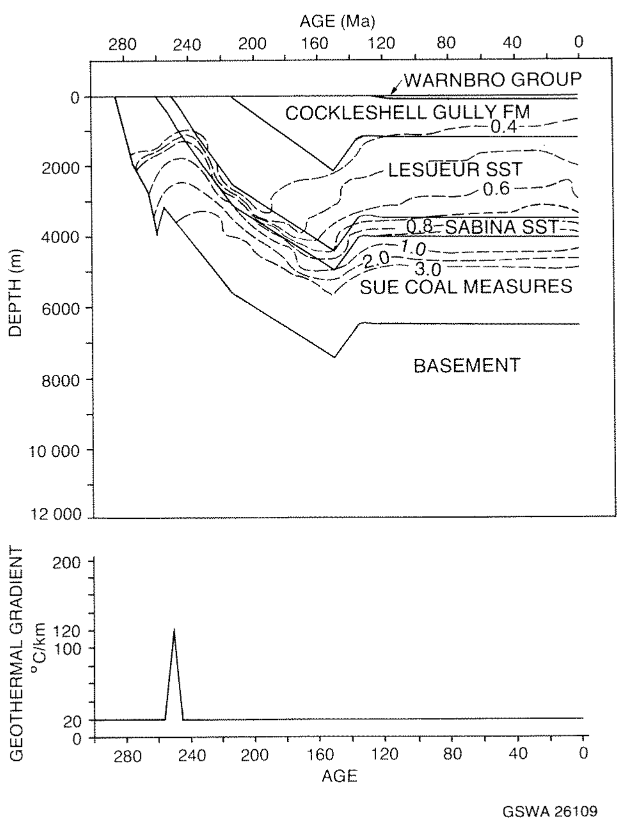

Figure 25. Geohistory plot and R_o contours for Lake Preston 1

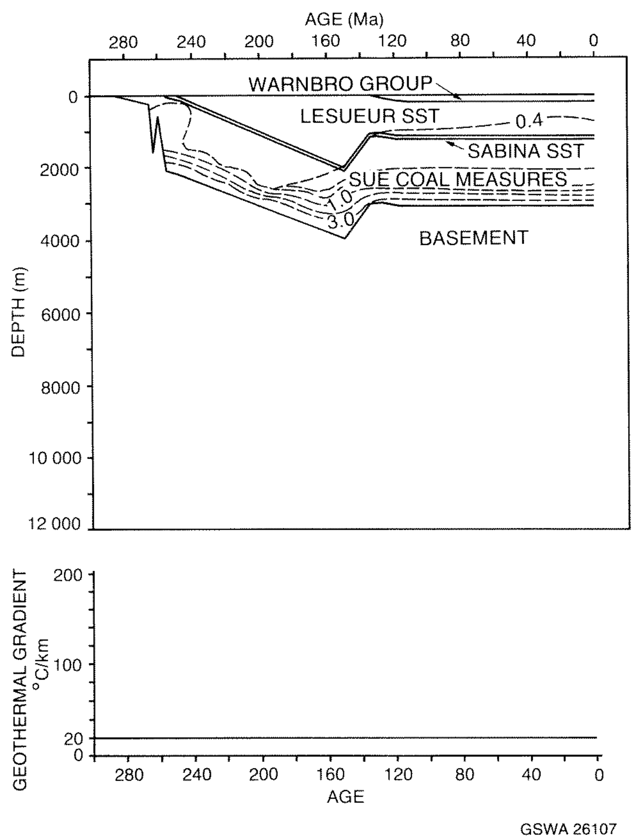

Figure 27. Geohistory plot and R_o contours for Sue 1

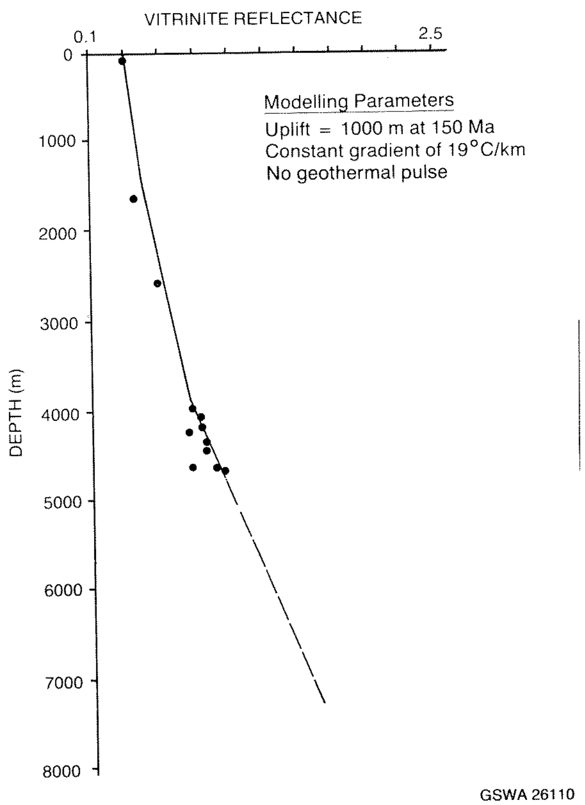

Figure 28. Whicher Range 1, vitrinite reflectance plotted against depth

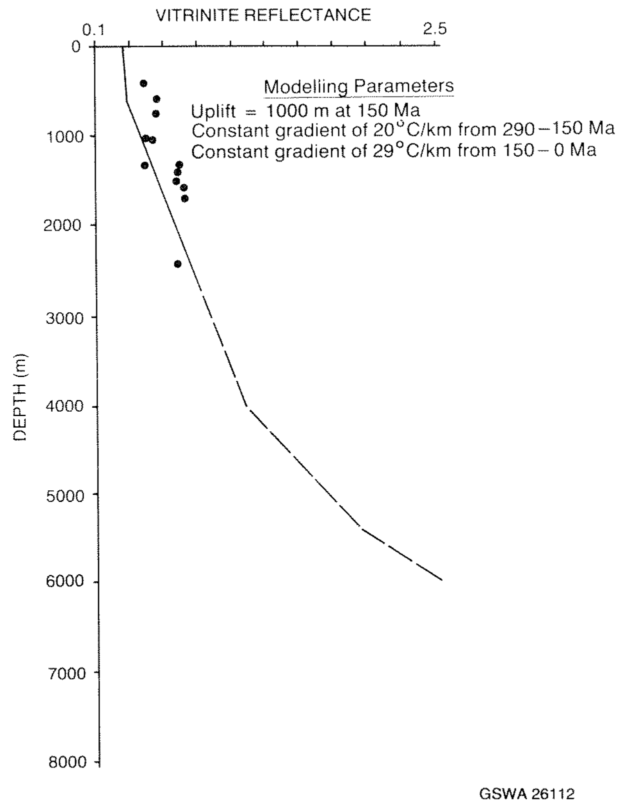

Figure 30. Sugarloaf 1, vitrinite reflectance plotted against depth

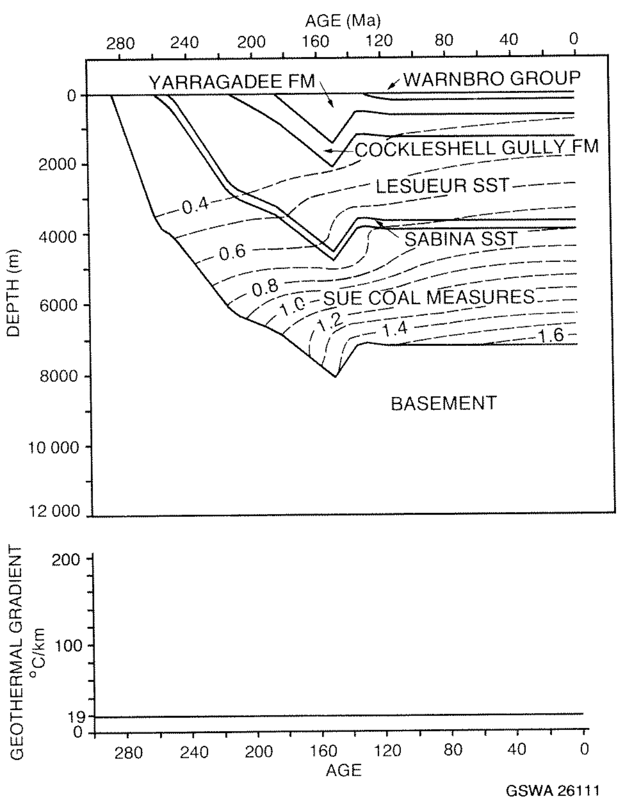

Figure 29. Geohistory plot and R_o contours for Whicher Range 1

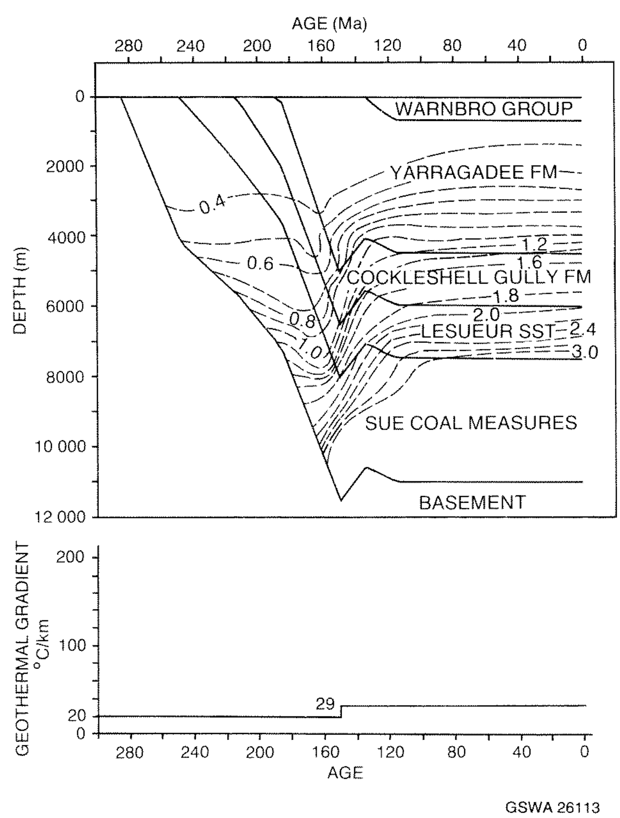

Figure 31. Geohistory plot and R_o contours for Sugarloaf 1

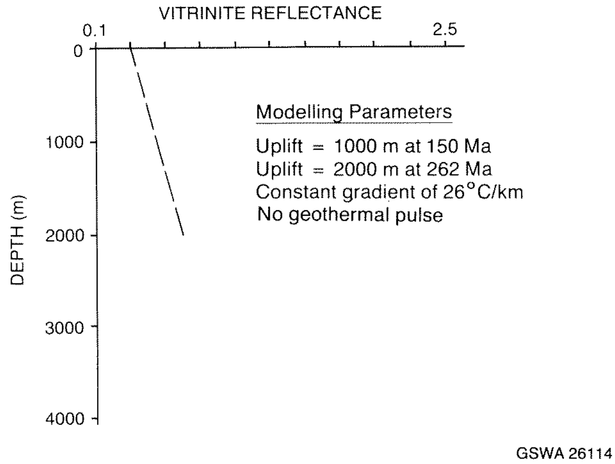

Figure 32. Alexandra Bridge 1, vitrinite reflectance plotted against depth

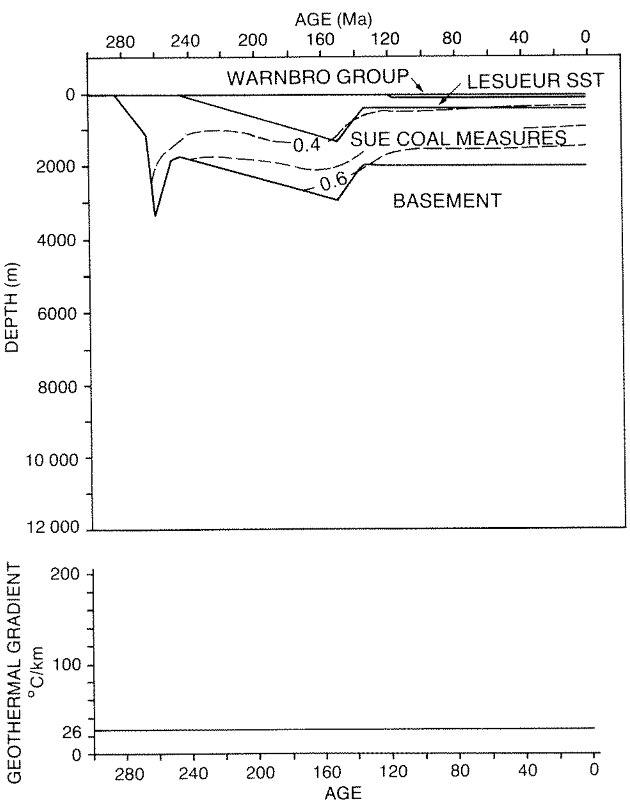

Figure 33. Geohistory plot and R_o contours for Alexandra Bridge 1

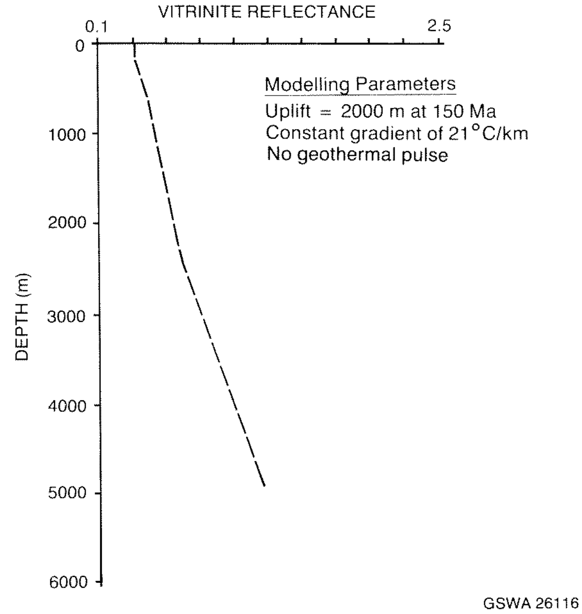

Figure 34. Blackwood 1, vitrinite reflectance plotted against depth.

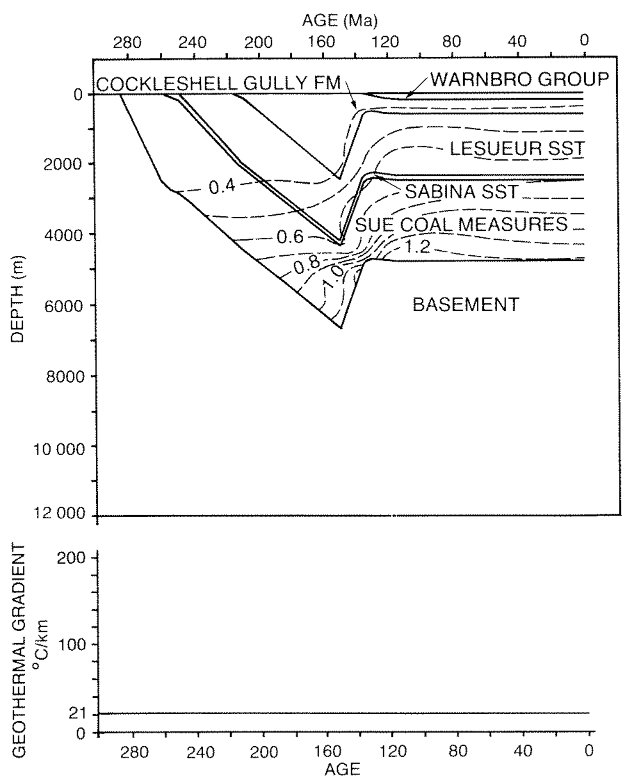

Figure 35. Geohistory plot and R_o contours for Blackwood 1

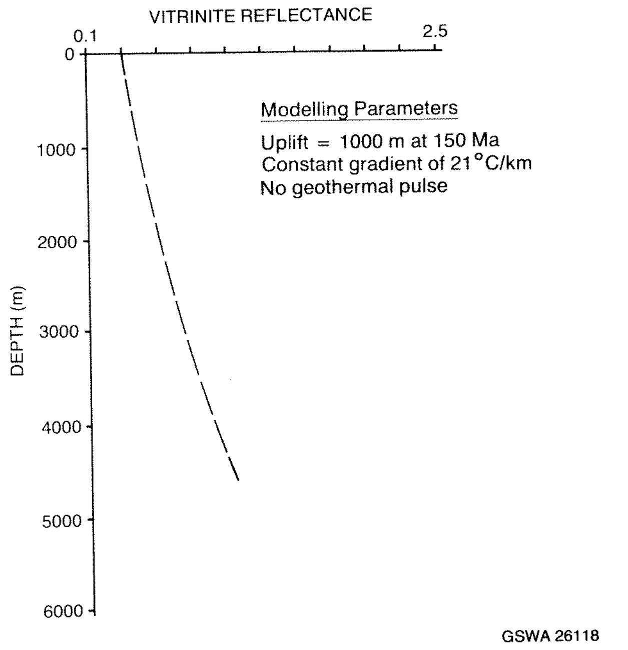

Figure 36. Canebreak 1, vitrinite reflectance plotted against depth

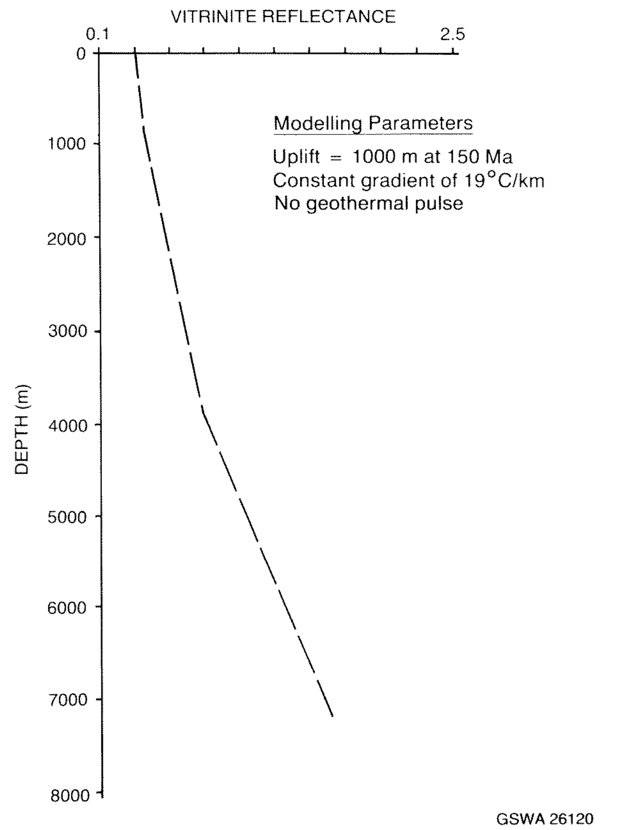

Figure 38. Sabina River 1, vitrinite reflectance plotted against depth

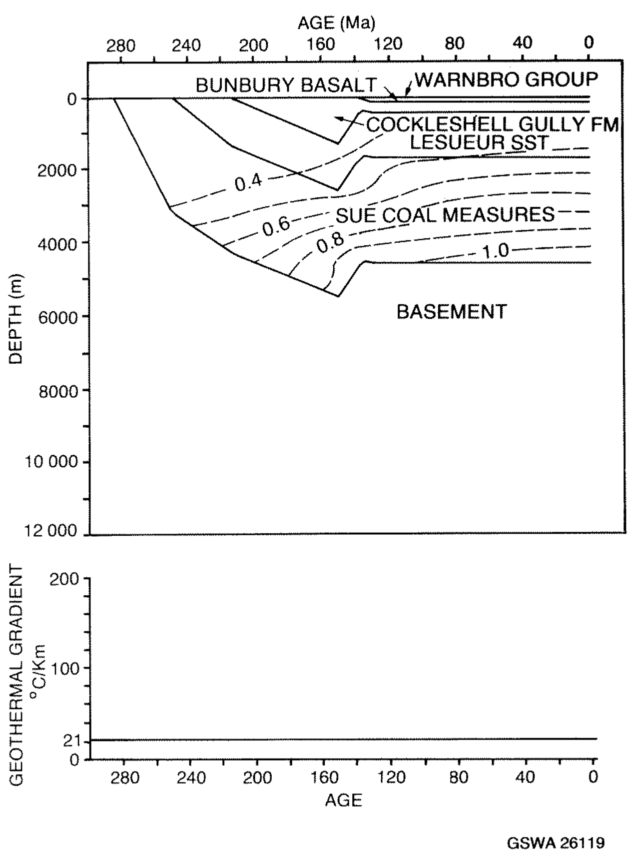

Figure 37. Geohistory plot and R_o contours for Canebreak 1

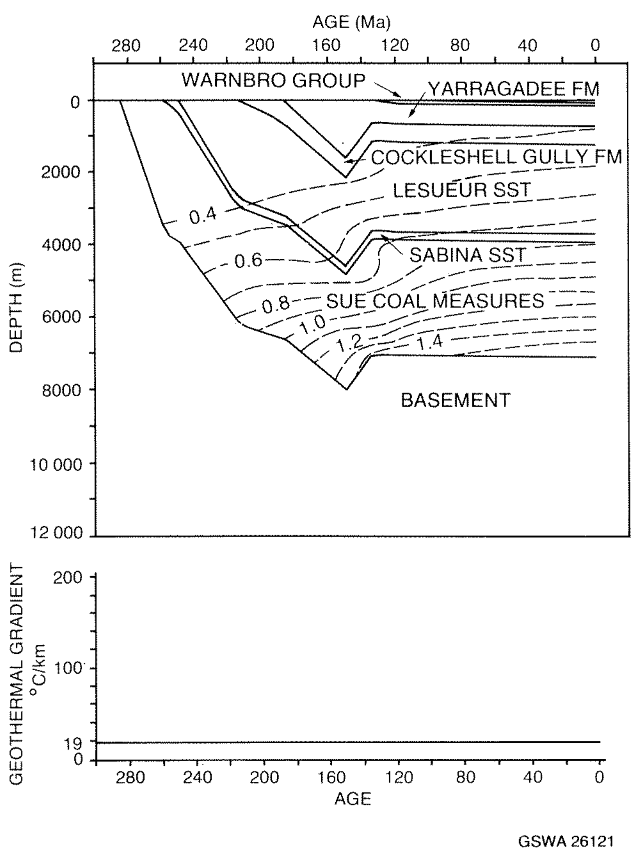

Figure 39. Geohistory plot and R_o contours for Sabina River 1

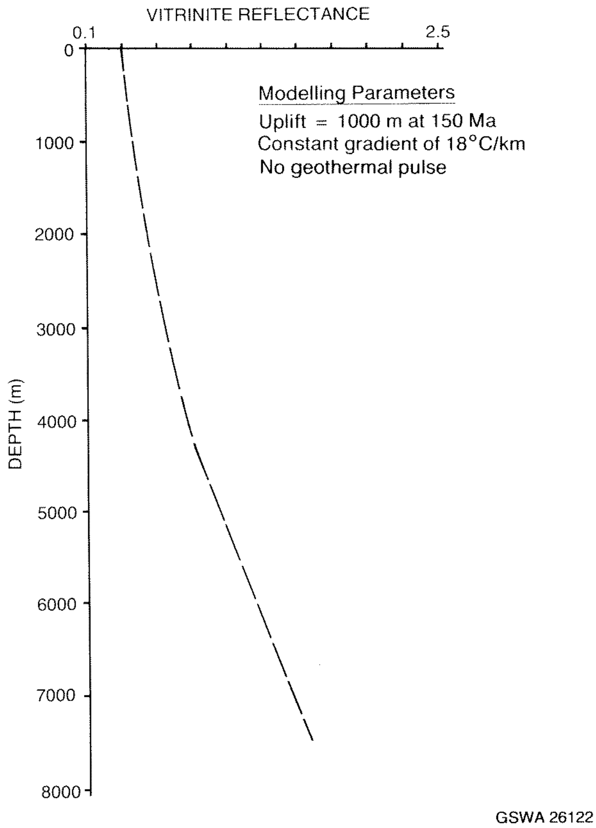

Figure 40. Wonnerup 1, vitrinite reflectance plotted against depth

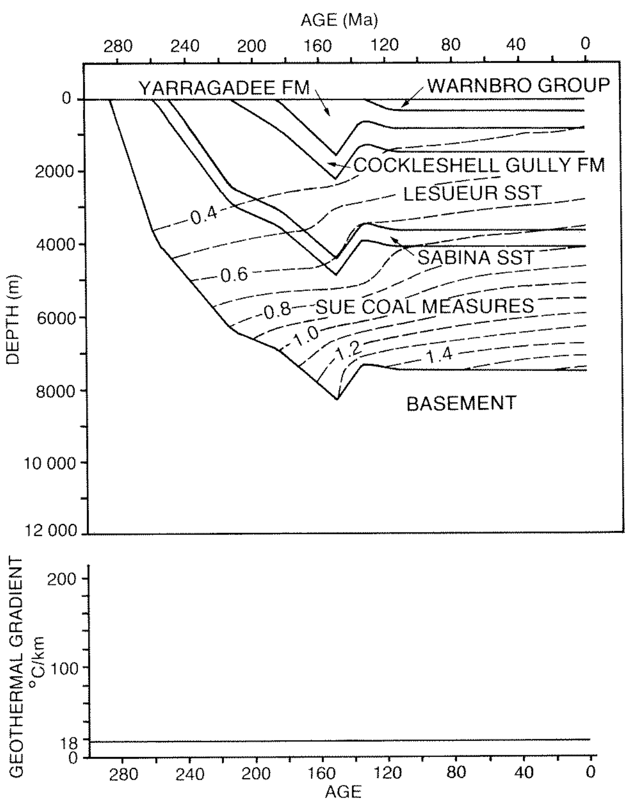

Figure 41. Geohistory plot and R_o contours for Wonnerup 1

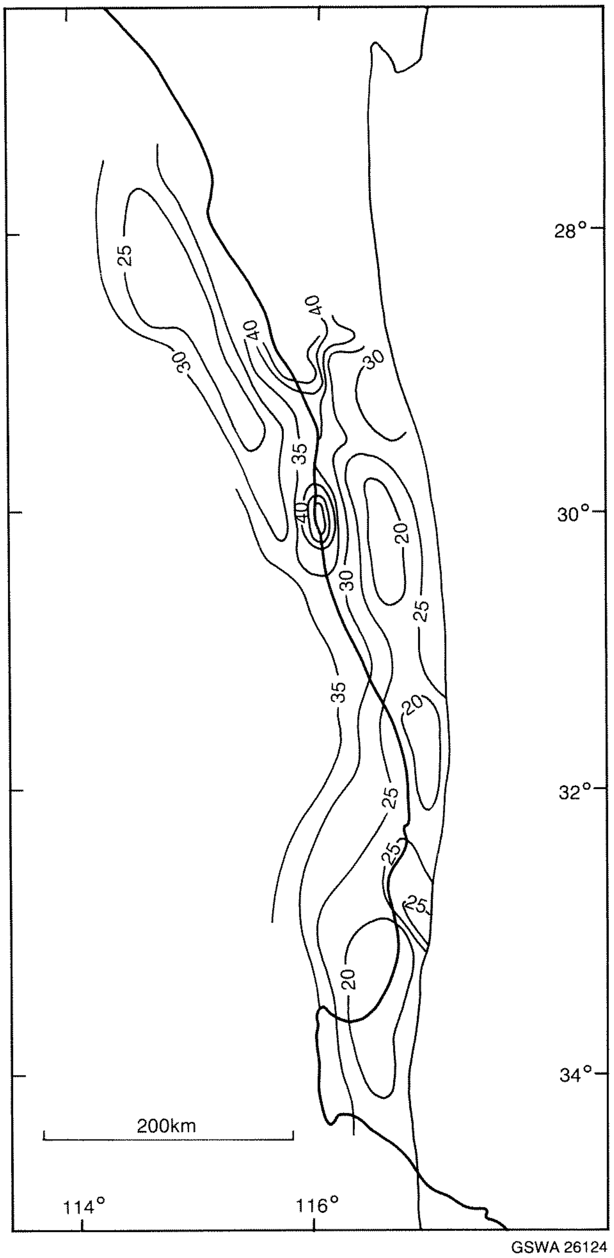

Figure 42. Zones of equal geothermal gradient. Contour interval 5 K/km

Alexandra Bridge 1 is on the Vasse Shelf, and the thermal modelling parameters used for Sue 1 were also applied to Alexandra Bridge 1 (Figures 32). The thermal parameters used to model Whicher Range 1 were applied for the remaining wells in the Bunbury Trough — Blackwood 1, Canebreak 1, Sabina River 1, and Wonnerup 1. Their vitrinite reflectance versus depth-curves are shown in Figures 34, 36, 38 and 40, and the geohistory diagrams, vitrinite reflectance contours and thermal histories are shown in Figures 35, 37, 39 and 41.

The contours of Figure 42 show that, in the onshore Bunbury Trough, the Lesueur Sandstone and the Sue Coal Measures are within the oil maturation window. In the offshore Bunbury Trough the sediments thicken and the geothermal gradient increases; consequently the maturation window is higher in the sequence. At Sugarloaf 1, the Otorowiri Member of the Parmelia Formation and the Yarragadee Formation are within the oil window, whereas the Cockleshell Gully Formation is within the gas window. The sedimentary section is thinner southeast of this well and both the Cockleshell Gully Formation and the Lesueur Sandstone are in the oil maturation window.

Regional cross-section analysis

Figure 43 shows the locations of the regional cross sections. The geological history for each traverse is shown by reconstructing geological cross sections from the beginning of sedimentation in the Permian to the present day (Figures 44 to 48).

The parameters used to model the individual wells were also used to model the traverses. The aim was to show the basin's evolution by reconstructing geological cross sections through time. Thermal maturation modelling was not done on the traverses, and consequently vitrinite reflectance contours were not constructed.

The reconstructions show that major period of vertical movement occurred in the Late Permian and at breakup in the Early Cretaceous. The Triassic and Jurassic sequence was deposited during a period of rapid subsidence. The Early Cretaceous breakup tectonism, together with downwarping related to subsidence in the depocentres, has had a pronounced effect on the present structure of the basin. The mid-Jurassic movement along the Dunsborough Fault, interpreted from the seismic structure maps on page 17, is not seen in the reconstructions because it would have had only minimal effect in the Bunbury Trough.

Discussion

The geohistory and maturation modelling indicate that there were two episodes of uplift in the Bunbury Trough. The first occurred in the Late Permian–Triassic when major faults such as the Darling and Busselton Faults were reactivated. Large quantities of sediment were subsequently deposited with little interruption throughout the Mesozoic. The second major event was the uplift during breakup of Australia and India in the Neocomian. The breakup was transtensional in nature (oblique strike-slip) and occurred after the deposition of the Yarragadee Formation. This event determined the present structure of the basin.

Vitrinite reflectance modelling has shown that there was a significant event in the Late Permian to Early Triassic, which resulted in uplift over parts of the Perth Basin and the activation of the Darling, Busselton, and Dunsborough Faults.

The low heat flow in the southern Perth Basin produced a slow rate of maturation of the potential source material. This is seen in the low (0.5–0.8%) vitrinite reflectance values in wells in the Bunbury Trough and Vasse Shelf (Mishra, 1986) where source rocks may be found at greater depths.

In the onshore Bunbury Trough, maturation modelling shows that the Permian–Triassic section falls within the oil maturation window with vitrinite reflectance values of 0.5 to 1.3% (Figs 24–29 and 33–41). Offshore, the Late Jurassic sedimentary sequence falls within the maturation window (Fig. 31).

Whicher Range 1 and Wonnerup 1 had good gas shows, and the Permian Sue Coal Measures have proved to contain reasonable source rocks. Reservoir sands have been encountered in Permian, Triassic, and Jurassic strata. However, post-Permian targets have been ignored in the southern Perth Basin although they are prospective in the northern Perth Basin (Early Jurassic Cattamarra Coal Measures and Early Triassic Kockatea Shale).

Offshore, Gage Roads 1 and 2 showed that the Late Jurassic Otorowiri Member of the Parmelia Formation is an attractive source rock in the Vlaming Sub-basin. This member extends south into the Bunbury Trough. Shales of the Yarragadee Formation also fall within the oil maturation window and are possible source rocks.

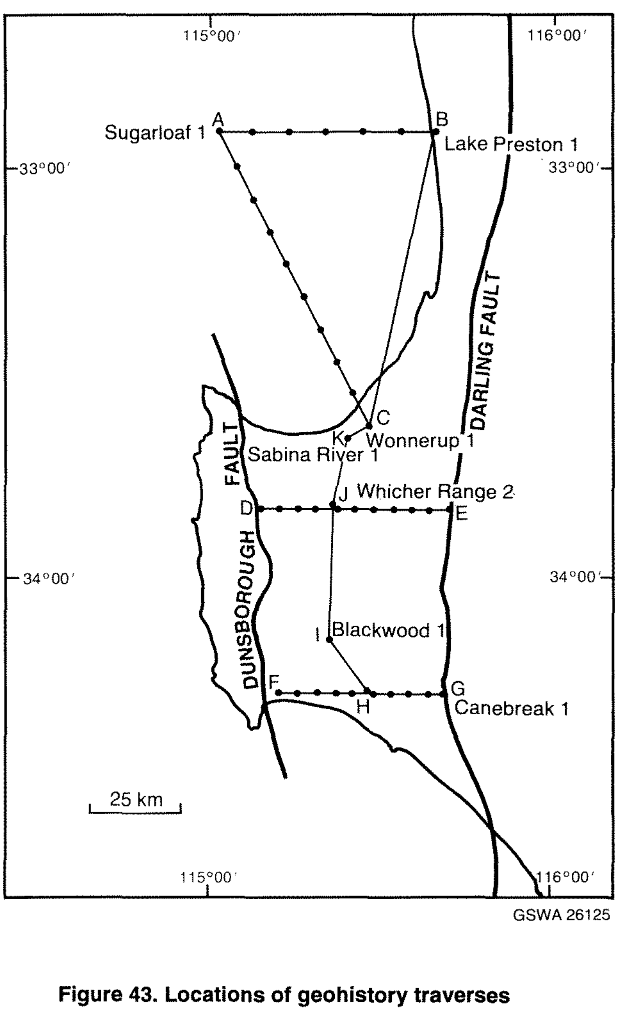

Figure 43. Locations of geohistory traverses

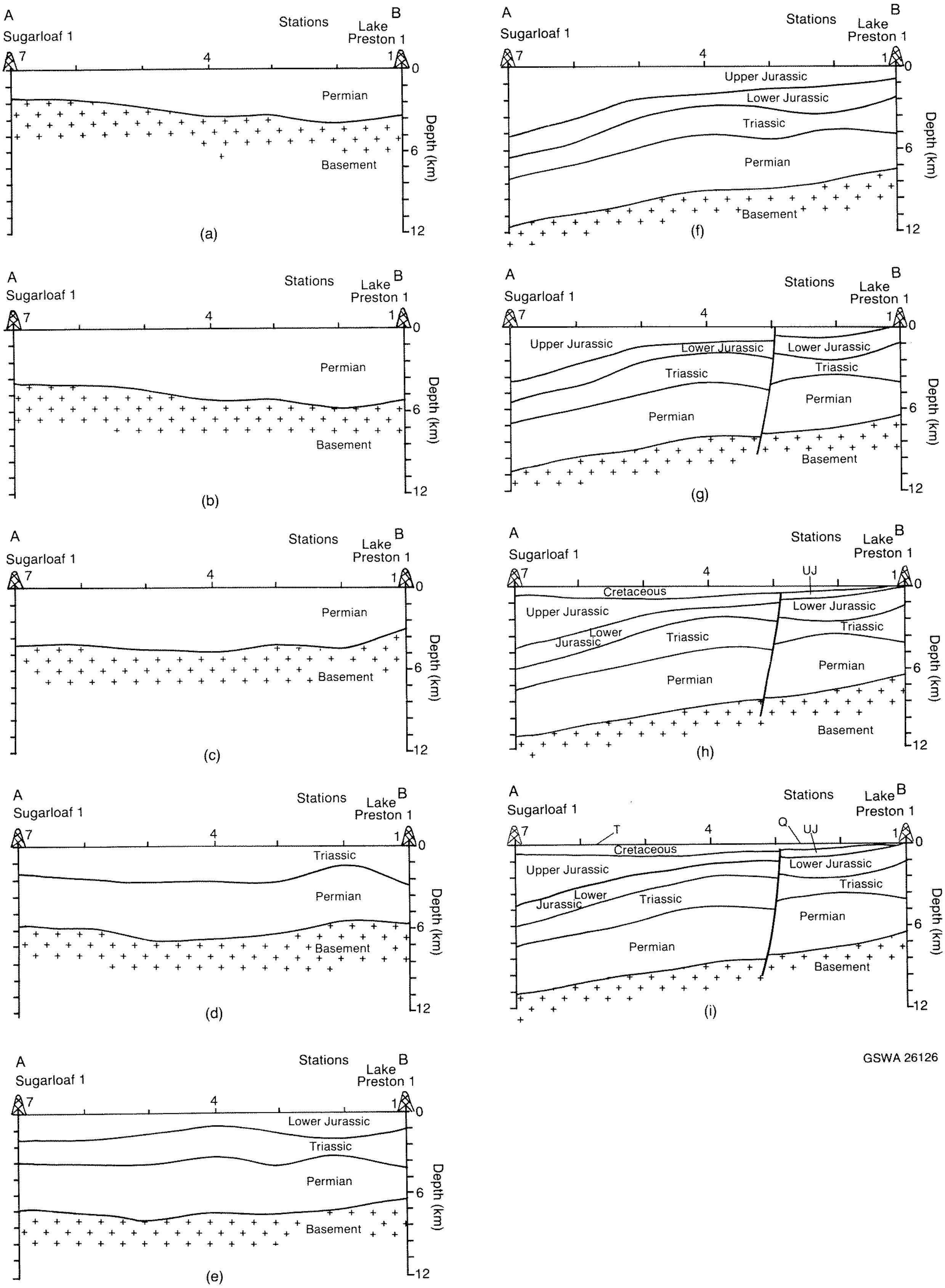

Figure 44. Geohistory reconstruction of traverse AB

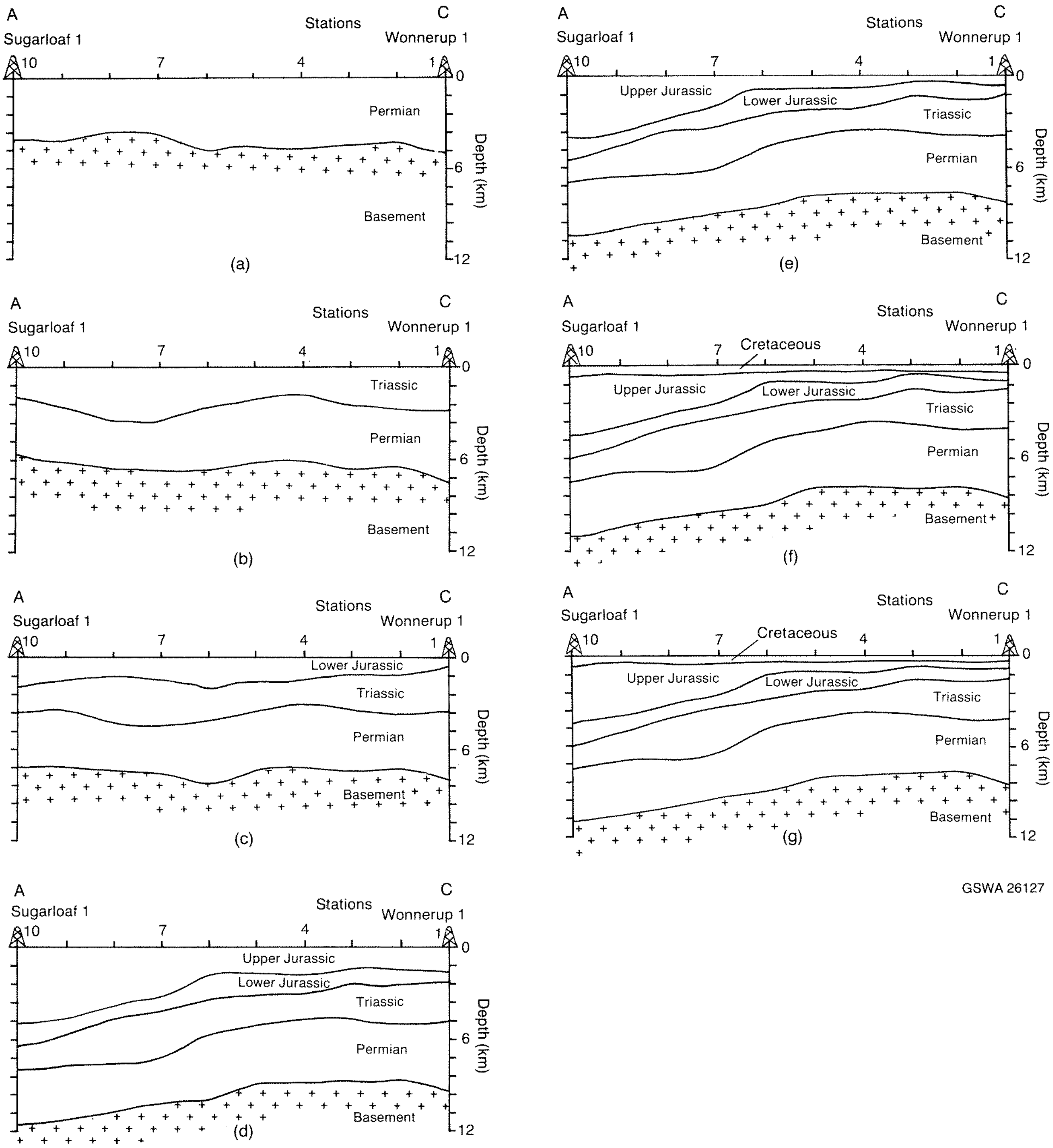

Figure 45. Geohistory reconstruction of traverse AC

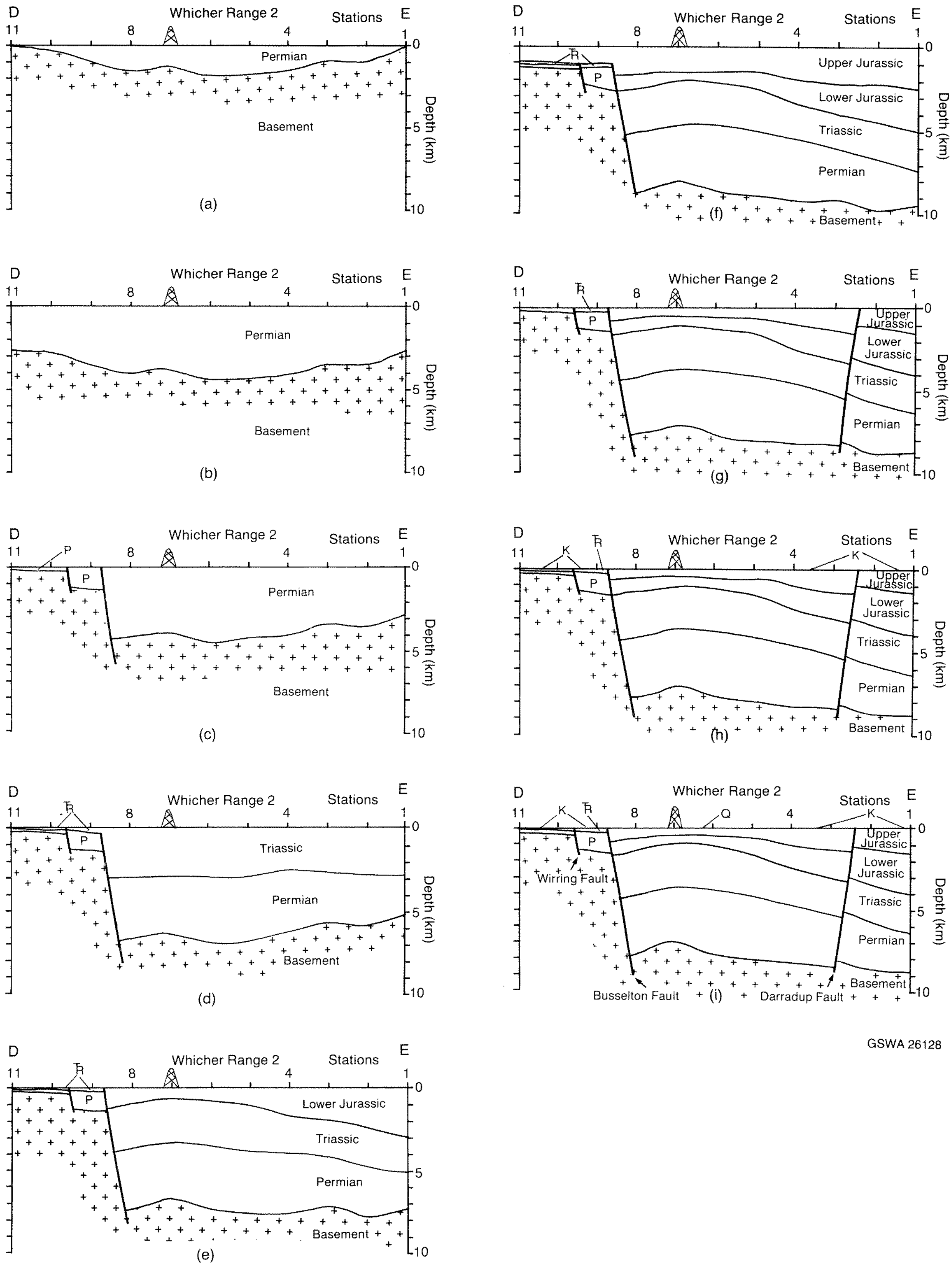

Figure 46. Geohistory reconstruction of traverse DE

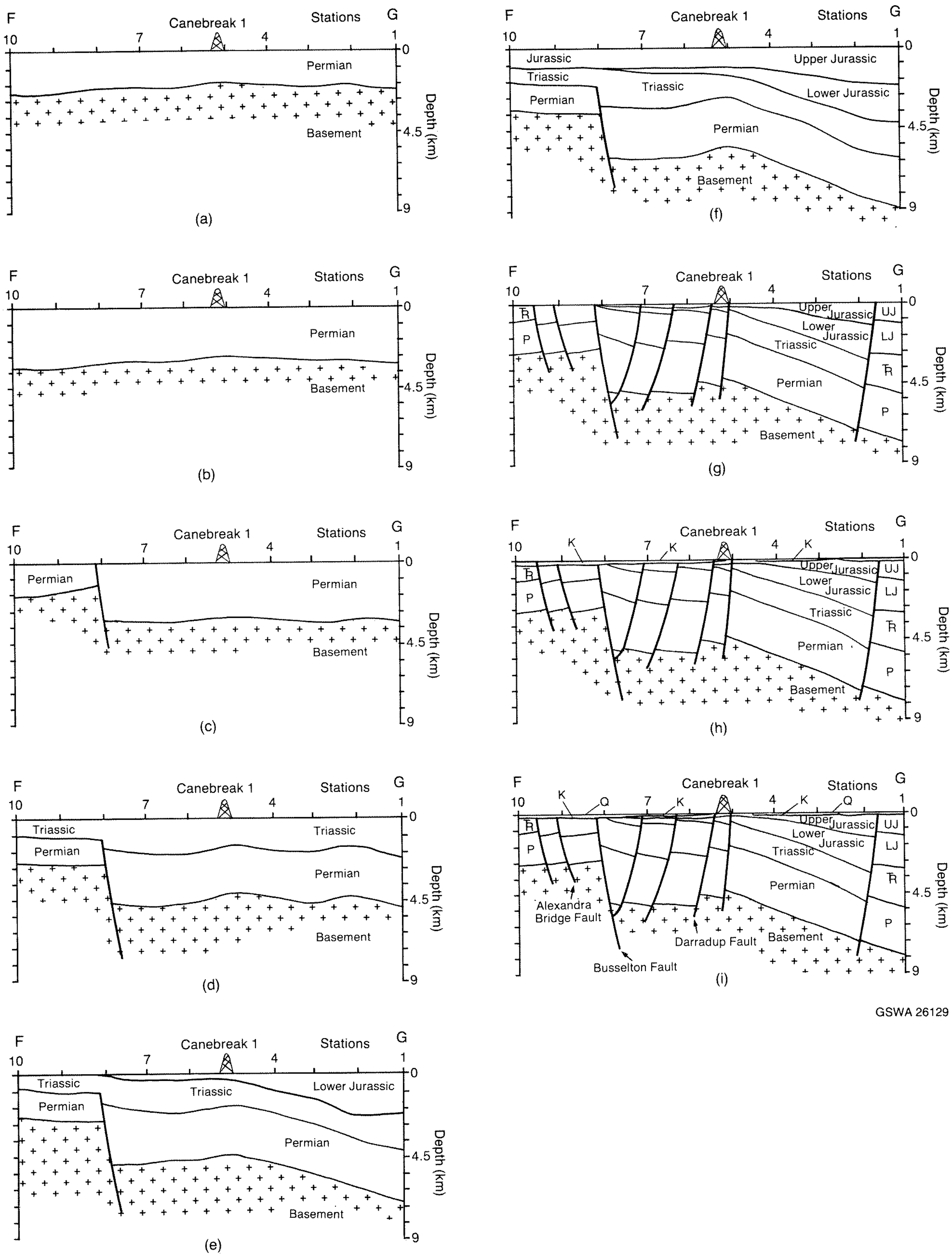

Figure 47. Geohistory reconstruction of traverse FG

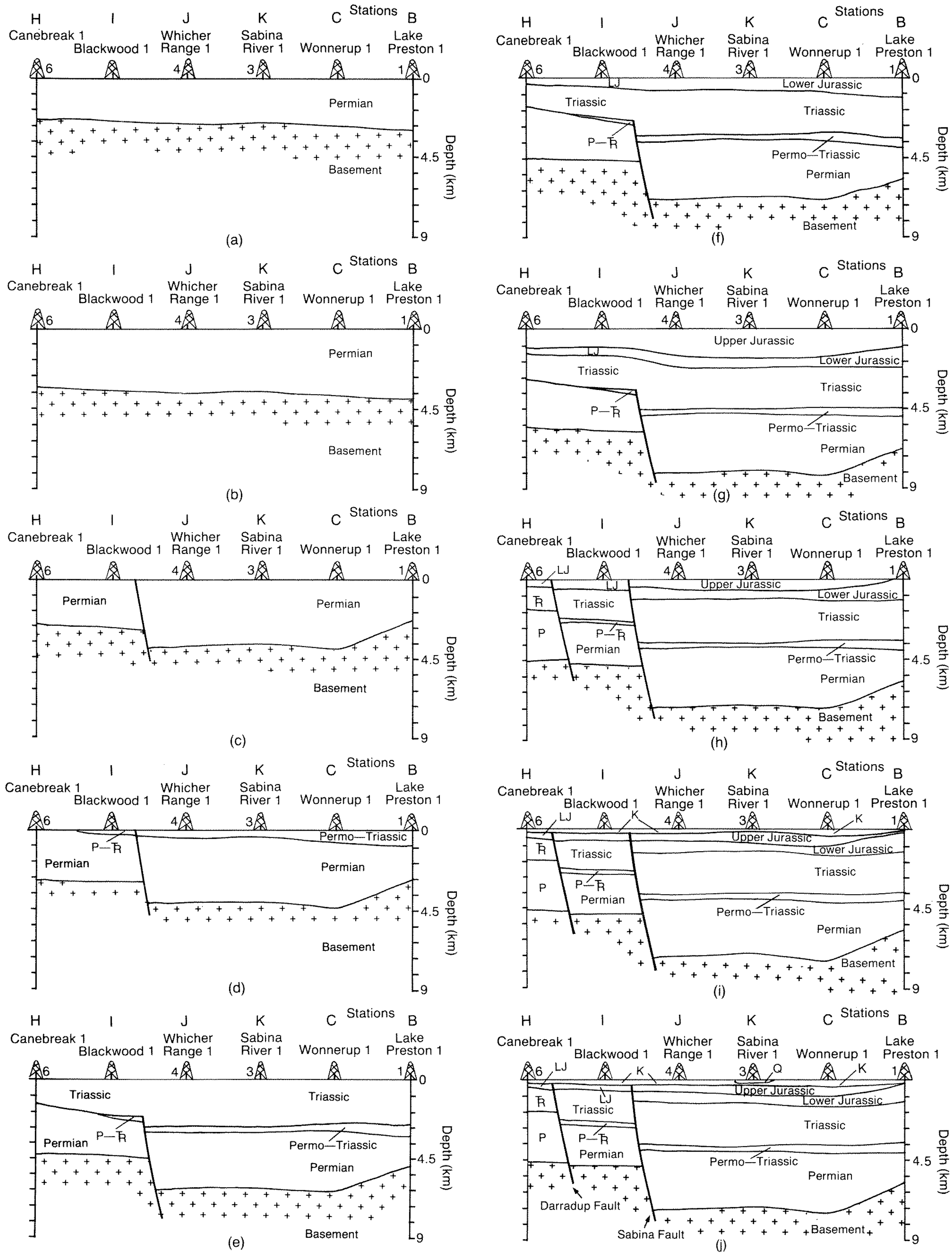

Figure 48. Geohistory reconstruction of traverse HIJKCB

References

ACHESON, C. H., 1981, Time–depth and velocity–depth relations in sedimentary basins — A study based on current investigation in the Arctic Islands and an interpretation of experience elsewhere: Geophysics, v. 46, p. 707–716.

ALLARD, F. J., 1983, Geochemical data for Sugarloaf 1 and Cockburn 1, Perth Basin, Australia: (B.P. Company, B.P. Research Centre): Western Australia Geological Survey, S-series open-file microfiche PEG621/A3).

APPLEYARD, S. J., 1989, The geology and the hydrogeology of the Cowaramup borehole line, Perth Basin, WesternAustralia: Western Australia Geological Survey, Hydrogeology Report 1989/34 (unpublished).

APPLEYARD, S. J., 1991, The geology and the hydrogeology of the Cowaramup borehole line, Perth Basin, Western Australia, *in* Professional Papers: Western Australia Geological Survey, Report 30.

AUSTRALIAN MINERAL DEVELOPMENT LABORATORIES, 1979, Source rock analysis of samples 51–100 (results of samples 96–100 only enclosed): (Australia, Bureau of Mineral Resources Report) Western Australia Geological Survey, S-series (S1468/A24) open-file microfilm 378.

BACKHOUSE, J. 1988, Late Jurassic and Early Cretaceous palynology of the Perth Basin, Western Australia: Western Australia Geological Survey, Bulletin 135.

BACKHOUSE, J. 1993, Palynology and correlation of Permian sediments in the Perth, Collie, and Officer Basins, Western Australia, *in* Professional Papers: Western Australia Geological Survey, Report 30, p. 111–128.

BACKHOUSE, J. and WILSON, A. 1989, New records of Permian and Cretaceous sediments from the southwestern part of the Yilgarn Block, *in* Professional Papers: Western Australia Geological Survey, Report 25, p. 1–5.

BADDOCK, L. J., 1991, The geology and the hydrogeology of the Karridale borehole line, Perth Basin, Western Australia: Western Australia Geological Survey, Hydrogeology Report 1991/18 (unpublished).

BAXTER, J. C. and HARRIS, J. L., 1979, The Darling Fault — Diamond drilling results at Harrisons Copper prospect: Western Australia Geological Survey, Annual Report 1979, p. 90–93.

BERKMAN, D. A., 1976, Field geologists' manual, *edited by* Berkman D. A. and Ryall W. R.: Australasian Institute of Mining and Metallurgy, Monograph 9.

BESTOW, T. 1982, The potential for geothermal-energy development in Western Australia: Western Australia Geological Survey, Record 1982/6.

BIRD, K. J. and MOYES, C. P., 1971, Sugarloaf 1 well completion report: (West Australian Petroleum Pty Ltd, PSSA Report) Western Australia Geological Survey, S-series (S621) open-file microfiche PEW621.

BLIGHT, D. F., COMPSTON W., and WILDE, S. A., 1981, The Logue Brook Granite — Age and significance of deformation zones along the Darling Scarp: Western Australia Geological Survey, Annual Report 1980, p. 72–80.

BOLT, B. A., DOYLE, H. A., and SUTTON, D. J., 1958, Seismic observations from 1965 atomic explosions in Australia: Geophysics Journal, v. 1, p. 135–145.

BURDETT, J. W., 1963, Hill River stratigraphic bores, Perth Basin, Western Australia: (West Australian Petroleum Pty Ltd, Report): Western Australia Geological Survey, S-series (S15) open-file microfilms 8A and 41.

BUREAU OF MINERAL RESOURCES, 1978, Vitrinite-reflectance analysis of samples from four wells — Tables of measurements only: Western Australia Geological Survey, S-series (S1468/A16) open-file microfiche PEG1468/A16.

BURGESS, I. R., 1978, Geology and Geochemistry, of the Cretaceous Bunbury Tholeiite Suite, Perth Basin, Western Australia: University of Western Australia, Bachelor of Science Thesis (unpublished).

CANDE, S. C. and MUTTER, J. C., 1982, A revised identification for the oldest sea floor spreading anomalies between Australia and Antarctica: Earth Planetary Science Letters, v. 58, p. 151–160.

CLARKE, E. de C., PRIDER R. T., and TEICHERT, C., 1944, Elements of geology: Perth, University of Western Australia Text Books Board, 301 p.

COCKBAIN, A. E., 1990, Perth Basin, *in* Geology and mineral resources of Western Australia: Western Australia Geological Survey, Memoir 3, p. 495–524.

COCKBAIN, A. E. and LEHMANN, P. R., 1971, Geology of the Perth Basin, Western Australia, part 1 — Regional stratigraphy and structure: (Ashburton Oil N.L. Report) Western Australia Geological Survey, S-series (S1129) open-file microfiche PEG1129-A1.

COMMANDER, D. P., 1981, The geology and hydrogeology of Bunbury: Western Australia Geological Survey, Hydrogeology Report 2327 (unpublished).

COMMANDER, D. P., 1982, The Bunbury shallow drilling groundwater investigation, *in* Professional Papers 1982: Western Australia Geological Survey, Report 12, p. 32–52.

COOK, A. C., 1979a, Vitrinite reflectance data for eight wells in the Perth Basin: (University of Wollongong, Department of Geology) Western Australia Geological Survey, S-series open-file microfiche PEG1490/A1.

COOK, A. C., 1979b, Vitrinite reflectance analysis for four wells in the Perth Basin: (University of Wollongong, Department of Geology) Western Australia Geological Survey, S-series open-file microfiche PEG1490/A2.

COOK, A. C. and KANTSLER, A. J., 1980, The maturation history of the epicontinental basins of Western Australia: UN ESCAP, CCOP/SOPAC, Technical Bulletin 3.

COPE, R. N., 1972, Tectonic style in the southern Perth Basin: Western Australia Geological Survey, Annual Report 1971, p. 46–50.

CRA EXPLORATION PTY LTD, 1984, Perth Basin well sampling, 1984 — Results of analysis by pyrolysis from 49 wells: Western Australia Geological Survey, S-series open-file microfiche PEG2969/A1.

CROSTELLA, A. and BARTER, T. P., 1980, Triassic–Jurassic depositional history of the Dampier and Beagle Sub-basin, Northwest Shelf of Australia: APEA, Journal, v. 20(1), p. 25–33.

DAVIES, H. L., SUN S-S, FREY, F. A., GAUTIER, I., McCULLOCH, M. T., PRICE, R. C., BASSIAS, Y., KLOOTWIJK, C. T., and LECLAIRE, L., 1989, Basalt basement from the Kerguelen Plateau and trail of a Dupal plume: Contribution to Mineralogy and Petrology, Springer-Verlag 1989, 103, p. 457–469.

DEENEY, A. C., 1989a, Hydrogeology of the Binningup borehole line, Perth Basin, *in* Professional Papers 1989: Western Australia Geological Survey, Report 25, p. 7–16.

DEENEY, A. C., 1989b, Hydrogeology of the Harvey borehole line, Perth Basin, *in* Professional Papers 1989: Western Australia Geological Survey, Report 26, p. 59–68.

de LAETER, J. R. and LIBBY, W. G., in press, Early Palaeozoic Rb–Sr dates in the Yilgarn Craton, Western Australia: Geological Society of Australia, Australian Journal of Earth Science.

DOOLEY, J. C. 1972, Seismological Studies of the upper mantle in the Australian region, *in* Proceedings of the second Indian symposium on the Upper Mantle Project, December 1970: Hyderabad, National Geophysical Research Institute, p. 113–146.

DOOLEY, J. C., 1976, Variation of crustal mass over the Australian region: BMR Journal of Australian Geology and Geophysics, v. 1(4), p. 291–296.

DOYLE, H. A. and EVERINGHAM, I. B., 1964, Seismic velocity and crustal structure in southern Australia: Geological Society of Australia, Journal, v. 11, p. 141–150.

EDWARDS, A. B., 1938, Tertiary tholeiite magma in Western Australia: Royal Society of Western Australia, Journal, v. 24, p. 1–12.

ELIE, R., COOPER, R., TRICOT, P. L. and SWEENEY, P., 1965, Cadda 1 well completion report: (French Petroleum Co. (Australia) Pty Ltd: PSSA Report (unpublished)): Western Australia Geological Survey, S-series S226.

ELLIOTT, R. M. L., IASKY, R. P., and CRANK, K. A., 1985, Review of petroleum exploration, development and production in Western Australia to the end of 1984: Western Australia Geological Survey, Record 1985/2.

ETHERIDGE, M. A., SYMONDS, P. A., and LISTER, G. S., 1989, Application of the detachment model to reconstruction of conjugate passive margins, *in* Extensional tectonics and stratigraphy of the North Atlantic margins, *edited by* A. J. Tankard and H. R. Balkwill: American Association of Petroleum Geologists, Memoir 46.

FAIRBRIDGE, R. W., 1948, Preliminary report on the geology of the coastal plain and other sedimentary areas between Busselton and Geraldton, Western Australia: Richfield Oil Corporation, Report (unpublished).

FAIRBRIDGE, R. W., 1953, Australian stratigraphy: Perth, University of Western Australia, Text Books Board, 516 p.

FALVEY, D. A., 1974, The development of continental margins in plate tectonics theory: APEA, Journal., v. 14(1) p. 95–106.

FALVEY, D. A. and MUTTER, J. C., 1981, Regional plate tectonics and the evolution of Australia's passive continental margins: BMR Journal of Australian Geology and Geophyisics, v. 6, p. 1–29.

FELCMAN, F. L. and LANE, E. P., 1963, Southern and central Perth Basin gravity survey by WAPET: Western Australia Geological Survey, S-series (S54) open-file microfilm 10.

FLETCHER, I. R., WILDE, S. A., and ROSMAN, K. J. R., 1985, Sm/Nd model ages across the margins of the Archaean Yilgarn Block, Western Australia, III — The western margin: Australian Journal of Earth Sciences, v. 32, p. 73–82.

FRANCIS, T. J. G. and RAITT, R. W., 1967, Seismic refraction measurements in the southern Indian Ocean: Journal of Geophysical Research, v. 72, p. 3015–3041.

GARDNER, G. H. F., GARDNER, L. W., and GREGORY, A. R., 1974, Formation velocity and density — The diagnostic basics for stratigraphic traps: Geophysics, v. 39, p. 770–780.

HAWKINS, L. H., HENNION, J. F., NAFE, J. E., and THYER, R. F., 1965, Geophysical investigation in the area of the Perth Basin, Western Australia: Geophysics, v. 30, p. 1026–1052.

HIRSCHBERG, K-J. B., 1989, Busselton shallow-drilling groundwater investigation, *in* Professional Papers: Western Australia Geological Survey , Report 25, p. 17–38.

HOCKING, R. M., 1991, The Tumblagooda Sandstone, Western Australia: Western Australia Geological Survey, Report 27.

IASKY, R. P., 1990a, A geophysical synthesis of the southern Perth Basin, Western Australia: Curtin University of Technology, Department of Exploration Geophysics, M Sc. thesis (unpublished).

IASKY, R. P. 1990b, Computer programs for analysing gravity and geothermal data: Western Australia Geological Survey, Record 1990/12.

JOHNSTONE, D. and PLAYFORD, P. E., 1955, Geology of the Shark Bay–Murchison River area, Carnarvon Basin: West Australian Petroleum Pty Ltd, Report (unpublished).

JOHNSTONE, M. H., LOWRY, D. C., and QUILTY, P. G., 1973, The geology of southwestern Australia — A review: Royal Society of Western Australia, Journal, v. 56, p. 5–15.

JONES, D. K., 1965, Alexandra Bridge 1 well completion report: (West Australian Petroleum Pty Ltd Report) Western Australia Geological Survey, S-series (S232) open-file microfilms 43 and 628.

KATZ, B. J., PHEIFER, R. N., and SCHUNK, D. J., 1988, Interpretation of discontinuous vitrinite reflectance profiles: American Association of Petroleum Geologists, Bulletin, v. 72(8), p. 926–931.

KING, D. and FALVEY, M., 1977, A seismic survey in the Cooper Basin in Queensland: APEA, Journal, p. 78–84.

LAMBECK, K., 1987, The Perth Basin — A possible framework for its formation and evolution: Australian Society of Exploration Geophysics, Bulletin, v. 18 (1–2), p. 124–128.

Le BLANC-SMITH, G., 1989, Structural evidence from the Collie Coalfield, *in* Offshore Perth Basin seminar, Perth, 5 October 1989: Western Australia Geological Survey, S-series S3914 A1 (unpublished).

LEHMANN, P. R., 1966, Preston 1 well completion report: (West Australian Petroleum Pty Ltd, PSSA Report): Western Australia Geological Survey, S-series (S316) open-file microfilm 42.

Le MAITRE, R. W., 1975, Volcanic rocks from Edel No. 1 petroleum exploration well, offshore Carnarvon Basin, Western Australia: Geological Society of Australia, Journal, v. 22, p. 167–174.

LIBBY, W. G. and de LAETER, J. R., 1979, Biotite dates and cooling history at the western margin of the Yilgarn Block: Western Australia Geological Survey, Annual Report 1978, p. 79–87.

LIU, H., 1979, Mantle convection and subcrustal stresses under Australia: Modern Geology, v. 7, p. 29–36.

LODWICK, K. B., 1962, Busselton seismic survey, Western Australia, 1955–56: Australia, Bureau of Mineral Resources, Record 1962/108.

LOW, G. H., 1972, Explanatory notes on the Phanerozoic of the western part of the Collie 1:250 000 geological sheet, Western Australia: Western Australia Geological Survey, Record 1972/10.

LOWELL, J. D., 1985, Structural styles in petroleum exploration: Tulsa, OGCI Publications.

LOWRY, D. C., 1967, Explanatory notes on the Busselton and Augusta geological sheets, Western Australia: Western Australia Geological Survey, 1:250 000 Geological Series — Explanatory Notes.

LOWRY, D. C., 1976, Tectonic history of the Collie Basin, Western Australia: Geological Society of Australia, Journal, v. 23(1), p. 95–104.

LOWRY, D. C., 1983, Canebreak 1 well completion report: Western Australia Geological Survey, S-series (S2020) open-file microfilm 628.

MAITLAND, A. G., 1919, A summary of the geology of Western Australia: Western Australia Geological Survey, Memoir 1, Chapter 1.

MARSHALL, J. F., LEE CHAO-SHING, RAMSAY, D. C., and MOORE, A. M. G., 1989, Tectonic controls on sedimentation and maturation in the offshore north Perth Basin: APEA, Journal, v. 29(1).

MATHUR, S. P., 1974, Crustal structure in southwestern Australia from seismic and gravity data: Tectonophysics, v. 24, p 151–182.

MATHUR, S. P., MOSS, F. J., and BRANSON, J. C., 1977, Seismic and gravity investigations along the geotraverse: Australia, Bureau of Mineral Resources, Bulletin 191.

McDOUGALL, I. and WELLMAN, P., 1976, Potassium-argon ages for some Australian Mesozoic rocks: Geological Society of Australia, Journal, v. 23(1), p. 1–9.

MIDDLETON, M. F., 1984a, Hydrocarbon maturity of the southern continental margin of Western Australia, *in* Geoscience in the Development of Natural Resources — Seventh Australian Geological Convention, Sydney, 1984: Geological Society of Australia, Abstracts 12.

MIDDLETON, M. F., 1984b, Formation of rifted continental margins — A discussion of mechanisms: First Break (April 1984), p. 9–14.

MIDDLETON, M. F., 1985, Depth to basement map: Western Australia Geological Survey.

MIDDLETON, M. F., 1991, Tectonic history of the southern continental margin of Western Australia: Western Australian, Geological Survey, Record 1990/8.

MIDDLETON, M. F., 1990, Analysis of wrench tectonics in the Perth and Canning Basins, Western Australia: Western Australia Geological Survey, Basin and Fossil Fuels Report 3/1990 (unpublished).

MIDDLETON, M. F. and HUNT, J. W., 1989, Influence of tectonics on Permian coal-rank patterns in Australia: International Journal of Coal Geology, v. 13, p. 391–411.

MISHRA, H. K. 1986, A comparative study of the petrology of Permian coals of India and Western Australia: University of Wollongong, PhD thesis (unpublished).

MYERS, J. S. and HOCKING, R. M. (compilers), 1988, Geological map of Western Australia, 1:2 500 000: Western Australia Geological Survey.

NOSIARA, M. and HOGG, P., 1982, Sabina River 1 well completion report: Western Australia Geological Survey, S-series (S2149) open-file microfilm 632.

NAFE, S. P. and DRAKE, C. L., 1961, Physical properties of marine sediments: Lamont Geological Observatory, Technical Report 2 (unpublished).

NETTLETON, L. L., 1976, Gravity and magnetics in oil prospecting: McGraw-Hill Book Company, Inc.

PIDGEON, R., 1989, *Comment in* Informal minutes of the third meeting of the Darling Fault Working Group, *edited by* R. Young and J. Scott: Perth, Curtin University of Technology.

PLAYFORD, P. E. and WILLMOTT, S. P., 1958, Stratigraphy and structure of the Perth Basin, Western Australia: West Australian Petroleum Pty Ltd (unpublished).

PLAYFORD, P. E., COCKBAIN, A. E., and LOW, G. H., 1976, Geology of the Perth Basin, Western Australia: Western Australia Geological Survey, Bulletin 124.

POYNTON, D. J. and HOLLAMS, R. F. F., 1980, Whicher Range 2 well completion report: Western Australia Geological Survey, S-series (S1628) open-file microfilms 629 and 630.

PROBERT, D. H., 1968, Groundwater in the Busselton area — Progress report on exploratory drilling: Western Australia Geological Survey, Annual Report 1967, p. 12–17.

QUILTY, J. H., 1963, Perth Basin aeromagnetic survey, Western Australia 1957: Australia, Bureau of Mineral Resources, Record 1963/74 (unpublished).

REECKMANN, S. A. and MEBBERSON, A. J., 1984, Igneous intrusions in the north-west Canning Basin and their impact on oil exploration, *in* The Canning Basin, WESTERN AUSTRALIA., *edited by* P. G.. Purcell: Perth, Geological Society of Australia and Petroleum Exploration Society of Australia, Symposium Proceedings p. 389–399.

ROBERTS, A. M., BADLEY, M. E., PRICE, J. D., and HUCK, I. W., 1990, The structural history of a transtensional basin — Inner Moray Firth, NE Scotland: Geological Society (London), Journal, v. 147, 1990, p. 87–103.

RYALL, A. M., 1989, Petroleum geology of the offshore Perth Basin, southern Western Australia (Offshore Perth Basin Seminar, 5 October 1989, Perth): Western Australia Geological Survey, S-series S3914 A1 (unpublished).

SAINT-SMITH, E. C., 1912, A geological reconnaissance of a portion of the South-West Division of Western Australia: Western Australia Geological Survey, Bulletin 44.

SMITH, R. A., 1982, Geology and hydrogeology of the Boyanup bore line, Perth Basin, *in* Professional Papers 1982: Western Australia Geological Survey, Report 12, p. 72–81.

SMITH, G. C. and COWLEY, R. G., 1987, The tectonostratigraphy and petroleum potential of the north Abrolhos Sub-basin, Western Australia: APEA Journal, p. 112–136.

SYLVESTER, A. G., 1988, Strike-slip faults: Geological Society of America, Bulletin, v. 100, p. 1666–1703.

TAYLOR, D. D., 1969, Seismic data problems on coastal limestone, Western Australia: APEA, Journal Vol. 9, p. 136–145.

TEICHERT, C., 1947, Stratigraphy of Western Australia: Royal Society of New South Wales, Journal and Proceedings, v. 80, p. 81–142 (*also* American Association Petroleum Geologists, Bulletin, v. 31, p. 1–70).

THYER, R. F., 1951, Gravity traverse near Bullsbrook, Western Australia: Australia, Bureau of Mineral Resources, Record 1951/45 (unpublished).

THYER, R. F. and EVERINGHAM, I. B., 1956, Gravity survey of the Perth Basin, Western Australia: Australia, Bureau of Mineral Resources, Bulletin 33, 11 p.

TRENDALL, A. F., 1963, Petrologist's report 33: Western Australia Geological Survey, Petrological Report (unpublished).

UNION OIL DEVELOPMENT COMPANY, 1968, Whicher Range 1 well completion report (PSSA report): Western Australia Geological Survey, S-series (S405) open-file microfilm 62.

UNION OIL DEVELOPMENT COMPANY, 1969, Blackwood 1 well completion report (PSSA report): Western Australia Geological Survey, S-series (S484) open-file microfilm 43.

UNION OIL DEVELOPMENT COMPANY, 1972, Wonnerup 1 well completion report (PSSA report): Western Australia Geological Survey, S-series (S716) open-file microfilm 62.

VENING MEINESZ, F. A., 1948, Gravity expeditions at sea, 1923–1938: Delft, Mulder, 233 p.

WHARTON, P. H., 1980, The geology and hydrogeology of the Picton borehole line: Western Australia Geological Survey, Annual Report 1979, p. 14–19.

WHARTON, P. H., 1981, The geology and hydrogeology of the Quindalup borehole line: Western Australia Geological Survey, Annual Report 1980, p. 27–35.

WILDE, S. A. and LOW, G. H., 1980, Pinjarra, W. A.: Western Australia: Western Australia Geological Survey, 1:250 000 Geological Series — Explanatory Notes.

WILDE, S. A. and WALKER, I. W., 1982, Collie, W. A.: Western Australia: Western Australia Geological Survey, 1:250 000 Geological Series — Explanatory Notes.

WILDE, S. A. and WALKER, I. W., 1984, Pemberton W. A.: Western Australia Geological Survey, 1:250 000 Geological Series — Explanatory Notes.

WILLIAMS, C. T. and NICHOLLS, J. 1966, Sue 1 well completion report (PSSA report): Western Australia Geological Survey, S-series (S268) open-file microfilm 43.

WILSON, A. F., 1958, Advances in the knowledge of the structure and petrology of the Precambrian rocks of the south-western Australia: Royal Society of Western Australia, Journal, v. 41, p. 57–83.

WOOLLARD, G. P., 1959, Crustal structure from gravity and seismic measurements: Journal of Geophysical Research, v. 64, p. 1521–1544.

WOOLLARD, G. P., 1968, The inter-relationship of the crust, the upper mantle and isostatic gravity anomalies in the United States, *in* The crust and upper mantle of the Pacific area, *edited by* L. Knopoff, C. Drake, and P. Hart: American Geophysical Union, Geophysical Monograph, v. 12, p. 312–341.

WOOLNOUGH, W. G., 1920, The physiographic elements of the Swan Coastal Plain: Royal Society of Western Australia, Journal and Proceedings, v. 5, p. 15–20.

YOUNG, R. J. B. and JOHANSON, J. N., 1973, Lake Preston 1 well completion report: West Australian Petroleum Pty Ltd (PSSA report): Western Australia Geological Survey, S-series (S811) open-file microfilm 42.

Appendix 1. Surveys conducted for petroleum exploration in southern Perth Basin

Survey name	*Year*	*Company*	*Tenement*	*Survey type*	*Kilo– metres*	*GSWA no.*	*Microform no.*
Aeromag S. of Perth Basin	1957	BMR	PE–27–H	mag	3219	S152	–
Alexandra Bridge S. Rec. S.	1964	WAPET	PE–27–H	refl	298	S132V1	12, 43
				refr	14		
Ambergate S. S.*	1980	MESA	EP–130	refl	388	S1751	629
			EP–112				
Augusta 1st Order Reg. Mag. S.	1970	BMR	EP–50	mag	–	S3009V2	–
Augusta–Moora Grav. S.	1963	WAPET	PE–27–H	grav	–	S54V1	10
Blackwood S. S.*	1965	WAPET	PE–27–H	refl	190	S206	17, 43, 62
Broadwater M. S. S.	1980	MESA	VACANT	refl	49	S1737	PES1737
Bunbury M. S. S.	1967	WAPET	PE–27–H	refl	96	S393	21, 311
Busselton S. Refl. S.	1956	BMR	PE–27–H	refl	64	S3007	–
Canebreak S. S.*	1982	WEAVER	EP–112	refl	113	S2010	628
Cape Leeuwin M. S. S.*	1980	WAINOCO	WA–135–P	refl	768	S1749	PES1749
Central Perth Basin Grav. S.	1963	WAPET	PE–27–H	grav	2534	S54V2	10
Charla S. S*	1966	WAPET	PE–27–H	refl	37	S278	40
Darradup S. S.*	1964	WAPET	PE–27–H	grav	185	S132V2	12
				refl	9		43,62
Flinders Bay M. S. S., &	1972	WAPET	WA–13–P	refl	155	S803V3	PES803
Grav. & Mag. S.			WA–14–P	grav	155		(634, 21)
				mag	289		
Four Mile Hill S. S.*	1981	BP	EP–130	refl	46	S1991	629
Grav. S. of Perth Basin	1951	BMR	PE–27–H	grav	–	S3001	–
Happy Valley S. S.*	1981	WEAVER	EP–112	refl	194	S1614	628
Harvey D1 S. S.*	1970	WAPET	PE–27–H	refl	136	S526	41
Harvey S. S.*	1969	WAPET	PE–27–H	refl	65	S471V2	41–43, 62
			PE–261–H				
Karnup Reconn. S. S.*	1966	WAPET	PE–27–H	refl	143	S277	41, 86
Koombana M. S. S.	1969	WAPET	WA–13–P	refl	1319	S456	21, 312
			WA–14–P				
Koombana Wedge Is M. S. S.	1969	WAPET	WA–13–P	refl	379	S520V1	21, 312
			WA–14–P				
Koombana 3 M. S. S. & Mag. S.	1975	WAPET	WA–14–P	refl	498	S1115	PES1115
Lake Preston S. S.*	1964	WAPET	PE–27–H	refl	74	S133V1	12, 39, 40
				refl	7		
Leeuwin Aeromag. S.	1969	WAPET	WA–13–P	mag	3701	S503	PES503
			WA–14–P				
			PE–261–H				
Margaret River S. S. *	1967	UNION	PE–261–H	refl	357	S396	43, 62
Perth M. S. S.	1965	WAPET	PE–27–H	refl	592	S243	PES243
			PE–225–H				(21, 311)
Perth Waters M. S. S.	1970	WAPET	WA–13–P	refl	24	S626V2	PES626
			WA–14–P				(21,53)
			WA–20–P				(309, 312)
Preston Detail S. S.*	1970	WAPET	EP–25	refl	88	S608	41
Preston Detail S. S. 1971/72	1971	WAPET	WA–14–9	refl	153	S788V2	639, 312
Preston D1 Detail S. S.	1971	WAPET	EP–25	refl	29	S666	41
Preston M. S. S.	1966	WAPET	PE–27–H	refl	–	S269V1	21, 311
Sabina S. Reconn. S.	1964	WAPET	PE–27–H	refl	185	S132V3	12
				refl	9		
Sabina S. S.*	1967	UNION	PE–261–H	refl	79	S356	43
Scientific Investigation 6SL	1972	SHELL	WA–13–P	refl	6194	S779	PES779
			WA–43–P	grav	6194		24, 31
			WA–44–P	mag	6194		637
			WA–47–P				
			WA–50–P				
			WA–51–P				

* Survey data used in this study

Appendix 1. (*continued*)

Survey name	*Year*	*Company*	*Tenement*	*Survey type*	*Kilo–metres*	*GSWA no.*	*Microform no.*
South Perth Basin Grav. S.	1963	WAPET	PE–27–H	grav	2317	S54V3	10
Stirling Rapids S. S.*	1980	MESA	EP–130	refl	169	S1580	628, 629
			EP–112	refl	146		
Sugarloaf M. S. S.	1968	WAPET	WA–13–P	refl	515	S437	PES437
			WA–14–P				21, 312
WA–174–P 1982 M. S. S.*	1982	BP	WA–174–P	refl	1633	S2030	PES2030
			WA–135–P				
WA–174–P 1983 M. S. S.	1983	BP	WA–174–P	refl	378	S2328	PES2328
			WA–13–P				
Wonnerup–Flinders S. S.*	1969	UNION	PE–261–H	refl	131	S462	43

Appendix 2. Reference for maturation data

Reference	*Type of analysis*	*Wells analysed*	*Microform*
Allard, 1983	Vitrinite reflectance	Cockburn 1, Sugarloaf 1	PEG621/A3
Cook, 1979a	Vitrinite reflectance	Eneabba 1, Sue 1, Walyering 1, Whicher Range 1, Whicherina 1, Woolamulla 1, Yardarino 1.	PEG1490/A1
Cook, 1979b	Vitrinite reflectance	Bullsbrook 1, Cockburn 1, Lake Preston 1, Pinjarra 1.	PEG1490/A2
CRA Exploration, 1984	Pyrolysis	49 wells in the Perth Basin *including*, Alexandra Bridge 1, Blackwood 1, Lake Preston 1, Preston 1, Sue 1, Sugarloaf 1, Whicher Range 1, Wonnerup 1	PEG2969/A1
Australian Mineral Dev. Labs, 1979	Vitrinite reflectance, Pyrolysis, TOC	Sue 1	Roll 378
BMR, 1978	Vitrinite reflectance	Whicher Range 1, Sue 1, Eneabba 1, Walyering 1	PEG1468/A16

Appendix 3. Wells drilled for petroleum exploration in the southern Perth Basin

Well name	*Year*	*Company*	*Latitude Longitude*	*Tenement*	*T.D. (m)*	*Status*	*Shows (G,O)*	*GSWA no.*	*Microform no.*
Alexandra Bridge 1	1965	WAPET	34°09'35" 115°15'40"	PE-27-H	766	P & A	0,0	S232	43, 628
Blackwood 1	1969	UNION	34°08'55" 115°21'28"	PE-261-H	3333	P & A	0,0	S484	43
Canebreak 1	1982	WEAVER	34°17'02" 115°28'06"	EP-112	2090	P & A	1,0	S2020	628
Lake Preston 1	1973	WAPET	32°55'13" 115°39'39"	EP-25	4565	P & A	0,0	S811	42
Preston 1	1966	WAPET	32°56'57" 115°42'40"	PE-27-H	765	P & A	0,0	S316	42
Sabina River 1	1982	BP	33°39'58" 115°24'35"	EP-130	4309	P & A	0,0	S2149	632
Sue 1	1966	WAPET	34°00'58" 115°19'12"	LP-152-H	3078	P & A	0,0	S268	43
Sugarloaf 1	1971	WAPET	32°54'58" 115°03'17"	WA-13-P	3658	P & A	0,0	S621	PEW621
Warren River 1	1902	WMO	34°34'00" 115°55'00"	EP-50	25	P & A	0,0	S3344V1	
Warren River 2	1902	WMO	34°35'00" 115°54'00"	EP-50	154	P & A	0,0	S3344V2	
Warren River 3	1902	WMO	34°37'00" 115°51'00"	EP-50	524	P & A	0,0	S3344V3	
Whicher Range 1	1968	UNION	33°50'19" 115°22'18"	LP-198-H	4653	P & A	3,0	S405	62
Whicher Range 2	1980	MESA	33°50'31" 115°22'57"	EP-130	4330	P & A	3,0	S1628	629, 630
Whicher Range 3	1982	BP	33°52'19" 115°23'34"	EP-130	4496	P & A	3,0	S1932	630-632
Wonnerup 1	1972	UNION	33°37'59" 115°28'24"	EP-50	4727	P & A	2,0	S716	62

NOTE: 1. Show rating is on a scale of 0 to 5. No show = 0, producing well = 5. 2. Status P & A means plugged and abandoned. 3. Company WMO = Westralian Mining and Oil Corporation.

Appendix 4. Water wells drilled in the southern Perth Basin by the Geological Survey of Western Australia

Well name	*Year*	*Latitude*	*Longitude*	*T.D. (m)*	*Reference*
Abba River 1	1956	33°43'24"	115°29'59"	522	GSWA file 125/02
Abba River 2	1956	33°44'12"	115°26'33"	226	
Abba River 3	1956	33°44'54"	115°27'40"	464	
Harvey 1B	1983	32°54'43"	115°42'05"	605	Deeney, 1989a
Harvey 2A	1983	32°55'08"	115°45'57"	810	
Harvey 3A	1983	32°54'31"	115°49'29"	603	
Harvey 4A	1984	32°53'51"	115°54'08"	602	
Binningup 1	1984	33°08'51"	115°41'46"	807	Deeney, 1989b
Binningup 2	1984	33°08'59"	115°44'28"	600	
Binningup 3	1984	33°09'37"	115°48'15"	801	
Binningup 4	1984	33°09'42"	115°51'09"	803	
Picton 1	1978	33°20'44"	115°41'36"	1200	Wharton, 1979
Picton 2	1978	33°22'07"	115°38'42"	782	
Picton 3	1978	33°20'55"	115°45'08"	794	
Picton 4	1978	33°20'59"	115°48'30"	824	
Boyanup 1	1981	33°28'13"	115°34'18"	1000	Smith, 1982
Boyanup 2	1981	33°28'29"	115°36'36"	1000	
Boyanup 3	1981	33°29'21"	115°40'01"	1000	
Boyanup 4	1981	33°28'36"	115°45'33"	998	
Quindalup 1	1966	33°39'36"	115°17'41"	588	Wharton, 1980
Quindalup 2	1967	33°39'26"	115°13'55"	551	
Quindalup 3	1967	33°38'37"	115°10'30"	453	
Quindalup 4	1967	33°38'13"	115°26'00"	585	
Quindalup 5	1967	33°38'38"	115°30'22"	613	
Quindalup 6	1974	33°38'56"	115°35'02"	1118	
Quindalup 7	1979	33°39'05"	115°38'39"	1044	
Quindalup 8	1979	33°38'17"	115°42'12"	1158	
Quindalup 9	1980	33°39'06"	115°46'52"	1465	
Quindalup 10	1979	33°39'53"	115°19'26"	1064	
Cowaramup 1	1988	33°52'15"	115°12'23"	500	Appleyard, 1989
Cowaramup 2	1988	33°51'58"	115°15'22"	759	
Cowaramup 3	1988	33°52'24"	115°19'07"	1055	
Cowaramup 4	1988	33°52'18"	115°24'15"	1072	
Cowaramup 5	1988	33°52'09"	115°28'44"	1500	
Cowaramup 6	1988	33°52'22"	115°33'04"	1494	
Cowaramup 7	1988	33°51'56"	115°38'28"	1668	
Cowaramup 8	1988	33°51'24"	115°43'08"	1448	
Karridale 1	1989	34°09'52"	115°11'12"	655	Baddock, 1991
Karridale 2	1989	34°09'22"	115°16'58"	1171	
Karridale 3	1989	34°09'06"	115°21'36"	1203	
Karridale 4	1989	34°09'46"	115°27'42"	1207	
Karridale 5	1989	34°10'06"	115°31'40"	1165	
Karridale 6	1990	34°10'55"	115°37'19"	1602	
Karridale 7	1989	34°11'21"	115°43'10"	1682	

Appendix 5. Coal exploration wells on the Vasse Shelf

Well name	*Year*	*Latitude*	*Longitude*	*T.D. (m)*	*Reference*
Vasse 1	1976	33°44'30"	115°08'48"	452	S1807, Roll
341					
Vasse 2	1976	33°42'31"	115°13'03"	450	
Bond DDH8	1983	33°49'36"	115°14'23"	337	S2353-A4 (not
Bond DDH9	1983	33°49'35"	115°15'46"	412	filmed)
Bond DDH11	1983	33°48'32"	115°13'38"	497	
Bond RDH1	1983	33°52'54"	115°15'45"	341	
Bond RDH2	1983	33°51'23"	115°15'35"	320	

Appendix 6. Formation tops of wells in the southern Perth Basin
(Depths in metres)

Well name	*AHD (m)*	*Warnbro Group*	*Bunbury Basalt*	*Parmelia Formation*	*Yarragadee Formation*	*Cockleshell Gully Formation*	*Lesueur Sandstone*	*Sabina Sandstone*	*Sue Coal Measures*	*Basement*
Alexandra Bridge 1	37	3	-	-	-	-	70	-	408	-
Blackwood 1	71	18	-	-	-	186	606	2344	2448	-
Canebreak 1	31	16	44	-	-	150	447	-	1709	-
Lake Preston 1	15	42	-	-	-	112	1219	3474	4035	-
Preston 1	8	26	-	-	-	205	-	-	-	-
Sabina River 1	13	61	-	-	150	700	1220	3614	3914	-
Sue 1	86	6	-	-	-	-	169	1137	1216	3054
Sugarloaf 1	30	390	-	710	-	-	-	-	-	-
Whicher Range 1	153	15	-	-	192	619	1271	3667	3915	-
Whicher Range 2	157	-	-	-	108	617	1257	3650	3896	-
Whicher Range 3	138	-	-	-	?	650	1240	3796	4017	-
Wonnerup 1	24	17	-	-	341	843	1482	3644	4105	-
Abba River 1	39	23	-	-	73	-	-	-	-	-
Abba River 2	21	-	-	-	0	-	-	-	-	-
Abba River 3	36	24	55	-	78	-	-	-	-	-
Harvey 1B	2	23	-	-	-	188	-	-	-	-
Harvey 2A	13	26	-	-	-	203	-	-	-	-
Harvey 3A	13	21	-	-	-	204	-	-	-	-
Harvey 4A	33	20	-	-	-	57	-	-	-	-
Binningup 1	2	29	-	-	-	194	-	-	-	-
Binningup 2	15	37	-	-	-	153	-	-	-	-
Binningup 3	13	22	-	-	-	145	-	-	-	-
Binningup 4	15	24	-	-	-	99	-	-	-	-
Picton 1	8	20	-	-	280	566	-	-	-	-
Picton 2	6	-	-	-	15	202	-	-	-	-
Picton 3	18	18	-	-	262	733	-	-	-	-
Picton 4	45	8	-	-	104	-	-	-	-	-
Boyanup 1	8	17	-	-	78	571	-	-	-	-
Boyanup 2	18	-	-	-	18	804	-	-	-	-
Boyanup 3	32	-	-	-	19	805	-	-	-	-
Boyanup 4	76	0	305	-	360	-	-	-	-	-
Quindalup 1	2	9	-	-	-	84	-	-	-	-
Quindalup 2	2	9	-	-	-	-	-	-	109	-
Quindalup 3	3	10	-	-	-	-	-	-	209	-
Quindalup 4	5	11	-	-	89	-	-	-	-	-
Quindalup 5	20	7	-	-	151	-	-	-	-	-
Quindalup 6	42	11	32	-	104	-	-	-	-	-
Quindalup 7	101	1			139	-	-	-	-	-
Quindalup 8	59	4	-	-	253	-	-	-	-	-
Quindalup 9	96	1	-	-	350	-	-	-	-	-
Quindalup 10	2	3	-	-	497	796	-	-	-	-
Cowaramup 1	95	0	-	-	-	-	-	-	188	-
Cowaramup 2	144	0	-	-	-	-	-	-	250	-
Cowaramup 3	134	0	-	-	160	680	-	-	-	-
Cowaramup 4	133	0	-	-	150	1010	-	-	-	-
Cowaramup 5	178	0	180	-	198	950	-	-	-	-
Cowaramup 6	116	0	-	180	250	1215	-	-	-	-

Appendix 6. (*continued*)

Well name	*AHD* (*m*)	*Warnbro Group*	*Bunbury Basalt*	*Parmelia Formation*	*Yarragadee Formation*	*Cockleshell Gully Formation*	*Lesueur Sandstone*	*Sabina Sandstone*	*Sue Coal Measures*	*Basement*
Cowaramup 7	110	0	72	135	?	?	-	-	-	-
Cowaramup 8	155	0	174	-	214	-	-	-	-	-
Karridale 1	13	0	-	-	-	-	88	139	200	-
Karridale 2	43	-	-	-	-	-	0	860	980	-
Karridale 3	65	0	-	-	180	-	-	-	-	-
Karridale 4	65	0	-	137	235	-	-	-	-	-
Karridale 5	61	-	-	-	45	394	-	-	-	-
Karridale 6	111	0	22	-	125	862	-	-	-	-
Karridale 7	121	0	235	263	480	-	-	-	-	-
Vasse 1	60	0	-	-	-	-	-	-	140	-
Vasse 2	20	0	-	-	-	-	-	-	145	-

Appendix 7. Two-way time to formation tops

(Times in milliseconds)

Well	*Warnbro Gp.*	*Bunbury Basalt*	*Parmelia Fm.*	*Yarragadee Fm.*	*Cockleshell Gully Fm.*	*Lesueur Ss.*	*Sabina Ss.*	*Sue Coal Measures*	*Basement*	*T.D.*
Alexandra Bridge 1	?	-	-	-	-	?	-	380	-	780
Blackwood 1	?	-	-	-	114	451	1 471	1 532	-	2 052
Canebreak 1	?	9	-	-	82	285	-	1 134	-	1 389
Lake Preston 1	34	-	-	-	92	830	1 863	2 068	-	2 335
Preston 1	27	-	-	-	185	-	-	-	-	548
Sabina River 1	66	-	-	153	584	960	2 207	2 268	-	2 460
Sue1	?	-	-	-	-	130	870	930	1 950	2 000
Sugarloaf 1	340	-	590	-	-	-	-	-	-	2 150
Whicher Range 1	?	-	-	46	390	830	1 940	2 070	-	2 420
Whicher Range 2	-	-	-	?	372	767	1 950	2 080	-	2 270
Whicher Range 3	-	-	-	?	410	830	2 060	2 160	-	2 435
Wonnerup 1	?	-	-	307	670	1 110	2 110	2 360	-	2 660

Appendix 8. Velocity function coefficients

Well	*a*	*b*	*Correlation coefficient*
Blackwood 1	1 412	1.195	0.9997254
Canebreak 1	1 478	1.009	0.9976796
Lake Preston 1	1 598	1.241	0.9997288
Sabina River 1	1 384	1.233	0.9991608
Sue 1	1 349	1.249	0.9994888
Sugarloaf 1	1 295	1.319	0.9993470
Whicher Range 1	1 527	1.191	0.9977934
Whicher Range 2	1 509	1.201	0.9988969
Whicher Range 3	1 470	1.221	0.9989041
Wonnerup 1	1 408	1.265	0.9993592

Appendix 9. Vitrinite reflectance data

Lake Preston 1		*Sue 1*		*Sugarloaf 1*		*Whicher Range 1*	
Depth	*Ro*	*Depth*	*Ro*	*Depth*	*Ro*	*Depth*	*Ro*
387.2	0.23	154.0	0.40	470.9	0.47	68.6	0.35
510.7	0.20	1 218.0	0.48	681.2	0.55	1 614.3	0.41
800.3	0.44	1 382.6	0.41	873.3	0.55	2 550.3	0.57
843.0	0.26	2 419.2	0.67	1 205.5	0.48	3 928.4	0.80
1 013.7	0.31	2 593.0	0.62	1 205.5	0.52	4 038.1	0.85
1 089.9	0.31	2 806.4	0.82	1 507.2	0.48	4 149.4	0.86
1 391.8	0.52	2 861.3	0.80	1 507.2	0.72	4 209.5	0.77
1 626.5	0.35	2 861.3	0.68	1 594.1	0.71	4 314.2	0.89
1 815.5	0.61	2 861.3	0.51	1 705.4	0.71	4 407.0	0.89
1 862.8	0.55	2 870.4	0.63	1 804.4	0.75	4 596.0	0.97
4 041.0	1.01	2 885.7	1.16	1 918.7	0.76	4 596.0	0.79
4 096.0	0.88	3 004.6	0.70	2 732.5	0.69	4 650.9	1.01
4 190.5	0.83			2 732.5	0.71		
4 190.5	1.21						
4 190.5	1.85						
4 214.9	0.92						
4 359.8	1.56						
4 410.0	1.73						
4 469.5	1.84						
4 542.7	1.97						

13843/11/93—400—L/6217

GARRY L. DUFFIELD, Government Printer, Western Austr

SOUTH PERTH BASIN

DRILL SITE LOCATIONS

Pl. 1 Rep. 31

REFERENCE

- Petroleum well
- G.S.W.A. Hydrogeological bore
- Coal bore

DEPARTMENT OF MINERALS AND ENERGY

DEPARTMENT OF MINERALS AND ENERGY
WESTERN AUSTRALIA

SOUTHERN PERTH BASIN

DRILLING SITE LOCATION MAP

SCALE 1:250 000

5 0 5 10 15 20 25

KILOMETRES

GSWA REPORT 31 PLATE 1

SOUTH PERTH BASIN (LOCATION MAP) COMPOSITE SEISMIC LINES (SHOT POINT) P/.2 Rp/.31

SOUTH PERTH BASIN

(DEPTH)

BASE WARNBRO GROUP

Pl. 3 Rep. 31

REFERENCE

- Abandoned well, dry
- Abandoned well, show of gas
- (St) Stratigraphic well
- (316) Depth to mapped horizon, metres
- H Structural high
- L Structural low

Contour interval 100 m

Datum MSL

DEPARTMENT OF MINERALS AND ENERGY WESTERN AUSTRALIA

SOUTHERN PERTH BASIN

Depth

STRUCTURE

BASE WARNBRO GROUP

SCALE 1:250 000

5 0 5 10 15 20 25 KILOMETRES

Interpretation by R.P. Iasky of the Geological Survey of Western Australia

GSWA REPORT 31 PLATE 3

SOUTH PERTH BASIN (SEISMIC TIME) BASE WARNBRO GROUP Pl. 4 Rep. 31

SOUTH PERTH BASIN (DEPTH) TOP COCKLESHELL GULLY Fm. Pl.5 Rep.31

REFERENCE

- Abandoned well, dry.
- Abandoned well, show of gas
- (687) Depth to mapped horizon, metres
- H Structural high
- L Structural low

Contour interval 250 m
Datum MSL

DEPARTMENT OF MINERALS AND ENERGY
WESTERN AUSTRALIA

SOUTHERN PERTH BASIN

Depth

STRUCTURE

TOP COCKLESHELL GULLY FM

SCALE 1:250 000
5 0 5 10 15 20 25
KILOMETRES

Interpretation by R. P. Iasky of the Geological Survey of Western Australia

GSWA REPORT 31 PLATE 5

SOUTH PERTH BASIN (SEISMIC TIME) TOP COCKLESHELL GULLY Fm. Pl. 6 Rep. 31

REFERENCE

- Abandoned well, dry
- Abandoned well, show of gas
- (687) Depth to mapped horizon, metres
- H Structural high
- L Structural low

Contour interval 100 ms (Two way time)
Datum MSL

DEPARTMENT OF MINERALS AND ENERGY
WESTERN AUSTRALIA

SOUTHERN PERTH BASIN

Seismic Time

STRUCTURE

TOP COCKLESHELL GULLY FM.

SCALE 1:250 000
5 0 5 10 15 20 25
KILOMETRES

Interpretation by R. P. Iasky of the Geological Survey of Western Australia

SOUTH PERTH BASIN (DEPTH) TOP LESUEUR SS. Pl.7 Rep 31

REFERENCE

- Abandoned well, dry
- Abandoned well, show of gas
- (St) Stratigraphic well
- (1612) Depth to mapped horizon, metres
- H Structural high
- L Structural low

Contour interval 250 m
Datum MSL

DEPARTMENT OF MINERALS AND ENERGY
WESTERN AUSTRALIA

SOUTHERN PERTH BASIN

Depth

STRUCTURE

TOP LESUEUR SS

SCALE 1:250 000
KILOMETRES

Interpretation by R. P. Iasky of the Geological Survey of Western Australia

GSWA REPORT 31 PLATE 7

SOUTH PERTH BASIN (SEISMIC TIME) TOP LESUEUR SS Pl. 8 Rep. 31

REFERENCE

- Abandoned well, dry
- Abandoned well, show of gas
- (St) Stratigraphic well
- (1612) Depth to mapped horizon, metres
- H Structural high
- L Structural low

Contour interval 100 ms (Two way time)
Datum MSL

DEPARTMENT OF MINERALS AND ENERGY
WESTERN AUSTRALIA

SOUTHERN PERTH BASIN

Seismic Time

STRUCTURE

TOP LESUEUR SS

SCALE 1:250 000
5 0 5 10 15 20 25
KILOMETRES

Interpretation by R.P. Iasky of the Geological Survey of Western Australia

GSWA REPORT 31 PLATE 8

SOUTH PERTH BASIN (DEPTH) TOP SUE COAL MEASURES

Pl. 9 Rep. 31

REFERENCE

◇ Abandoned well, dry

◇ Abandoned well, show of gas

(St) Stratigraphic well

(3900) Depth to mapped horizon, metres

H Structural high

L Structural low

Contour interval 250 m

Datum MSL

DEPARTMENT OF MINERALS AND ENERGY
WESTERN AUSTRALIA

SOUTHERN PERTH BASIN

Depth

STRUCTURE

TOP SUE COAL MEASURES

SCALE 1:250 000

5 0 5 10 15 20 25

KILOMETRES

Interpretation by R.P. Iasky of the Geological Survey of Western Australia

SOUTH PERTH BASIN (SEISMIC TIME) TOP SUE COAL MEASURES

Pl. 10 Rep. 31

SOUTH PERTH BASIN (DEPTH) BASEMENT STRUCTURE Pl. 11 Rep. 31

REFERENCE

◇	Abandoned well, dry
(2968)	Depth to mapped horizon, metres
H	Structural high
L	Structural low

Contour interval 250 m

Datum MSL

DEPARTMENT OF MINERALS AND ENERGY
HON. GEORGE CASH, J.P., M.L.C. MINISTER FOR MINES
L.C. RANFORD, ACTING DIRECTOR GENERAL

PIETRO GUJ
DIRECTOR, GEOLOGICAL SURVEY OF WESTERN AUSTRALIA

DEPARTMENT OF MINERALS AND ENERGY WESTERN AUSTRALIA

SOUTHERN PERTH BASIN

Depth

STRUCTURE

BASEMENT

SCALE 1:250 000

5 0 5 10 15 20 25 KILOMETRES

Interpretation by R.P. Iasky of the Geological Survey of Western Australia

GSWA REPORT 31 PLATE 11

SOUTH PERTH BASIN (SEISMIC TIME) BASEMENT STRUCTURE Pl. 12 Rep. 31

REFERENCE

◇ Abandoned well, dry

(2968) Depth to mapped horizon, metres

H Structural high

L Structural low

Contour interval 100 ms (Two way time)
Datum MSL

DEPARTMENT OF MINERALS AND ENERGY
WESTERN AUSTRALIA

SOUTHERN PERTH BASIN

Seismic Time

STRUCTURE

BASEMENT

SCALE 1:250 000

5 0 5 10 15 20 25

KILOMETRES

Interpretation by R.P. Iasky of the Geological Survey of Western Australia

GSWA REPORT 31 PLATE 12